ACUSTICA

Vol. 3 1953 No. 5

CALCULATION OF SOUND PROPAGATION IN STRUCTURES

by L. CREMER, München

Summary

The different types of structure-borne sound waves are described and the wavelengths deduced. Especially the radiation into the air and the reciprocal transition are discussed.

The impedances of simple types of structure are calculated and also the spectrum of impact sounds.

Finally the paper deals with the reduction of longitudinal and flexural wave amplitudes afforded by change of section, transition from rod to plate, corners, elastic layers and impeding masses.

Sommaire

On décrit les différents types d'ondes sonores qui sont transmises par les éléments de construction et on en calcule les longueurs d'onde. On étudie spécialement le cas du rayonnement dans l'air et de la transition en sens inverse.

On calcule les impédances d'éléments simples de construction ainsi que le spectre des sons d'impact.

Enfin, le présent article traite de la réduction de l'amplitude des ondes longitudinales et de flexion qui est produite par les variations de section, le passage d'une tige à une plaque, les angles, les couches élastiques et les masses réflectantes.

Zusammenfassung

Es werden zunächst die verschiedenen Wellenarten, die bei Baukonstruktionen hauptsächlich interessieren, beschrieben und die Wellenlängen berechnet. Dabei wird besonders die Frage der Abstrahlung in Luft und die des reziproken Überganges aus Luft diskutiert.

Es werden dann einige Impedanzen berechnet und aus ihnen wird das Körperschallspektrum für Stoßvorgänge abgeleitet.

Schließlich wird die Körperschalldämmung behandelt, die sich bei Longitudinal- und Biegewellen ergibt bei Querschnittswechsel, beim Übergang Stab—Platte, an Ecken, bei elastischen Zwischenlagen und bei aufgesetzten Sperrmassen.

INTRODUCTION

A great part of the noise which annoys us in buildings or cars is due to the fact that sound travels through the supporting or separating constructions. This is true for all those noises in particular which are directly produced within these solids, such as knocking, rubbing, etc.

In constructional acoustics little attention has been paid thus far to the study of the problem how the wave propagation actually takes place in solids; this may be due to the fact that most of the disturbing noises are produced in air and finally reach our ear through the air.

Furthermore, the physics of sound propagation in solids is far more complicated than in the case of sound propagation in gases and liquids. In the case of continua of unlimited extension there are two different types of waves, namely the longitudinal waves (dilatation waves) also occurring in liquid or gaseous media and, due to the possibility of transmitting shearing stresses, transverse shear waves (rotational waves). These two types of waves are mostly produced at the same time and when one type strikes an obstacle or a reflecting surface the other type arises as a secondary effect. If the reflecting surfaces lie close together, as is the case with all plates and rods, a great variety of resultant wave types will be produced.

In general the useful representation of a problem of wave propagation in finite structures depends on the ratio of their dimensions to the respective wavelengths. Since the audio-frequencies cover 9 octaves, we have to deal with very different problems. If low frequencies are of interest a construction can be considered as one unit, i.e. as a mass or a compliance. In this case the whole construction can be treated like a coupled system with a finite number of degrees of freedom. This treatment does not differ from that usual in the mechanics of oscillations.

On the other hand, if very high frequencies are of interest, in particular in the field of ultrasonics, all dimensions are large as compared with the wavelength and it will be best to use laws of propagation proper to a three dimensional continuum. For this case seismology has done a great deal of useful preparatory work.

The characteristic domain of "sound propagation in constructions" is the medium range. Most of the constructional elements, no matter whether these are buildings or steel constructions of ships, consist either of rods with very different cross-sections or of plates. The appropriate representation of problems concerning these structures and the frequencies which are of chief interest depend upon the fact that, compared with the wavelength, they are considered to be small in respect to the small lateral dimensions and to be large in respect to their longitudinal dimensions. Only one or two dimensional propagation problems are of interest in so far as sound in constructional elements is concerned.

I. WAVE-LENGTHS

1. Longitudinal waves

If the acoustical properties of a given structure are to be determined, first the ratio between the dimensions and the wavelengths in question has to be considered. If the disturbance occurs in a certain narrow frequency range, the problem is relatively simple to solve. If the frequency range is unknown, the whole audio-frequency range or that part of it which is of interest in architectural acoustics, i.e. 100 to 3200 c/s, has to be considered.

The computation of wavelengths can only be based upon certain physical properties of the building materials. This immediately involves a first difficulty. The density ϱ of most materials is a quantity well-known or easy to determine. Things are quite different with Young's modulus E, the modulus of rigidity G, and the coefficient of lateral contraction μ related to both. The results of earlier measurements of Young's modulus mostly refer to its static value and have moreover proved to be much dependent on the load.

In architectural acoustics, however, the dynamic value of Young's modulus has to be considered and this may differ considerably from the static value. The dynamic value is best determined from the longitudinal natural vibrations of a free-free rod. Its length l equals half a wavelength λ_L or a multiple of this distance:

$$l = n\,\frac{\lambda_L}{2}\,. \tag{1}$$

From the associated frequency f_n

$$f_n = \frac{c_L}{\lambda_L} = n\,\frac{c_L}{2l} \tag{2}$$

we obtain the velocity of propagation c_L of a longitudinal wave:

$$c_L = \sqrt{E/\varrho}. \tag{3}$$

Young's modulus can be calculated from c_L if the density ϱ is known. It is, however, easy to refer all the formulae to c_L and ϱ instead of E. So it is sufficient to note the values of c_L, which moreover represent a more obvious physical conception.

Such determinations of c_L for various building materials have been made by R. Schmidt [1]. Rods suspended by means of wires were set into vibration at one end by a bone-conduction receiver, and the vibrations were received by a pick-up at the other end. Every resonance, i.e. agreement of driving and natural frequencies, resulted in a narrow peak on the record. Thus he was able to determine many values of c_L within a large frequency range:

Material	c_L
Iron	5170 m/s
Reinforced concrete	3700 m/s
Bricks with mortar	2350 m/s
Timber (fir) lengthwise	4900 m/s

These values, however, were obtained from single specimens of each material. Only the value for the metal, i.e. the iron, may also be applicable to specimens of other composition. The term "concrete", even when restricted to heavy concrete, involves materials differing in density by a factor of 2 and in Young's modulus by a factor of 2.5. As long as we can suppose that both properties of different compositions vary in the same sense, the value given above would not differ by more than 12 %. For bricks, however, the data given in the literature vary considerably, perhaps owing to the differences in mortar. E. Lübcke [2] e.g. gave $c_L = 4300$ m/s instead of the above value. The data concerning timber are similarly different. Compared with the above value obtained by Schmidt the well-known pocket-book "Hütte" gives $c_L = 4180$ m/s for fir and 3380 m/s for oak. In the direction transverse to the fibres the stiffness and velocity of propagation may be considerably lower. For plywood, which is nearest to an isotropic material, an average value of $c_L = 3000$ m/s can be taken.

Since the known data are partly contradictory, partly not precisely defined, it is to be expected that new data gained by systematic tests according to Schmidt's method will soon be published.

At present we only can refer to the data given above when estimating the effects to be expected in architectural structures. In most cases we have to restrict ourselves to an estimate of the order of magnitude since on the one hand the theoretical presuppositions are mostly not fulfilled and on the other hand the composition and the dimensions of the materials and the building methods are far from being uniform and exact.

Under these circumstances some minor differences can be disregarded. The difference, for example, between the velocity of longitudinal waves in a rod, as mentioned above, and that in a plate

$$c_{L_1} = \sqrt{E/[\varrho(1-\mu^2)]} \tag{4}$$

which with $\mu = 0.3$ is about 5% higher, can be ignored in comparision with the uncertainties in E and ϱ. The velocity of longitudinal waves in an infinite medium, which is again somewhat higher, is of no interest in most buildings.

The calculation of the wavelength from equations (2) and (3) is easy but if it is required repeatedly it is convenient to read it from a diagram. Fig. 1 shows the wavelengths plotted against the frequency as straight lines on a logarithmic scale.

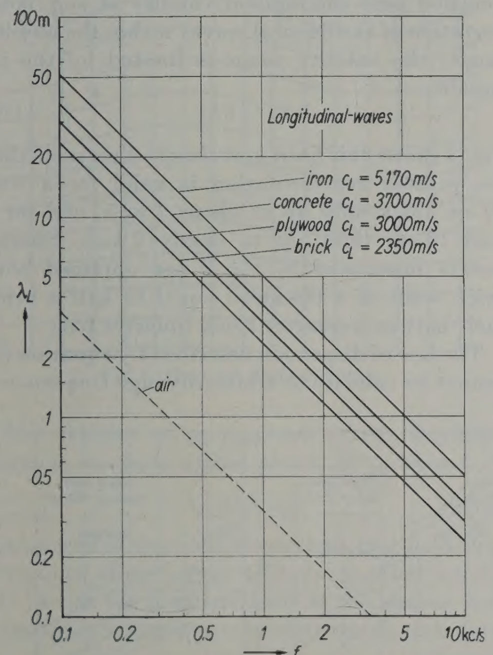

Fig. 1. Wavelengths of longitudinal waves.

This diagram shows, for example, that in concrete the wavelength is 37 m at 100 c/s and is still 1.15 m at 3200 c/s. From this result it can be deduced that a pillar 3 m high can be considered as a quasi-stationary element at 100 c/s, i.e. it can be considered as a mass or a spring according as its base is soft or rigid. Further, it can be deduced that a partition wall $h = 20$ cm thick is, even at 3200 c/s, still thin with respect to the wavelength so that the necessary restriction for the validity of the formula for longitudinal waves is not surpassed. This restriction requires about

$$\lambda_L > 3h. \tag{5}$$

Finally the magnitude of the wavelength is of interest for estimating possible resonances. At a frequency of about 600 c/s the above mentioned pillar would be equal in length to half a wavelength, in other words it would vibrate at a natural frequency if it is equally terminated at both ends either by a hard or a soft medium.

2. Transverse and torsional waves

Fig. 2 is a similar diagram showing the wavelengths of transverse waves (shear waves). They were derived from the longitudinal waves by putting $\mu = 0.3$ for all materials, because more exact data were not available. This means:

$$c_T = \sqrt{G/\varrho} = \sqrt{E/2\varrho(1+\mu)} = 0.62\, c_L. \tag{6}$$

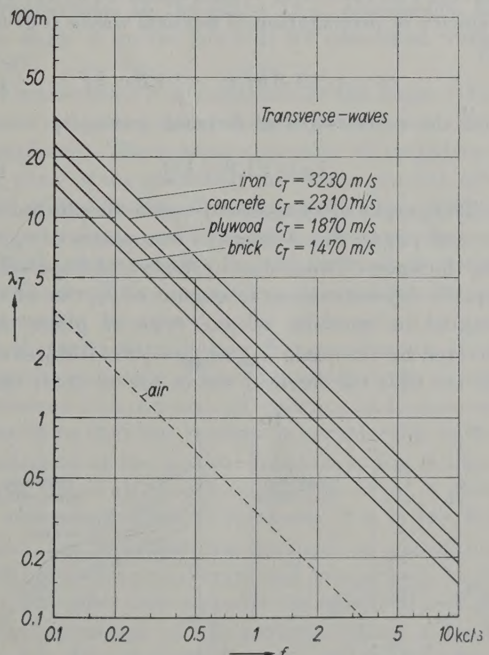

Fig. 2. Wavelengths of transverse waves.

These pure transverse waves are of little importance in architectural structures. The conditions are quite different in vehicles and machines especially because at the same time c_T is equal to the velocity of propagation of torsional waves in structural elements of a circular symmetric cross-section. An iron shaft, e.g. 5 m in length, between two heavy masses would show its fundamental resonance at 320 c/s.

In other cross-sections, e.g. in a flat steel strip, the torsional waves are propagated more slowly. For a narrow rectangle of breadth b and height H we have

$$c_{T_1} = \sqrt{G/\varrho} \cdot 2b/H. \tag{7}$$

With values of say $b = 5$ and $H = 50$ mm the velocity is one fifth of that of the pure transverse wave. A bar of this cross-section having a length of 1 m would have its fundamental natural frequency at 320 c/s.

3. Flexural waves

Flexural waves are the waves of highest importance in architectural acoustics. Their velocity of propagation depends not only on the material but also on the thickness of the plate or bar and the frequency. The dependence on frequency is associated with that on thickness since in a sound field every length has to be referred to the respective wavelength, e.g. that of longitudinal waves. The ratio h/λ_L is equivalent to hf/c_L. The velocity of propagation of flexural waves is given by

$$c_B = c_L \sqrt{1.8\, hf/c_L} = \sqrt{1.8\, c_L\, hf} \tag{8}$$

and the wavelength of flexural waves by

$$\lambda_B = \sqrt{1.8\, c_L\, h/f}. \tag{9}$$

The graphs of λ_B against f had to be plotted on several pages. Fig. 3 refers to iron plates of varying thickness. On account of the law of dispersion, i.e. the dependence on frequency of c_B, the wavelengths in question of one type of plates are covered by the ratio $\lambda_{100}:\lambda_{3200} = \sqrt{32}:1$. Moreover we see that the flexural waves are so short that even at low frequencies several wavelengths can occur in a structural element. Thus the consideration of semi-infinite structural elements is justified. A sheet of iron 1 mm thick, for example has $\lambda_{100} = 30$ cm. A plate of 1.2×1.2 m^2 of this material shows at least three wavelengths in every direction.

Fig. 3 is also useful for determining resonances. For an iron bar supported at both ends we have

$$l = n\lambda_B/2 \tag{10}$$

which corresponds to equation (1). For a small steel plate 5 mm thick and 25 cm long, supported at the edges, we obtain a fundamental natural frequency of about 190 c/s. If the plate is clamped at both ends the natural frequency would be 2.25 times higher. The boundary condition of perfect clamping, however, can hardly be fulfilled. For this reason a value between the two has to be expected but cannot be determined more exactly.

In the same manner Fig. 4, 5 and 6 refer to plates of concrete, brick and plywood and to thicknesses h which are of interest.

The thickness of the structural elements in question puts the limit of validity of our representation of the flexural waves within the audible range: the validity range is limited by the inequality

$$\lambda_B > 6h. \tag{11}$$

Fig. 4 shows this limit and clearly illustrates that the present representation is valid for a wall 20 cm thick only up to about 1 kc/s, and for a wall 10 cm thick up to nearly 2 kc/s. Similar results illustrated in Fig. 5 are obtained with brick walls of a thickness equal to half a brick (half bat) or a quarter brick (quarter bat).

The law of dispersion described by equation (8) cannot be valid up to arbitrarily high frequencies.

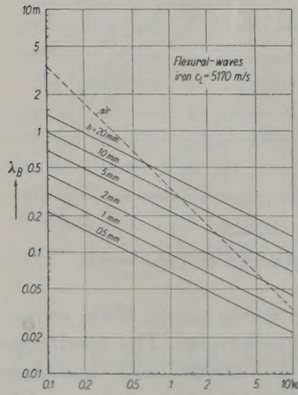

Fig. 3. Flexural wavelengths in iron plates.

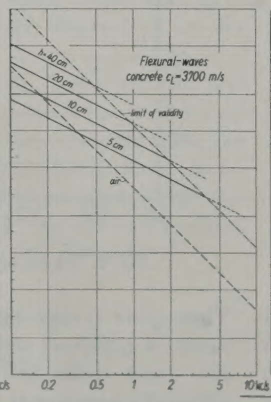

Fig. 4. Flexural wavelengths in concrete walls.

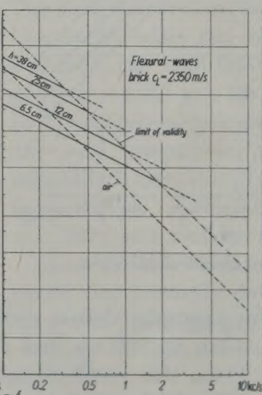

Fig. 5. Flexural wavelengths in brick walls.

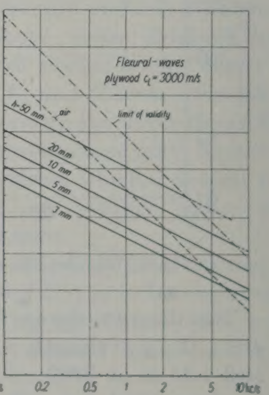

Fig. 6. Flexural wavelengths in plywood panels.

This can be concluded from the fact that this equation would describe a velocity of propagation approaching infinity. The highest velocity of propagation occurring in solids is, however, that of the longitudinal waves (without any lateral contraction). The velocity of the flexural waves could at most tend asymptotically towards this value.

In fact, the velocity of flexural waves tends towards a lower limiting value which is (for $\mu = 0.3$) given by

$$c_R = 0.57\ c_L. \tag{12}$$

The subscript R characterizes a special type of waves called Rayleigh waves after its discoverer. The Rayleigh wave is a surface wave (as illustrated by Fig. 7). This asymptotic behaviour of a wall struck by sound waves is understandable. At low frequencies, or with a wall thin compared with λ_L, both sides of the wall vibrate in phase. Normal to its surface the wall acts as a diaphragm. The thicker the wall with respect to λ_L, i.e. the higher the frequency, the smaller is the depth of penetration of the forced vibration.

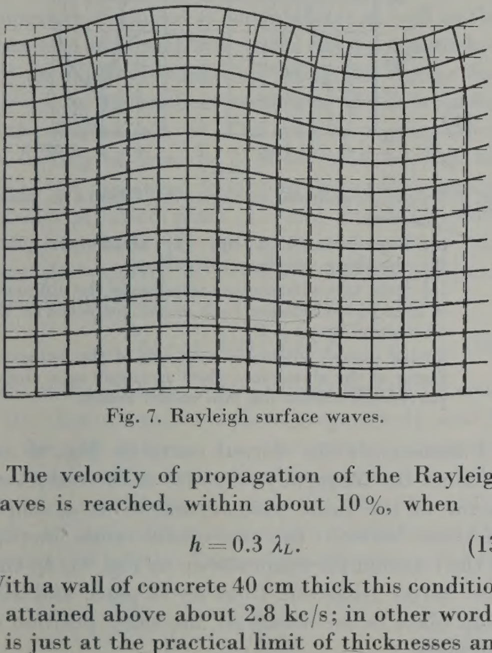

Fig. 7. Rayleigh surface waves.

The velocity of propagation of the Rayleigh waves is reached, within about 10%, when

$$h = 0.3\ \lambda_L. \tag{13}$$

With a wall of concrete 40 cm thick this condition is attained above about 2.8 kc/s; in other words, it is just at the practical limit of thicknesses and frequencies occurring in architectural acoustics.

4. The radiation from a plate into the air and the reciprocal transition

An important part is played by the ratio of the lengths of flexural waves to the wavelengths of sound in air of the same frequencies. For this reason Fig. 3 and the following figures show the wavelengths in air by a broken straight line. The slopes of these lines are steeper than that of the parallel lines describing the wavelengths of flexural waves. For this reason there is a critical frequency for every thickness of plate, characterized by the equality of both wavelengths. The critical frequency f_c can either be seen from the points of intersection in Fig. 3 ff. or calculated from an equation obtained by putting equal the formulae:

$$\lambda_B = \sqrt{1.8\, c_L\, h/f} = \lambda_0 = c_0/f$$

where c_0 denotes the velocity of sound in air. Hence:

$$f_c = c_0^2/1.8\, c_L\, h. \tag{14}$$

The importance of this critical frequency may be understood in regarding the radiation of an unlimited flexural wave [3], [6] and [15]. If its wavelength λ_B is larger than the wavelength in air λ_0 corresponding to the same frequency HUYGHENS' principle proves that there is a wave radiated in air on either side of the plate forming the angle

$$\vartheta = \arcsin\,(\lambda_0/\lambda_B) \tag{15}$$

between the direction of propagation and the perpendicular to the plate. If λ_0 approaches λ_B, the angle ϑ moves towards its maximum value of 90°.

Furthermore if λ_0 surpasses λ_B the angle ϑ becomes imaginary which means that radiation fails completely. The contrary motions of neighbouring parts of the plate only produce a quasi-steady field of flow in the surrounding medium, shifting the particles to and fro without compression.

With respect to the limited dimensions of the partition walls we cannot expect a sudden change between a frequency range with radiation and another without radiation. Yet experiments show that the radiation of plates excited at the centre increases with increasing frequency and moreover they show that this increase is considerable in the proximity of the critical frequency. Fig. 8 illustrates the result of such an experiment [4]. A plate of aluminium 5 mm in thickness, 1 m in breadth and 1.7 m in height, was arranged as a partition wall between a reverberant and an anechoic chamber. The plate was excited in the middle at a single point by means of the moving coil of a loudspeaker. The alternating force could be estimated from the intensity of the alternating current and thus the supplied power N_1 could be calculated. The power N_2 radiated from the plate was calculated from the mean value of sound pressure measured at several points in the reverberant chamber. Curve a of Fig. 8 shows the quotient N_2/N_1 thus obtained (disregarding a constant)

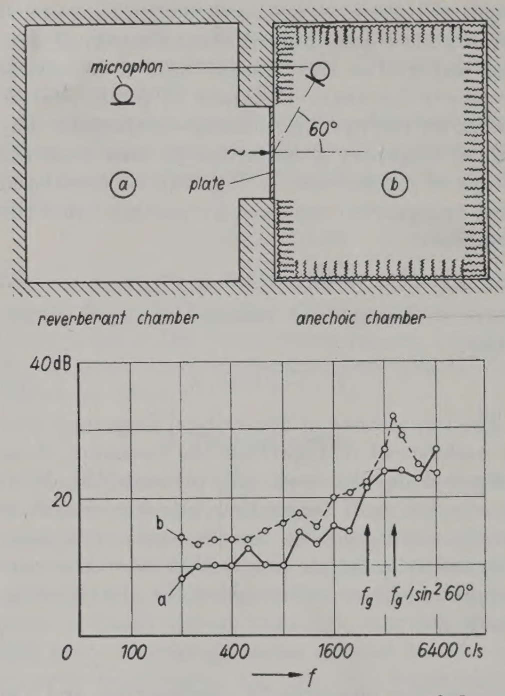

Fig. 8. Frequency response of the radiation of flexural waves.

plotted on a logarithmic scale. In spite of the relatively small dimensions of the plate we see clearly the sudden increase by 10 dB of radiation in the proximity of the critical frequency which is about 2.6 kc/s.

In order to gain a second proof of the theory, the pressure p_2 in the anechoic chamber was also measured at a distance of 2 m from the driving point under an angle of 60° with respect to the normal on the plate. The result is represented in curve b of Fig. 8 and clearly shows a maximum value at the frequency:

$$f = f_c/\sin^2 60°.$$

According to the law of reciprocity we also may expect a better transition from air-borne sound in flexural waves of solid plates above the critical frequency. Both phenomena are of great importance for the by-pass-transition in buildings over side-walls and ceilings common to adjacent rooms. K. Gösele[1] succeeded in checking this phenomenon. He used an aluminium plate 2 mm in thickness which was placed through a slot of a fourfold partition separating two small model rooms (Fig. 9a). Both rooms are reverberant so that the sound waves in the room containing the source struck the plate at all possible angles of incidence. In Fig. 9b the solid curve shows the frequency response of the difference in level between both rooms diminished by the tenfold logarithm of the absorptive power of room B. We see that above 4 kc/s this difference suddenly decreases about 20 dB and rises again above 7 kc/s. The critical frequency may be calculated as 6.2 kc/s.

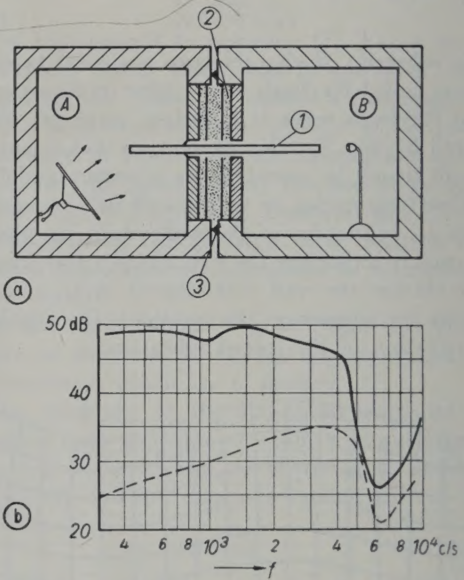

Fig. 9. By-pass-transition, measured by Gösele in model chambers.

(a) Experimental set-up: (1) aluminium plate, (2) absorbing material, (3) rubber.

(b) Solid curve: frequency response of the difference in sound level between both rooms, corrected for the absorption in room B,

dotted curve: frequency response of the reduction factor of the aluminium plate arranged as a simple partition between the two model rooms.

Furthermore the dotted curve in Fig. 9b represents the frequency response of the reduction factor of the same plate arranged as a simple partition between the two model rooms instead of the fourfold partition shown in Fig. 9a. In this case better transition from air to plate and also from plate to air occurs at the same position of the plate.

Regarding formula (14) we may remark that a plate radiates the better, the thicker it is. On the other hand a thicker plate requires more energy to set it in vibration. The above relations give an explanation of the fact that impact sound caused by hammering a thicker sheet of iron is, in spite of lower amplitude, equally as audible as sound caused by hammering of thinner sheets which show larger amplitudes.

---

[1] I am very much indebted to Herrn K. Gösele, Stuttgart, for the permission to use his results taken from a paper not yet published. The experiments in question were subsidised by the "Forschungsgemeinschaft Bauen und Wohnen, Stuttgart".

Moreover equation (14) explains the fact that in water sounds coming from structural elements are of higher pitch than sounds radiated by equal elements in air. In water the critical frequency is higher by the factor $(1460/340)^2 = 18$, since c_0 denotes the velocity of propagation in the surrounding medium. Thus in water the radiation of the lower partial tones is feebler.

The relative positions of the wavelength in air as against the wavelengths of flexural waves in iron plates on the one hand and on the other hand in walls and ceilings constructed of bricks or concrete are quite different. This is not caused by the difference in material but by the quite different order of magnitude of the plate thicknesses. The values of c_L in masonry are even smaller. In almost the whole frequency range the transition between air and the wall is rather easy. Only the heavy weight and high stiffness counteract an observable increase of sound transition as compared with plates of sheet iron.

With plywood plates (see Fig. 6) the critical frequencies are distributed between about 400 and 6000 c/s. Therefore, the sound radiating properties of thicker wooden plates as well as the transition of sound into them can be diminished and their sound-insulating properties can be improved by an artifical reduction of the velocity of the flexural waves. This can be accomplished by cutting of grooves as illustrated by Fig. 10, where the measured reduction factor for a homogeneous plywood plate (1.5 cm) and for a plate with grooves is plotted against frequency [5], since the velocity of flexural waves in inhomogeneous plates is:

$$c_B = \sqrt[4]{B/m} \cdot \sqrt{2\pi f}. \tag{16}$$

Here m denotes the mass per unit length, or area, in the case of a rod or a plate, respectively, and B the flexural stiffness, i.e. the quantity given by the relation of a static bending moment and the resulting curvature, which in the case of a rod is given by the product of Young's modulus and the moment of inertia. The critical frequency can be written:

$$f_c = \frac{c_0^2}{2\pi}\sqrt{\frac{m}{B}}. \tag{17}$$

By grooving the plates the mass is practically not altered, the flexural stiffness, however, is considerably diminished which results in a higher critical frequency.

This particular measure is an illustration of the general rule that it is often advantageous to use structural elements of low flexural stiffness if they are available. This measure can be applied in a building of low sound-insulation in order to protect certain rooms from noise propagated in the walls or the skeleton of reinforced concrete. This aim can be attained to an astonishing degree by providing an internal covering of the walls or the ceiling by light-weight plates of wood-shavings which are nailed to laths and coated by plaster on the surface directed towards the room [7]. The chief reason for this action of the additional plates is that they are of low flexural stiffness relative to their mass.

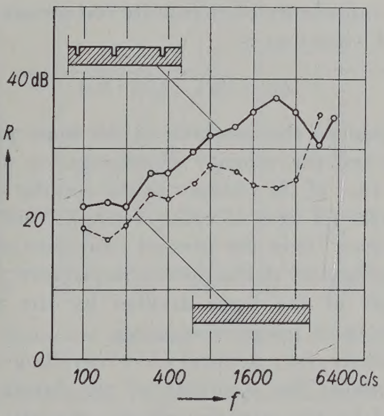

Fig. 10. Reduction factor of plywood panel without and with grooves.

In the case of inhomogeneous plates or building materials of unknown c_L, the critical frequency can be determined in the simplest way by a measurement of the sag η_m in the middle of a strip of the length l made of the material of the plate and supported at its ends. The appropriate formula reads:

$$f_c \approx 5200\sqrt{\eta_m}/l^2 \tag{18}$$

where η_m is measured in centimeters and l in metres. This formula says that a strip 2 m in length has to show a sag of about 10 cm if the critical frequency is to be above 4000 c/s. The abovementioned panels or wainscots can be made from such plates of low flexural stiffness since they are unloaded structural elements. One precaution only has to be observed, namely, long nails must not be driven into the wall at arbitrary spots. The application of pictures and other decorations, however, will remain unrestricted if two horizontal strips 20 cm in height are provided for long nails, one just below the ceiling, and the other at sight level. All other spots can be reached by inserting chains or wires. This demand is likely to be fulfilled by every architect, whereas the further recommendation to mark the nail-proof strips may not be generally adopted.

II. IMPEDANCES

1. Some simple formulae for impedances

A second factor of interest in all investigations of structure-borne sound is the mechanical impedance

$$\overline{Z} = \overline{F}/\overline{v} \tag{19}$$

of the respective structural element at the point of application of an alternating force $\overline{F}$. ($\overline{v}$ is velocity of particles. The bar denotes complex quantities.)

The impedance of an infinite rod set into longitudinal vibration is

$$Z_L = m c_L = \sqrt{m \cdot EA} \tag{20}$$

i.e. equal to the product of the mass per unit length and the velocity of propagation or equal to the root of the product of the specific stiffness and mass (A area of cross-section). This "input impedance" is in the present case identical with the mechanical characteristic impedance, i.e. the quotient of the force divided by the particle velocity in a progressive wave.

Similarly, for a flexural wave travelling in a rod or a plate, the quotient of the lateral force divided by the particle velocity is given by the product of the mass per unit length and the velocity of propagation:

$$Z_B = m c_B = \sqrt[4]{m^3 B \omega^2}. \tag{21}$$

Since for this type of wave, however, the velocity increases as the square root of the frequency, the impedance of a rod with respect to excitation of flexural waves by lateral forces is the higher the higher the frequency.

In a flexural wave the transport of energy is represented by the sum of the product of the force and the particle velocity and the product of the moment M and the angular velocity w, the latter being also in phase. It might be suggested that an impedance should be introduced differing by the square of a length, viz. the impedance with respect to moments, equal to the quotient of the moment divided by the angular velocity in a progressive wave. This impedance would read:

$$Z_{BM} = \overline{M}/\overline{w} = B/c_B = \sqrt[4]{m B^3/\omega^2}. \tag{22}$$

(A subscript M has been added to point to the moment. Correspondingly a subscript F should be added in equation (21) when confusion is possible.) This impedance of moments decreases with growing frequency. Thus a rod is the more resilient with respect to moments the higher the frequency.

The geometric mean of the two impedances yields a quantity which involves the structural data of the rod only:

$$\sqrt{Z_{BF} \cdot Z_{BM}} = \sqrt{Bm}. \tag{23}$$

It involves only the root of the product of stiffness and mass as in equation (20).

If a lateral force acts upon the free end of an infinite rod, the quotient of the force and the particle velocity is not equal to the expression of equation (21). The reason is that a quasi-stationary near-field is also excited. The latter adds to the resistive part (real part) of the input impedance a reactive part (imaginary part) which is equal in magnitude and in dependence on frequency. Moreover, a factor 1/2 turns out to be added. Thus we have

$$\overline{Z}_0 = \frac{m c_B}{2}(1 + \mathrm{i}). \tag{24}$$

If the point of excitation is in the middle of a rod (infinite in both directions) the impedance takes a value four times higher:

$$\overline{Z}_0 = 2 m c_B (1 + \mathrm{i}). \tag{25}$$

One of the most important and, at the same time, unexpected results of the theory of structure-borne sound is the fact that the mechanical impedance of a plate (infinite in all directions) excited at a single point is real and independent of frequency [8], [9], [10].

$$\overline{Z}_0 = 8 \sqrt{Bm}. \tag{26}$$

This formula, too, shows the root of the specific stiffness and mass, already considered in equation (23). Equation (26) can for a homogeneous plate of the thickness h be transformed into:

$$Z_0 = \frac{4}{\sqrt{3}} c_L \varrho h^2. \tag{26a}$$

Since the thicknesses of the plates in question lie between 0.5 mm and nearly 50 cm, i.e. vary by 10^3, the values of Z_0 vary by nearly 10^6 in spite of the small differences in the quantity c_L. Fig. 11 shows the values in question for iron and plywood, Fig. 12 those for concrete and bricks. The thickness h has been plotted as the abscissa. The diagram has been subdivided because the values for iron and wood lie in a different range to those for walls and ceilings. Z_0 has been plotted as the ordinate. The validity of the graphs is based on two assumptions. First the wavelength of the flexural wave has to exceed six times the value of the plate thickness; in other words, the upper frequency limits are the same as in the diagrams 3 to 6. Secondly, the point of excitation must be at a sufficient distance from any edge, and the attenuation during the propagation and at the edges has to be so considerable that any influence of reflected waves can be neglected. This assumption implies that any focal concentration of energy is avoided, in other words, that e.g. a circular plate is not excited at its centre.

2. Spectrum of impact sound

Knowledge of the mechanical impedance is important for several reasons. First, it is the basis of an estimation of the force acting upon the structural element, or of the particle velocity, caused by a transmitter of sound, the internal impedance of which can only be estimated roughly. Thicker structural elements, the mechanical impedance of which mostly exceeds the internal impedance of the transmitter, require an estimation of the force; thinner elements of lower impedance that of the particle velocity.

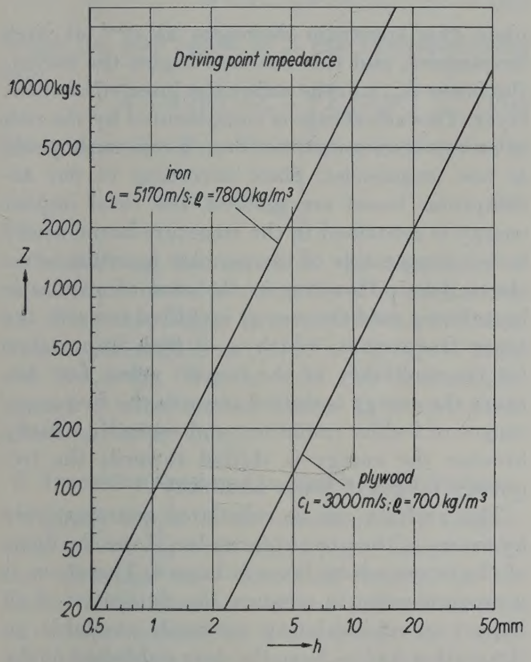

Fig. 11. Mechanical impedance of iron-plates and plywood-panels.

Secondly, the reaction due to the properties of a measuring instrument attached to a structural element can be judged. The reaction can only be neglected if the mechanical impedance of the instrument is small compared with that shown by the object under test at the point of attachment.

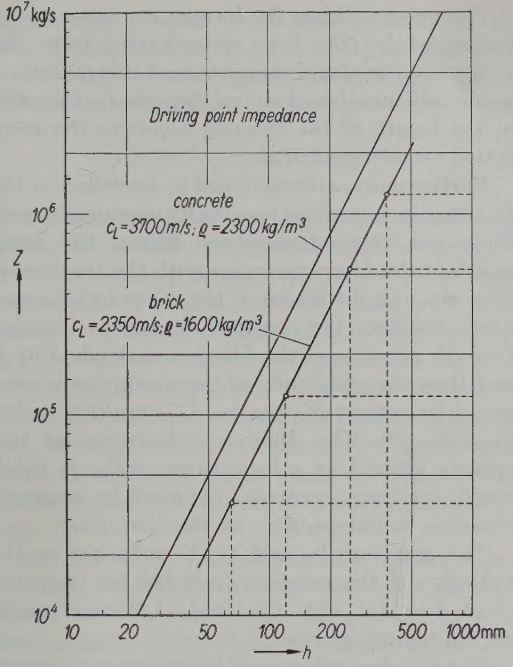

Fig. 12. Mechanical impedance of concrete and brick walls.

Moreover, the process caused by the impact of a mass m_0 striking the structural element at a velocity v_{00} can be calculated, especially its frequency spectrum, which is of chief interest. Since at any rate all values of Z in question increase with frequency to a lesser degree than does the mass impedance of the striking mass ($i\omega m_0$), this process can be dealt with as if the striking mass were already in contact with the structural element before the impact and experiences a very strong but very short pulse containing all frequencies in the same magnitude. The spectrum of the resulting velocity amplitude simply comprises the resulting impedance $i\omega m_0 + \overline{Z}_0$ in the denominator, the absolute value of the amplitude of a partial tone reading:

$$|\overline{a}_0| = \frac{m_0 v_{00}}{\pi |i\omega m_0 + \overline{Z}_0|}. \qquad (27)$$

At high frequencies this expression decreases as ω^{-1}. At low frequencies and in the case of constant Z_0, i.e. in a rod set into longitudinal vibration and a plate set into transverse vibration, we obtain a constant value, whereas in a rod set into transverse vibration we have a value increasing towards lower frequencies as $\omega^{-1/2}$. In the latter case the lower frequencies are relatively stronger and the impact sound is hollower. Similarly, and in accordance with experience, equation (27) shows that the decrease as ω^{-1} begins later the lighter the striking mass m_0 and the higher Z_0, i.e. the heavier and stiffer the structural element struck by m_0. This results in a clearer tone.

The noise striking the human ear is moreover influenced by the laws of radiation from the respective structural elements, and this radiation, as already mentioned above, depends on the ratio of the length of the flexural waves to the associated wavelengths in air.

Furthermore, attention has to be called to the fact that in measuring spectra by means of octave filters, or third-of-an-octave filters, the band width of the filters increases with the frequency. This means a distortion of the curve to be measured because the portion of energy passing through any one of the filters is multiplied by f, and thus the amplitude of the partial tone computed by means of equation (27) appears multiplied by $f^{1/2}$. The difference, however, of two spectra plotted on a logarithmic scale, in other words the "improvement" obtained by a certain measure, is independent of this distortion.

The same can be said of the influence on the radiation if the measure intended for improvement does not alter the field of flexural waves on the radiating area.

The simplest measure of improvement consists in the insertion of a resilient layer between the striking mass m_0 and the radiating structural member which be characterized by Z_0. Denoting the stiffness of this resilient layer by K_0 we obtain another expression for the resulting impedance acted upon by the impact $\overline{F}'_0$:

$$\begin{aligned}\overline{F}'_0/\overline{v}'_0 &= \mathrm{i}\omega m_0 + 1\Big/\left(\frac{\mathrm{i}\omega}{K_0}+\frac{1}{\overline{Z}_0}\right)\\ &= \mathrm{i}\omega m_0 + \frac{\overline{Z}_0}{1+\mathrm{i}\omega\overline{Z}_0/K_0}.\end{aligned} \tag{28}$$

This expression, however, cannot be substituted for the denominator of the spectrum, for it would characterize the spectrum of the particle velocity $\overline{v}'_0$ of the mass m_0. What we want is the particle velocity of the structural element $\overline{v}_0$, and this is related to $\overline{v}'_0$ inversely as the associated partial impedances:

$$\overline{v}_0/\overline{v}'_0 = \left[1\Big/\left(\frac{\mathrm{i}\omega}{K_0}+\frac{1}{\overline{Z}_0}\right)\right] : Z_0 = \frac{1}{1+\mathrm{i}\omega\overline{Z}_0/K_0}. \tag{29}$$

Hence the spectrum in which we are interested reads:

$$\begin{aligned}|\overline{a}_0| &= \frac{m_0 v_{00}}{\pi\,|[\mathrm{i}\omega m_0+\overline{Z}_0/(1+\mathrm{i}\omega\overline{Z}_0/K_0)](1+\mathrm{i}\omega\overline{Z}_0/K_0)|}\\ &= \frac{m_0 v_{00}}{\pi\,|\mathrm{i}\omega m_0+\overline{Z}_0(1-\omega^2 m_0/K_0)|}.\end{aligned} \tag{30}$$

Fig. 13 illustrates this expression for constant real values of Z_0, i.e. specially for a given plate. In contrast with the case of direct impact on the plate this spectrum decreases as ω^{-2} at high frequencies, and this decrease begins the earlier, the lower K_0, i.e. the softer the inserted resilient layer. This advantage is compensated by the risk of an increase, sometimes even a resonance peak, at low frequencies. Since according to our assumptions losses are ignored, the total impact energy is contained in the structure-borne sound waves irrespective of the possible insertion of an elastic layer. However in the case of an elastic layer being used the energy is shifted towards the lower frequencies, which is of high importance for the audibility of the impact noise, first because the energy is shifted towards the frequency ranges of feebler radiation, and secondly, chiefly because the energy is shifted towards the frequency ranges of lower audibility[2].

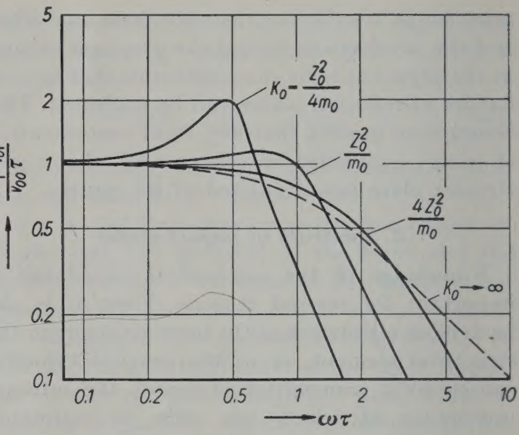

Fig. 13. Structure-borne sound spectrum of an impact on a plate with resilient layers of stiffness K_0 (m_0 striking mass, v_{00} its velocity, Z_0 impedance of the plate and $\tau = m_0/Z_0$).

This shifting can be calculated quantitatively by means of the present formulae, if the elasticity of the intermediate layer is known. Therefore, it is recommended to measure the elasticities of all impact sound-insulating materials available on the market and to have the data published in the prospectuses.

Moreover, there is a certain elasticity in every plate of wood, concrete, or even iron, so that the idealized spectrum given by equation (27) cannot be attained in practice.

III. REDUCTION FACTORS

1. Pure longitudinal transition

The knowledge of the mechanical impedances finally permits us in many cases to estimate the transition of sound from one structural element to another. The transition of longitudinal waves is governed by the simple "matching" formula:

---

[2] A more important measure of improvement is offered by the "floating floor" [11].

$$\overline{r} = \frac{\overline{Z}_1 - \overline{Z}_2}{\overline{Z}_1 + \overline{Z}_2} \qquad (31)$$

where $\overline{r}$ is the generally complex reflection factor, i.e. the quotient of the particle velocity of the reflected wave and that of the incoming wave, $\overline{Z}_1$ the characteristic impedance with respect to longitudinal waves in the first medium, e.g. a rod, and $\overline{Z}_2$ the input impedance of the second medium subsequent to the rod. From $\overline{r}$ we obtain the ratio of the energy which is not reflected but transmitted to the second medium divided by the incident energy; in other words the so-called transmission coefficient:

$$d = 1 - |\overline{r}|^2 \qquad (32)$$

which for real values of Z can be transformed into

$$d = 4/(\sqrt{Z_1/Z_2} + \sqrt{Z_2/Z_1})^2. \qquad (32a)$$

From d we finally obtain the reduction factor

$$R = 10 \log \frac{1}{d}. \qquad (33)$$

Considering, for instance, the transition of sound from one rod into another of equal material but five times bigger in cross-section, we obtain from equation (31) to (33): $\overline{r} = -4/6$; $d = 20/36$ and $R \approx 3$ dB. We see that this considerable change in cross-section results in a very small insulation effect only.

2. Transition from rod to plate (sound-bridges)

Equally simple is the transition of a longitudinal wave from a rod into a plate normal to the rod, although the vibrational motion in the second medium consists of a cylindrical flexural wave superimposed on a quasi-stationary near-field, since the process is governed by Z_2 only, which according to equation (26) has a real value. The most important property of the present example is the fact that here, too, total transmission of energy is possible in spite of the differences between the structural elements and types of waves occurring. This total transmission occurs in the case of perfect matching of the mechanical impedances:

$$Z_1 = Z_2 \qquad (34)$$

which in the present case means

$$m_1 c_{L_1} = \frac{4}{\sqrt{3}} \varrho_2 c_{L_2} h_2^2. \qquad (34a)$$

In the case of equal media this condition is fulfilled if the cross-sectional area A_1 of the rod is made equal to the square of a length about 1.5 times the thickness of the plate

$$A_1 = \frac{4}{\sqrt{3}} h_2^2 \approx (1.5\, h_2)^2. \qquad (35)$$

This dimension is not only easy to design but even within the order of magnitude usual in all structures involving pillars for support of plates and rods between plates. Already from the first example we have seen that mismatching even up to 1:5 does not result in much insulation. Thus it is to be expected that the usual combinations of pillars and ceilings in buildings (and in vehicles) lead to considerable transmissions of sound and noise. It is, therefore, necessary to choose very extreme mismatch in order to secure high insulation.

This statement is of importance for the studs between double partitions, which are already known as "sound bridges" on account of this disadvantage. These bridges should be so designed that the characteristic impedance of the stud is much smaller than that of the plate or, on the contrary, is much higher. In the first case, the second plate acts as a rigid terminal for the stud, and such a stud usually acts like a spring when it is short compared to the longitudinal wavelength. In the second case, the stud is not hindered by the second plate from vibrating, and thus it acts by its inertia. In both cases, calculations show that the sound insulation is better, the longer the stud, and since all linear extensions in a sound field have to be referred to the wavelengths in question—in the present case longitudinal wavelengths—the insulation grows with the frequency.

States of mismatch can be arrived at from two directions. Which of them is more suitable depends on the properties of the plates connected by the stud. Between thick walls it would, of course, be useless to design connecting studs of high mechanical impedance. Such connecting studs should be as thin and resilient as permitted by their static destination. Even unusual designs are worth considering; this is confirmed by ASTON's experiments with his so-called "butterfly-shape ties", i.e. wires bent into bows for higher resiliency [12].

In order to connect thin plates, e.g. double shells of vehicles, it is mostly easier to choose the impedance of the stud to be high in comparison with that of the plates, in other words, to connect the plates by heavy structural elements. This rule seems to be still relatively unknown. Based on experience of statics, of thermal conduction, ro of electric current, it has often been concluded that the thicker element would result in more transmission of sound, but this, however, is erroneous. Already in 1937 E. Meyer [13] had shown by experimental tests that the insulation of a double partition made of plywood is lower with connecting wooden studs than with iron connecting elements and gave a qualitative explanation derived from the better matching between the wooden studs and the plywood plates[3].

3. Corners and other junctions

Equation (31) also permits us to estimate the transmission of sound energy entering a rod in the form of longitudinal waves and transmitted to another rod perpendicular to it. The second rod may be connected to the first rod either by a swivel link or by a rigid T-joint. The quantity Z_2 has to be taken from equations (24) or (25), respectively. In the first case, with rods of equal properties, we obtain

$$\overline{r} = \frac{2c_L - c_B(1+\mathrm{i})}{2c_L + c_B(1+\mathrm{i})} = \frac{2-\beta(1+\mathrm{i})}{2+\beta(1+\mathrm{i})} \tag{36}$$

where β denotes the ratio of the velocities of flexural waves and of longitudinal waves. This ratio increases as the root of the frequency. The new parameter reads

$$\beta = c_B/c_L = \sqrt{1.8\,hf/c_L}. \tag{37}$$

Generally this quantity is small and according to equation (11) limiting the representation of pure flexural waves, it is bounded by the inequality

$$\beta < 0.3. \tag{38}$$

Thus we have a mismatch in any case since the input impedance of the second rod set into flexural vibrations is always low compared with the longitudinal characteristic impedance of the first rod. With increasing frequency the matching conditions are improved owing to the input impedance growing as the root of the frequency. Equation (36) yields a quantitative expression of the transmission coefficient:

$$d_{LB} = 1 - |\overline{r}|^2 = \frac{2\beta}{1+\beta+\beta^2/2}. \tag{39}$$

The double subscript LB is to indicate that the waves arrive as longitudinal ones and depart as flexural waves.

According to the reciprocity theorem this relation also holds for the energy transmission from a flexural wave arriving in the first rod to a longitudinal wave departing in the second rod:

$$d_{LB} = d_{BL}. \tag{40}$$

The frequency response of d_{LB} described by equation (39) is illustrated by a full line in Fig. 14.

The figure also shows (by a broken line) the transmission coefficient d_{LB} calculated for two rods or plates connected by a rigid joint. This is the case occurring most usually in practice. Unfortunately its calculation is more difficult than that of a swivel joint. The six boundary conditions, viz. the continuity of the two particle velocities perpendicular to each other, of the angular velocities, of the two forces perpendicular to one another and of the moments, are so intricate that the input impedance Z_2 is also dependent on the data of the first medium and leads to a very complicated expression. Nevertheless a rough estimate of the question of matching between the longitudinal characteristic impedance of the first rod—Z_{L1}—and the impedance with respect to flexural waves of the second rod—Z_{BF2}—already yields a true picture of the frequency response, viz. the transmission described by d_{LB} decreases with decreasing frequency.

In the figure β^2 has been chosen as the abscissa. The respective frequencies depend not only on β but also on the material and its thickness. For a corner formed by two walls of concrete 10 cm thick we have

$$f = \frac{c_L}{1.8h}\beta^2 \approx 20\,000\,\beta^2 \text{ c/s}.$$

In other words, the highest value permissible in this calculation, i.e. $\beta^2 = 0.1$, is associated with a frequency of about 2000 c/s. For two plates of sheet iron 1 mm thick we obtain

$$f = 512\,000\,\beta^2/0.18 \text{ c/s}.$$

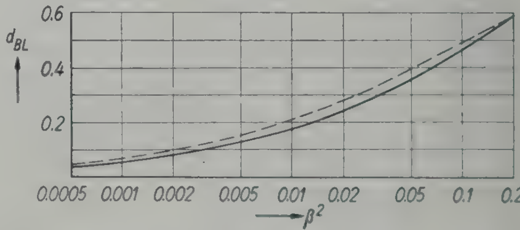

Fig. 14. Transmission coefficient versus frequency (parameter $\beta^2 = 1.8\,hf/c_L$) for a longitudinal wave in a rod to a flexural wave in another rod perpendicular to the first one.

solid line: rods connected by a swivel link,
dotted line: rods connected by a rigid joint.

---

[3] A complete theory of "sound bridges" should also take into account that not only forces but also moments can be transmitted by the connecting elements. It would be much more complicated to deal with this problem exactly. The contribution of the moments, however, seems to be in general of less importance.

In this example the upper frequency limit of the present calculation lies in the ultrasonic range at 290 kc/s.

The other limit of the calculated frequency response is given by $\beta^2 = 0.0005$. In the first example it corresponds to 10 c/s, in the second to 1450 c/s. Below this frequency the transition of longitudinal waves into flexural waves, and vice versa, can in general be neglected, or expressed in terms of a boundary condition: each of the rods hinders the other from a transverse motion.

In the case of two plates joined at a right angle and rigidly connected with respect to flexural vibrations an energy transmission by way of the product of moment and angular velocity remains possible. Thus a flexural wave arriving in the first plate can be partially transmitted into the second plate. Moreover, it is not surprising that the formula for d_{BB} involves the ratio of the impedances with respect to the moments as defined by equation (22):

$$d_{BB} = \frac{2}{\left(\sqrt{\frac{B_1}{c_{B1}}\Big/\frac{B_2}{c_{B2}}} + \sqrt{\frac{B_2}{c_{B2}}\Big/\frac{B_1}{c_{B1}}}\right)^2} \qquad (41)$$

describing the condition of matching which evidently is important in the present problem. Similarly it is clear that even in the case of perfect matching:

$$B_1/c_{B1} = B_2/c_{B2} \qquad (42)$$

i.e. for instance with structural elements of equal dimensions and the same material, there is not total transmission but we have

$$d_{BB} = 0.5 \qquad (43)$$

since a transmission of energy by way of the product of force and particle velocity is totally hindered by the corner. It is worth mentioning that in the case of equal structural elements the insulating effect of a corner is only 3 dB. In this case, too, the insulation is not much augmented by those degrees of mismatch which may usually occur. If, for example, the second structural element is of double thickness and the same material, the ratio of impedances with respect to the moments is augmented by $2^{5/2} = 5.7:1$ but the insulation only rises to a value still somewhat below 6 dB.

Similarly worth keeping in mind are the numerical values describing the transition of energy at a T-joint of equal structural elements. The reflected portion is 5/9 instead of 5/10 as above, and the transmitted portions are 2/9 each. Finally in a joint of four equal structural elements in the form of a cross, the energy of a flexural wave arriving in one element is so distributed that 5/8 are reflected and 1/8 is transmitted in each of the three other elements.

Quantitative confirmations of the present theoretical results are still lacking. We are, however, able to state that qualitatively the processes are in accordance with the general experience of propagation of sound in buildings constructed of one material only (e.g. reinforced concrete). No sufficient insulating effect can be expected from the changes in cross-section and direction which are mostly given in buildings.

4. Elastic layers

An essential improvement in sound insulation[4] can only be obtained by the insertion of special structural elements. The insertion of elastic layers has proved useful in practice. For longitudinal waves the effect is in perfect analogy with the insertion of heavy masses between two rooms for the insulation of air-borne sound. Formula (44) represents the reduction factor valid for the present example:

$$R = 20 \log \frac{\omega\, h_2\, z_1}{2\, E_2} = 20 \log \frac{\pi\, h_2\, E_1}{\lambda_{L1}\, E_2} \qquad (44)$$

where z_1 is the characteristic impedance and E_1 Young's modulus of the interrupted structural element (pillar or wall), E_2 Young's modulus and h_2 the thickness of the elastic layer, and λ_{L1} the length of longitudinal waves in the medium 1. This formula is quite similar to the well-known formula of the insulation of air-borne sound by a wall of the density ϱ_2:

$$R = 20 \log \frac{\omega\, h_2 \varrho_2}{2 z_1} = 20 \log \frac{\pi\, h_2 \varrho_2}{\lambda_1 \varrho_1}. \qquad (45)$$

One formula shows the influence of the stiffnesses, the other that of the densities. In both cases the effect is increased by the thickness of the layer for any given material, and as the thickness has to be referred to the wavelength, it grows with the frequency, too.

If, as an example, we consider a cork layer 3 cm thick, for which we may assume a modulus

$$E_2 = 3 \cdot 10^7\ \mathrm{N/m^2}\ (= 3 \cdot 10^8\ \mathrm{dyne/cm^2})$$

and if this layer is inserted in a pillar or wall of concrete, the above approximate formula yields an insulation of 7 dB at 100 c/s and 27 dB at 1000 c/s. The assumptions of equation (44), viz. that both parts of the structural element interrupted by the elastic layer extend over several wavelengths, are not always fulfilled. Nevertheless the relatively simple equation (44) is useful in permitting us to estimate whether a noticeable insulating effect is to be expected at all.

---

[4] Recently the term "isolation" has been proposed for solid-borne sound, whereas "insulation" is kept for air-borne sound.

The insulating effect with respect to flexural waves of an elastic layer is also characterized by the fact that the reduction factor does not reach higher values except at higher frequencies, as is illustrated by the example of Fig. 15. The increase is even steeper and the difference between the behaviour of flexural waves as compared with longitudinal waves is, moreover, characterized by a frequency of total transmission occurring in the range of low, but still audible, frequencies.

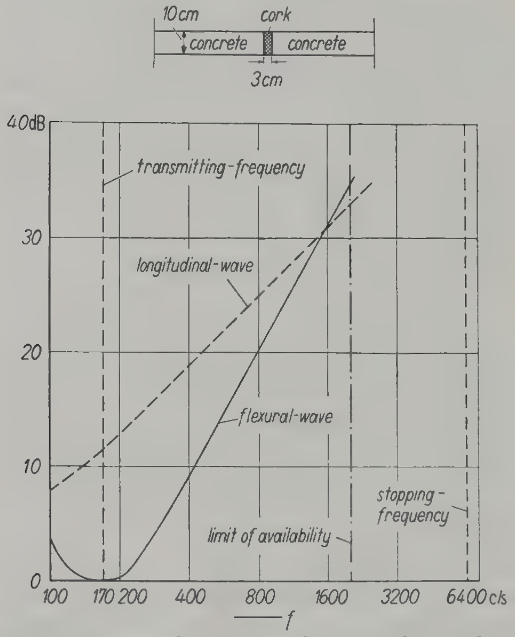

Fig. 15. Reduction factor versus frequency for an elastic layer of cork between two concrete walls forming a straight line.

This is astonishing since the intermediate layer, at any rate, causes a disturbance of the sound field, so that an alteration of the field pattern is to be expected. This is the case, indeed. It is, however, a special feature of the flexural waves that such a disturbance consists not only of reflected waves but also of a quasi-stationary near-field which after being generated does not need any further supply of energy. In exceptional cases the disturbance in front of the obstructing layer consists exclusively of such a near-field. This means that no energy is reflected, and thus the total incident energy is transmitted[5].

In the present example the associated frequency of total transmission can be calculated approximately from

$$\lambda_{B0} = \pi \sqrt[3]{H^2 h\, E_1 / E_2}. \tag{46}$$

The frequency of total transmission is therefore given by:

$$f_0 = \frac{1.8\, c_L}{\pi^2} \sqrt[3]{\frac{E_2^2}{E_1^2 H h^2}} = 0.18 \sqrt[3]{\frac{E_2^2}{E_1^{1/2} \varrho_1^{3/2} H h^2}}. \tag{47}$$

This frequency is lower, the lower the modulus and the thicker the layer. It is also dependent on the data of the interrupted structural element.

It is desirable to try to place this frequency at a sufficiently low value, not only to avoid the "effect of total transmission" but also so that the slope of the frequency response, which also is a function of the ratio f/f_0 will begin earlier. The response, as illustrated by Fig. 15, can be described by the function:

$$R = 10 \log \{1 + [1 - (f/f_0)^{3/2}]^2\} \tag{48}$$

which even one octave above the frequency of total transmission can already be given approximately by

$$R = 30 \log (f/f_0). \tag{48a}$$

With flexural waves it is also possible that the field behind the obstructing layer consists of a quasi-stationary near-field only. In this case the obstructing layer is vibrating but does not cause any flexural waves in the following medium, i.e. it completely hinders the transmission of flexural waves. Thus, from the point of view of sound insulation, the "effect of total insulation" is as welcome as its counterpart, the effect of total transmission, is undesirable.

The interruption of a pillar or wall by an intermediate layer also results in a similar effect of total insulation, but this lies in a frequency range which is beyond the limits of validity of our calculation. Nevertheless the approach to this effect is already observable in the considerable slope of the reduction factor vs. frequency curve according to equation (48a).

The effect of total insulation as a particular feature of the flexural waves can also occur in the frequency range in question even at low frequencies. This is shown by the calculation of the equally important problem of an elastic intermediate layer at a corner, e.g. between a ceiling and its supporting walls. This example, dealt with and illustrated by Fig. 17, clearly shows the physical conditions necessary for the occurrence of total insulation. Fig. 16 has been drawn to explain this example. The deflections, shown in the figure at intervals of a quarter-period, represent a pure near-field and obey the law:

---

[5] Recently this has been verified experimentally by M.-L. Exner and W. Böhme [16].

$$\eta = \eta_{00}\, \mathrm{e}^{-2\pi x/\lambda_B} \sin \omega t. \tag{49}$$

This field is caused when the bending moment acting at $x = 0$,

$$M_0 = -B \left[\frac{\partial^2 \eta}{\partial x^2}\right]_{x=0} = -B \left(\frac{2\pi}{\lambda_B}\right)^2 \sin \omega t \tag{49a}$$

and the alternating force acting at the same point,

$$F_0 = -\left[\frac{\partial M}{\partial x}\right]_{x=0} = -B \left(\frac{2\pi}{\lambda_B}\right)^3 \sin \omega t \tag{49b}$$

are in phase (with respect to the signs chosen here) and satisfy the proportion

$$M_0 : F_0 = \lambda_B : 2\pi. \tag{50}$$

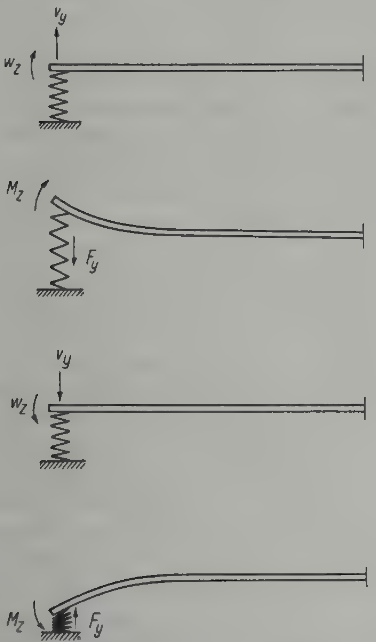

Fig. 16. Quasi-steady motion of a rod driven by a bending moment and connected with an elastic layer at the end.

In general it is difficult to predict the frequency at which these relations are fulfilled. At a corner with an elastic layer the relations are exceptionally clear since the only quantity given by the incident flexural wave is the moment whereas the force is generated by the deformation of the elastic layer only. Now we have:

$$F_0 = -K \eta_0 \tag{51}$$

where K is the stiffness of the layer. The force resulting from equations (51) and (49) is of equal phase to that described by equation (49b) which is required in the case where only a near-field and no propagated wave is caused. Both expressions are in perfect agreement, i.e. only a near-field is caused, when we have:

$$K = B \left(\frac{2\pi}{\lambda_B}\right)^3 \tag{52}$$

in other words at the frequency of total insulation described by

$$f = \frac{1}{2\pi} \left(\frac{K}{B}\right)^{2/3} m^{-1/2}. \tag{52a}$$

In the arrangement illustrated by Fig. 17 two values of K come into question. If the energy is transmitted from the x-direction into the y-direction, the rigidity

$$K_1 \approx \frac{G_2 H}{h} \approx \frac{E_2 H}{3h} \tag{53a}$$

hinders the vibration of the second structural element; for a wave arriving from the y-direction the stiffness with respect to pressure

$$K_2 \approx E_2 H / h \tag{53b}$$

has to be substituted. By virtue of the reciprocity theorem the insulating effect is the same in either direction. For this reason we obtain two frequencies of total insulation, viz.

$$f_1 = 0.115\, c_L \sqrt[3]{\left(\frac{E_2}{E_1}\right)^2 \frac{1}{H h^2}} \tag{54a}$$

according to equation (53a) and

$$f_2 = 0.24\, c_L \sqrt[3]{\left(\frac{E_2}{E_1}\right)^2 \frac{1}{H h^2}} \tag{54b}$$

according to equation (53b). The example illustrated by Fig. 17 is based on the same data as Fig. 15, viz. a 3 cm cork layer between concrete plates 10 cm thick. A comparison of the formula (54) with the formally similar expression in equation (47) shows that the two frequencies of total insulation lie somewhat below and somewhat above the frequency of total transmission shown in Fig. 15. Hence both frequencies lie in the lower frequency range.

With a perfect total insulation R ought to tend towards infinity at the above frequencies. The height of the insulation peaks, however, is restricted by the generation of secondary longitudinal waves and by the internal losses in the cork layer.

Assuming that in cork 10 % of the deformation energy is irreversibly dissipated, we may expect insulation values of 50 dB.

In the range of high frequencies the insulation is also satisfactory since here the slope of the insulating effect of an elastic layer with growing frequency is favourable. The frequency response of the reduction factor tends to the values given by the approximate formula:

$$R = 20 \log \left(\frac{\pi h}{\lambda_{B1}} \frac{E_1}{E_2} \right). \qquad (55)$$

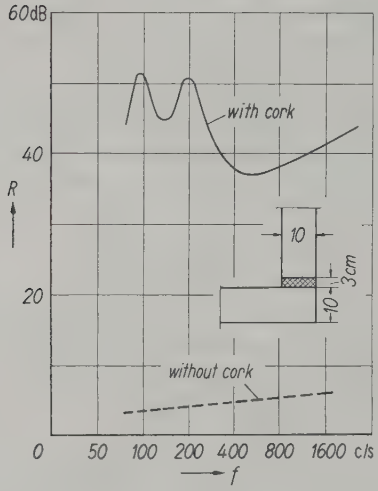

Fig. 17. Reduction factor versus frequency for a corner formed by concrete walls.
full line: with
dotted line: without
an elastic layer of cork.

This expression is similar to that given in equation (44) for the insulation of longitudinal waves by an elastic layer, only differing in that equation (44) involved the wavelength of longitudinal waves, which is inversely proportional to the frequency. In the present example we have the wavelength of the flexural wave which is inversely proportional to the root of the frequency, and this results in a smaller increase of R with frequency according to

$$R = 10 \log f + 10 \log \left(5.5\, h^2 H^{-1} E_1^{3/2} \varrho_1^{1/2} E_2^{-2}\right). \qquad (55a)$$

In the example of Fig. 17 the second term of this sum proves to be so large that in the interesting range the associated straight line always runs above 36 dB.

For the present problem of flexural waves a simple solution has been found that is similar to the corresponding problem of longitudinal waves. The reason is that at high frequencies the transmission due to the product of force and particle velocity is no longer effective since the impedance due to the compliance of the elastic layer decreases with ω^{-1} and is finally so small in comparison with the increasing impedance Z_{BF1} that the plates can be regarded as being free with respect to transverse vibrations. The difference between the impedance with respect to the moments of the flexural wave Z_{BM1} which decreases with $\omega^{-1/2}$ and the corresponding impedance of an elastic layer of the thickness h is not so high. For a plate of the thickness H the former impedance is

$$B_1/c_{B1} \approx E_1 H^3/12\, c_{B1}$$

and the absolute value of the latter is

$$|\overline{M}_1/(\overline{w}_1 - \overline{w}_2)| = E_2 H^3/12\, h \omega.$$

Moreover, it is obvious that the reduction factor depends on the ratio of these two quantities just as in equation (44) it depends on the ratio of the longitudinal characteristic impedance $z_1 A$ and the longitudinal impedance $A E_2/\omega h_2$ due to the compliance. The fact that we have only to substitute one of these ratios for the other without any alteration of the numerical factor is rather difficult to derive but easy to keep in mind.

In the above calculations the elastic layer has been dealt with as pure compliance. This involves the assumption that the thickness of the layer is always small compared with the lengths of longitudinal waves in the material in question. The velocity of longitudinal waves in cork is about the same as in air. Hence a 3 cm layer can be regarded as small compared with the wavelengths of the frequencies of interest in architectural acoustics. This condition is not fulfilled with sponge rubber, in which the appropriate velocity can be reduced to 60 m/s. Moreover, it is usual to apply thicker layers of this material. Hence it is possible that already at medium frequencies such a layer must be dealt with as a continuous medium. The thickness of a 5 cm layer of a material of this low velocity would at 600 c/s equal half a wavelength and permit total transmission if the damping could be ignored. But owing to internal damping, we need not be afraid of total transmission. Nevertheless the fact that the insulation can be considerably lower than would result from the relations and formulae given above has to be considered.

The usefulness of applying intermediate layers of cork between ceilings and supporting walls has been well recognized for a long time, but only in a qualitative sense. Their quantitative calculation would be an advance in the art of building. The present formulae are intended to aid in solving this problem. Moreover the effect of total insulation derived in this paper could be used in principle.

Considering the effect of mismatch of the impedance of the intermediate layer and that of the interrupted medium, we tend to insert layers of high acoustical “softness”. In other words, the insertion of layers of little stiffness and big thickness between solid bodies promises a successful insulation. Where no static forces have to be transmitted an intermediate layer of air is the best material. Nevertheless such a layer has a certain stiffness which is often undervalued. At high frequencies the air particles cannot give way by moving sideways.

For this reason the dynamical stiffness of the elastic layer below a “floating” floor is nearly equal to that of the air volume if this is filled by a very yielding and porous material such as glass wool [4], [11], [14].

5. Impeding masses

On the other hand it is in principle also possible, just as in the corresponding problem of airborne sound, to obtain a certain insulation by the insertion of materials of higher acoustic impedance. These materials act as inert masses, and their effect can be calculated for longitudinal waves from equation (45) taken from the corresponding problem in air, or more exactly from the original equation:

$$R = 10 \log \left[1 + \left(\frac{\omega\, h_2 \varrho_2}{2 z_1} \right)^2 \right]. \qquad (56)$$

From this formula we can deduce that for example an iron plate 3 cm thick inserted in a vertical wall of concrete would even at 10 000 c/s result in a reduction factor of 3 dB only. This small effect shows that acoustically there is so little difference between iron and concrete that it is permissible to deal with reinforced concrete as a homogeneous medium.

The insulating effect of the inserted mass can be augmented by giving it a larger cross-section than that of the interrupted structural element. In house building this measure would require very heavy and bulky structures for obtaining useful insulating effects, whereas in steel structures, e.g. in ships, this possibility may be taken into account.

In shipbuilding any insertion of elastic layers seems to be almost impossible for fear of leakage.

Experience has shown that ribs provided to give stiffness to the hull and acting as heavy masses from the view point of structural acoustics result in a high sound-insulating effect. This could hardly be expected from equation (56). Here, too, the “effect of total insulation” of the flexural waves causes the high reduction factors with respect to these waves. It was this problem which led to the theoretical discovery of this effect, confirmed by experiments.

In this problem the frequencies of total insulation can be estimated approximately by means of the very simple rule that the wavelength of the blocked flexural wave is equal to the circumference of a circle whose radius equals the radius of gyration of the additional heavy mass:

$$\lambda_B = 2\pi r. \qquad (57)$$

This simple formula is more difficult to derive than equations (54). Nevertheless it is clear that equation (50), being the relation between the moment and the force, involves the ratio of the impedance of the hindering object with respect to moments ($\omega m_0 r^2$) divided by the translatory inertia ωm_0 and this ratio is equal to the square of the radius of gyration r (m_0 denoting the additional mass provided at a rod or, in the case of a plate, that of a transverse rib expressed by its mass per unit width). At any rate this consideration shows that the additional mass must be compelled to follow the rotational vibrations of the plate or rod as a rigid body. Therefore the radius of gyration cannot be obtained by designing a lumped mass maintained at a certain distance by spokes. An absolutely rigid design is required. The theory as well as tests have shown that the length of the connection between the additional mass and the extended structural element (in the direction of propagation) has to be small compared with the wavelength.

A design combining high stiffness with a large radius of gyration and a small connecting length is that of a wedge fixed at its edge to the structural element in which the flexural waves are propagated. Its radius of gyration is 0.7 of the “height” of the wedge. Its height depends on the material, the thickness of the carrying structural element, and the desired frequency of total insulation. For plates of the thickness h equation (57) yields:

$$r = \frac{1}{2\pi} \sqrt{1.8\, c_L\, h / f} \qquad (58)$$

In the special case of iron we have

$$r \approx 150 \sqrt{\frac{h[\mathrm{cm}]}{f[\mathrm{c/s}]}}\ [\mathrm{cm}]. \qquad (58a)$$

As an example a sheet iron 0.5 cm thick and a frequency $f = 200$ c/s lead to a radius $r = 7.5$ cm, and a “height” of the wedge of 11 cm. These dimensions are easily applicable in practice. The choice of 200 c/s as the frequency of total insulation involves a useful insulation over the whole frequency range in question, the frequency of total transmission which occurs in this example, too, is mostly two octaves lower so that one

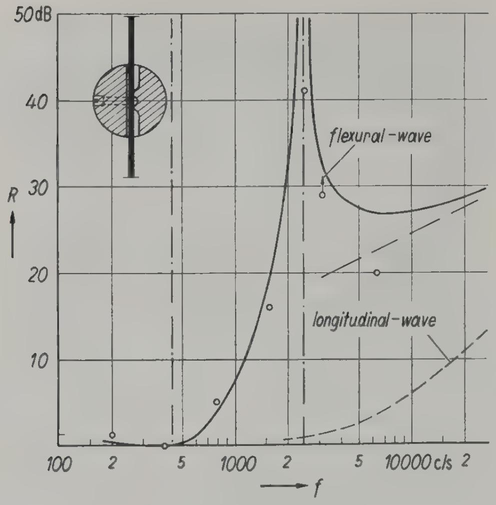

Fig. 18. Reduction factor versus frequency for an impeding mass.
circles: measurements } for flexural wave,
full line: calculation }
dotted line: calculation for longitudinal wave.

octave lower the insulation may be expected to be still fairly good.

At frequencies above that of total insulation the insulation value decreases but soon turns to a new increase in an asymptotic approach to the approximate response we are going to derive. Also in this example the range of higher frequencies is governed by a formula similar to equation (45) obtained when considering the attenuation of longitudinal waves by a heavy mass, viz.:

$$R = 20 \log \left(\frac{\pi m_0}{\lambda_B m} \right) \tag{59}$$

where m refers to the mass of the structural element carrying the flexural waves, i.e. in the case of a rod m denotes the mass per unit length, and in the case of a plate the mass per unit area. Similarly, as in equation (55), the transmission of energy only depends on one of the products. In the present case the product of the moment and the angular velocity is ineffective, since the impedance with respect to rotation of the additional mass due to its inertia grows as the frequency ω whereas the impedance with respect to moments of the flexural wave Z_{BM} decreases with $\omega^{-1/2}$; in other words the last mentioned impedance is so small in comparison with the first mentioned that any angular velocity vanishes. Instead of this equation (59), there is involved the ratio of the impedance according to translatory inertia ωm_0 divided by the impedance with respect to forces of the flexural waves $Z_{BF} = m c_B$. With c_B growing as the root of the frequency, R also in this example increases with $10 \log f$:

$$R = 10 \log f + 10 \log \left(1.6\, m_0^2\, m^{-3/2}\, B^{-1/2}\right). \tag{59a}$$

In Fig. 18 the full line shows the frequency response of the reduction factor due to an additional mass. The typical features can be clearly seen: a frequency of total transmission in the range of low frequencies, a peak at the frequency of total insulation, and finally the transition to an asymptotic slope. The curve refers to the structure indicated by the sectional drawing, an additional mass of 115 g attached to a flat steel rod 2.7 mm × 2 cm in cross-section. The reduction factor of this arrangement could be determined experimentally. The measured values have been plotted and prove that the effect of total insulation can be practically brought about and its frequency chosen by a prior calculation.

6. Problems of oblique incidences

All formulae discussed as yet have concerned either rods or plates at normal incidence of the waves on the interface. Since in practice also oblique incidence is of importance, its most important cases have to be dealt with. The process of oblique incidence is governed by a general rule known from the physics of optical refraction. This rule deals with the transition from a medium 1 with a velocity of propagation c_1 into a medium 2 with a velocity c_2 and says that the angles of incident and outgoing direction are related by

$$\frac{c_1}{\sin \vartheta_1} = \frac{c_2}{\sin \vartheta_2}. \tag{60}$$

This may be interpreted as the equality of the "trace velocities". If the velocity in the second medium exceeds that in the first, $c_2 > c_1$, the angle ϑ_2 reaches 90° at an angle of incidence

$$\vartheta_1 = \arcsin \left(\frac{c_1}{c_2} \right) \tag{61}$$

and at higher values of ϑ_1 no waves pass into the second medium. As an example we consider two plates of sheet iron, one being of double thickness compared with the other. The velocities of flexural waves are as $\sqrt{2}:1$. At an angle of incidence exceeding 45° no flexural wave enters the second sheet iron.

But also in the case of equal thickness of the two sheet iron plates, i.e. in the case of matching, the transmission coefficient depends on the angle of incidence. It decreases with oblique incidence according to

$$d = \frac{1}{2} \cos^2 \vartheta. \tag{62}$$

A discussion of further examples which mostly involve very complicated problems will be renounced, since this essay is meant to show that many fundamental problems of structure-borne sound can be judged and estimated by means of simple considerations and formulae.

Acknowledgement

This article is adapted from a Report—Sponsored Research (Germany) No. 1, Series B—entitled "The propagation of structure-borne sound",[5] which was carried out under arrangements with the Department of Scientific and Industrial Research, London, whose assistance and interest are gratefully acknowledged. It is published with the permission of the Department.

(Received 10th December, 1952.)

---

[5] There the reader may find the derivations of the formulae mentioned and the discussion of further details and problems. This report is obtainable on loan from the Building Research Station, Garston, Herts, England.

References

[1] Schmidt, R., Ing. Arch. **5** [1934], 352.
[2] Lübcke, E., Schallabwehr im Hochbau. Springer-Verlag, Berlin 1940.
[3] Cremer, L., Wellentheoretische Raumakustik, § 62. S. Hirzel Verlag, Leipzig 1950.
[4] Cremer, L., Tekn. Tidskr. **80** [1950], 393.
[5] Eisenberg, A. und Cremer, L., Baupl. u. Bautechn. **2** [1948], 235.
[6] Brillouin, J., Acustica **2** [1952], 65.
[7] Gösele, K., Bauzeitung **2** [1949], 632.
[8] Zener, C., Phys. Rev. **59** [1942], 669.
[9] Sneddon, J. N., Proc. Camb. phil. Soc. **41** [1945], 27.
[10] Cremer, H. und Cremer, L., Frequenz **2** [1948], 61.
[11] Cremer, L., Acustica **2** [1952], 167.
[12] Aston, G. H., Report of the 1948 Summer Symposium of the Acoustics Group of the Physical Society London, p. 13, Fig. 7.
[13] Meyer, E., Akust. Z. **2** [1937], 74.
[14] Gösele, K., Bauzeitung **4** [1951], 264.
[15] Gösele, K., Acustica **3** [1953], 243.
[16] Exner, M.-L. and Böhme, W., Acustica **3** [1953], Beiheft 1, 105.

ÜBER DEN GEHÖRSINN VON STECHMÜCKEN

Von H. TISCHNER

Physikalisches Institut der Universität Tübingen

Zusammenfassung

Messungen des Schallpotentials an männlichen Tieren einer Stechmückenart, Anopheles subpictus, ergaben, daß die Tiere in einem schmalen Frequenzbereich von 150…550 Hz hören. Die größte Empfindlichkeit wird bei 380 Hz erreicht. Sie entspricht der Empfindlichkeit des menschlichen Ohres bei 2 kHz. Der Hörumfang vom Schwellwert bis zur Sättigung beträgt 28 Phon. Die beobachtete Bandpaßwirkung ist auf die Abstimmung der Geißeln zurückzuführen. Das Fluggeräusch der Weibchen enthält einen subjektiv deutlich wahrnehmbaren Anteil von 380 Hz, so daß dieser Ton aus dem Geräusch der Umgebung herausgehoben wird. Das eigene Fluggeräusch wird, da es höher liegt, von den Geißeln des Männchens nur wenig erfaßt. Die beobachtete frequenzverdoppelnde Wirkung des Johnston-Organs geht aus seinem Aufbau hervor. Die Grundfrequenz der auf die Stifte wirkenden Spangenbewegung ist bei einer Geißelbewegung in Richtung der Antennenachse stärker vertreten als bei einer Bewegung senkrecht zu ihr. Das Tier ist trotz der gegenüber der Wellenlänge sehr kleinen Ausdehnung der Geißeln in der Lage, die Richtung zu bestimmen, aus der das weibliche Fluggeräusch kommt. Eine besondere biologische Bedeutung kommt der Überlagerung zweier Töne zu, die als Schwebung in der unmittelbaren Umgebung von 380 Hz ablaufen. Die relativ große Schwebungslaufzeit des Schallpotentials hat physikalische Ursachen, die durch die Resonanzeigenschaften der Antenne bedingt sind.

Summary

Measurements of the sound potential in male animals of a species of mosquitoes, Anopheles subpictus, show that these insects are hearing in a small range of frequency between 150 and 550 c/s. The maximum sensitivity occurs at 380 c/s. It corresponds to the sensitivity of the human ear at 2 kc/s. The difference between the threshold level and the level of saturation is 28 phon. The noise produced by the flying female mosquitoes contains a clearly perceptible tone of 380 c/s so that this tone is of great use to the male insect in spite of the general noise of the environment. The noise of flying of the male mosquito will practically not be picked up by its own feelers as the loudest tone of the spectrum is at the upper limit of its auditory range. The observed effect of doubling the frequency of the Johnston Organ may be understood from its construction. The first harmonic of the movement of the clasps working on the pins is larger at a motion of the feeler in the direction of the axis of the antennae than at a motion perpendicular to it. In spite of the small dimensions of the feeler compared with the wavelength the mosquito is able to find the direction from which the female noise of flying is coming. A particular biological importance belongs to the superposition of two sinusoidal sounds which form beats near 380 c/s. The relatively high time of delay of these beats observed in the sound potential has physical origins in the resonance effect of the antennae.

Sommaire

Des mesures faites sur le sens de l'ouïe de sujets mâles d'une certaine espèce de moustiques, Anopheles subpictus, ont montré que ces insectes entendent dans une gamme de fréquences étroite, de 150 à 550 Hz, la fréquence de plus grande sensibilité étant 380 Hz. Cette sensibilité correspond à celle de l'oreille de l'homme pour 2 kHz. Il y a 28 phones entre le seuil d'audition et la saturation. L'effet de bande passante observé est dû à l'accord des flagella. Le bruit du vol de la femelle contient une composante nettement perceptible subjectivement à 380 Hz, de sorte que ce son ressort du bruit ambiant. Le bruit de vol lui-même, de fréquence plus élevée, n'est presque pas perçu par le mâle. L'effet observé de doublement de la fréquence par l'organe de Johnston est dû à la constitution propre de cet organe. La fréquence fondamentale du mouvement de serrage agissant sur les tiges est plus marquée quand le mouvement des flagella a lieu dans la direction de l'axe que dans la direction perpendiculaire. Malgré la très faible dimension des flagella devant la longueur d'onde, l'insecte peut déterminer la direction d'où vient le bruit du vol de la femelle. La superposition de deux sons qui forment un battement au voisinage de 380 Hz a une importance biologique particulière. La réponse relativement retardée du sens de l'ouïe à ce battement a une origine physique liée aux propriétés de résonance des antennes.

1. Einleitung

Die Frage, ob Stechmücken (Moskitos) hören, bildet seit langer Zeit den Gegenstand der Erörterungen von Entomologen. Seit dem Jahre 1855, in dem C. **Johnston** [1] das nach ihm benannte Gehörorgan von Anopheles beschrieb und C. M. **Child** [2] in seiner Leipziger Dissertation dieses Organ im Jahre 1894 schon recht genau dargestellt hatte, wurde diese Frage gelegentlich immer wieder behandelt. Man beobachtete, daß Schwärme von Stechmücken durch Violin-, Cello- oder Zitherspiel [3] und durch Singen angelockt wurden und als die elektrotechnischen Erzeugnisse Eingang ins praktische Leben fanden, stellte man fest, daß der von bestimmten Telegraphenapparaten und einem tönenden Lichtbogen abgestrahlte Schall Moskitos anzog. Sir H. **Maxim** [4] bemerkte beim Bau einer Kraftanlage, daß eine schadhafte Lampe, welche als Telephon wirkte, von einem Mückenschwarm umgeben war.

Untersuchungen von A. M. **Mayer** [5] mit Stimmgabeln aus dem Jahre 1874 zeigten, daß die Geißelenden von Moskitos besonders kräftig bei 520 Hz ausschlugen. Bei zwölf Tieren war die Resonanzfrequenz ungefähr gleich. Eine klare Vorstellung von der Wirkungsweise des Johnston-Organs fehlte jedoch bisher. Die führenden amerikanischen Entomologen L. C. **Howard**, H. G. **Dyer** und F. **Knab** [6] faßten ihre Meinung im Jahre 1912 in dem folgenden Satz zusammen: Wenn der Schall mit den Antennen empfangen wird, wie es auf Grund des Baues der Antennen der Fall zu sein scheint, so ist noch zu bezweifeln, ob das Tier wirklich auf Schall reagiert oder ob die Geißeln nicht vielmehr auf den Luftstrom ansprechen. Es ist auch unklar, wie die Antennen auf Schall verschiedener Tonhöhe reagieren.

Die ersten zuverlässigen Untersuchungen über das Verhalten von männlichen Tieren einer Moskitoart, Aëdes aegypti, des Gelbfieberüberträgers, wurden von L. M. **Roth** [7] im Jahre 1948 mitgeteilt. Er arbeitete ebenfalls mit Stimmgabeln. Der Frequenzbereich, auf den Aëdes aegypti bei sinusförmigem Schall anspricht, erweitert sich etwas mit dem Alter der Tiere. Er liegt nach den auf statistischem Wege gefundenen Ergebnissen zwischen 200⋯500 Hz. Anschließend registrierten M. C. **Kahn** und W. **Offenhauser** jun. [8] das Fluggeräusch weiblicher Aëdes aegypti auf einer Schallplatte. Sie fanden bei der Wiedergabe mit einem Lautsprecher, daß männliche Insekten der gleichen Art beinahe sofort nach dem Einschalten auf den Lautsprecher zuflogen.

Für die Beurteilung des Hörvermögens hat man von drei verschiedenen Seiten auszugehen: Einmal ist die Morphologie des Gehörorgans zu studieren, das bei männlichen Culiciden ungleich besser entwickelt ist als bei den Weibchen, zum anderen ist das Verhalten der Tiere gegenüber dem weiblichen Fluggeräusch zu untersuchen und schließlich sind mit elektrophysiologischen Methoden die elektrischen Potentiale zu erfassen, die entstehen, wenn Stechmücken sich im Schallfeld aufhalten. Die morphologische Seite wurde jüngst von H. **Risler** [9], ausgehend von der Arbeit von C. M. **Child** [2], wieder aufgegriffen, der im Anschluß an die hier wiedergegebenen Beobachtungen die Anatomie des Gehörorgans von Anopheles stephensi studierte. Ergebnisse über das Verhalten der Tiere liegen von L. M. **Roth** sowie M. C. **Kahn** und W. **Offenhauser** jun. vor.

In der vorliegenden Arbeit wurde der dritte Weg beschritten. Mit den Untersuchungen von E. G. **Wever** und C. W. **Bray** [10] über die Cochlearpotentiale an der Schnecke von Wirbeltieren als Grundlage wird über Messungen der Schallspannung an einer Moskitoart, Anopheles subpictus, berichtet, die während eines Aufenthaltes in Indien am Indian Institute of Technology zur Verfügung stand und die mit A. stephensi eng verwandt ist. Die drei Wege müssen zusammenführen und eine einheitliche Vorstellung von der Wirkungsweise des Gehörorgans von Stechmücken ergeben.

2. Elektrophysiologische Untersuchungen

In Abb. 1 ist die Schaltung zur Messung des Schallpotentials an der lebenden Mücke dargestellt. Zwei spitze Stahlelektroden führen vom Tier zu dem Eingang eines erdunsymmetrischen, einstufigen Verstärkers, der sich mit dem Moskito, den Elektroden und deren Haltevorrichtung in einem geräumigen, doppelt geschirmten Faradayschen Käfig befindet. An den Ausgang des zweiten, einstufigen Verstärkers sind handelsübliche Röhrenvoltmeter R.V. und zwei Kathodenstrahloszillographen [11] K.O. I und K.O. II angeschlossen. Vor dem Faradayschen Käfig ist ein Lautsprecher L angeordnet, in dessen Schallfeld das Tier liegt. Zur Messung des Schalldruckes befindet sich in seiner unmittelbaren Nähe (Abstand des Moskitos kleiner als ein Sechstel der Wellenlänge) ein dynamisches Mikrophon M. Zwischen 100···800 Hz war die gemessene Spannung praktisch unabhängig von der Frequenz. Die an den Eingangsklemmen des ersten Verstärkers auftretende Rauschspannung betrug 6 μV. Da sich dieser Verstärker im Schallfeld des Lautsprechers befindet, und eine Klingfrequenz bei 750 Hz auftrat, wurde er in zwei gut schalldicht voneinander getrennte Kästen eingebaut.

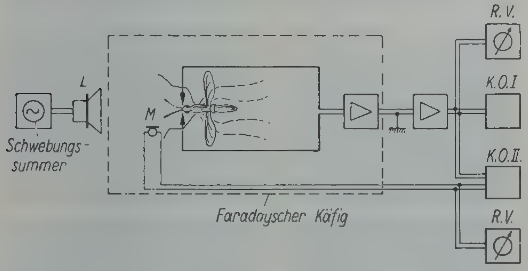

Abb. 1. Schaltung zur Messung des Schallpotentials.

Die Tiere wurden mit Chloroformdampf schwach betäubt, mit ihren Beinen auf einen Objektträger geklebt und eine Elektrode in das linke Auge gestochen. Die andere Elektrode wurde langsam in die Gelenkfalte an der Pedicellusbasis der rechten Antenne geführt und in diese eingestochen, bis das Braunsche Rohr eine Spannung anzeigte. Auch Versuche, bei denen eine Elektrode in das linke Auge, die andere in den Hinterleib des Tieres gestochen wurden, verliefen erfolgreich, wenn auch die gemessene Spannung viel kleiner war als in der unmittelbaren Umgebung des Johnston-Organs. Belegte man die zweite Elektrode mit einer feuchten Graphitschicht, so wurde ebenfalls eine Spannung beobachtet, wenn die Elektrode zart auf den Pedicellus gelegt wurde. Sie hob sich gerade vom Störpegel ab. Das Kriterium der „richtigen“ Meßstelle ist so ein rein elektrisches und kein optisches. Es ist möglich, daß der umfangreiche Nervenstrang vom Johnston-Organ zum Gehirn des Tieres nicht getroffen wurde, da die nachfolgend beschriebenen Ergebnisse nicht das zeigen, was von physiologischer Seite als Nervenaktionspotential (Impulsfrequenzmodulation) bezeichnet wird.

Ersetzte man den Kopf der Mücke durch einen Leimtropfen der gleichen Größe und stach beide Elektroden in ihn hinein, so blieb der Störpegel auch im relativ starken Schallfeld unabhängig von der Größe des Schallfeldes konstant. So war es sicher, daß die gemessenen Erscheinungen wirklich zum Tier gehören.

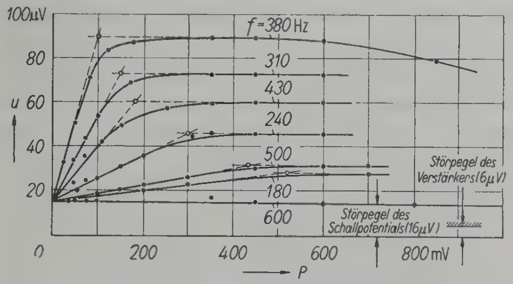

Abb. 2. Verlauf des Schallpotentials in Abhängigkeit vom Schalldruck.

Das Ergebnis einer Meßreihe zeigt Abb. 2. Mit steigendem Schalldruck P, in willkürlichen Einheiten (mV) gemessen, erhebt sich das Schallpotential u über den durch den Anschluß des Tieres erhöhten Störpegel von 16 μV zunächst linear, um bei einem bestimmten Schalldruck einen Sättigungswert zu erreichen. Da kein geeichter Schalldruckmesser zur Verfügung stand, wurde bei verschiedenen sinusförmigen Tönen der Schwellwert des Schalldruckes in der Nähe des Moskitos subjektiv bestimmt und über den in Spannungseinheiten geeichten Schwebungssummer und die bekannte Fletscher-Munson-Kurve auf die absolute Größe des Schalldruckes, bei dem die Sättigung erreicht ist, geschlossen. Dieser Sättigungsdruck (Schnittpunkt der gestrichelten Linien) hängt stark von der Frequenz ab. In Abb. 3 ist er als Funktion der Frequenz dargestellt. Während im Bereich um 150···600 Hz der Sättigungsdruck relativ groß ist, zeigt er bei 380 Hz ein scharf ausgeprägtes Minimum.

Ein Versuch, den Schwellwert zu ermitteln, führte zu der zweiten Kurve für A. subpictus.

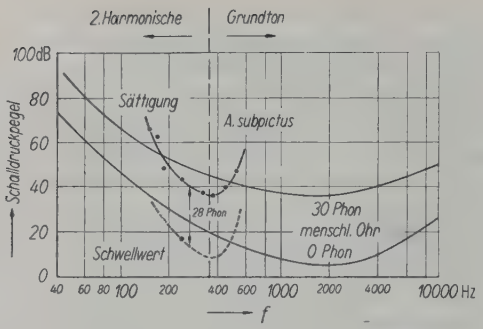

Abb. 3. Empfindlichkeitskurve des Gehörorgans von A. subpictus.

Das Schallpotential wurde oszillographisch kontrolliert und derjenige Schalldruck bestimmt, bei dem sich dieses Potential gerade vom Störpegel abhob. Bei 240 Hz gelang dies noch bei dem gleichen Tier, mit dem die Sättigungskurve erhalten wurde. Die Messungen erfolgten im Februar 1952 und mußten aus äußeren Gründen für acht Tage unterbrochen werden. Nach der Wiederaufnahme der Versuche war das Leben im dicht benachbarten Dschungel so laut geworden, daß Versuche, den Schwellwert erneut auf der alten Grundlage zu bestimmen, erfolglos verliefen. Der Störpegel, vorwiegend von Insekten hervorgerufen, war auf den dreifachen Betrag angestiegen. Ein schalltoter Raum stand nicht zur Verfügung. Der Verlauf der Schwellkurve wird sich jedoch nicht wesentlich von dem der Sättigungskurve unterscheiden. Es ergibt sich so ein Hörumfang von 28 Phon. Der Schwellwert ist im Bereich der größten Empfindlichkeit sehr klein. Er ist etwa gleich dem Schwellwert des menschlichen Ohres bei 2 kHz. Das Männchen der Stechmücke hört damit das relativ leise Fluggeräusch des Weibchens besonders gut, aus dem ein Ton von 380 Hz stark hervortritt.

Über die Höhe des subjektiv wahrgenommenen Flugtones von Culiciden liegen Untersuchungen von O. Sotavalta [12] (Abb. 4) vor. Die Tonhöhe des Flügelschlages ist von der Temperatur abhängig. Wichtig ist, daß bei allen Stechmückenarten der Unterschied zwischen dem männlichen und weiblichen Flugton deutlich in Erscheinung tritt. Die bei 28 °C durchgeführten eigenen Messungen zeigen dies ebenfalls. Der Unterschied beträgt auch bei A. subpictus etwa 200 Hz. Die Flugtonhöhe des Männchens ist ungefähr 540 Hz; sie liegt also an der Grenze seiner eigenen Wahrnehmungsfähigkeit. So ist die Möglichkeit gegeben, daß die männlichen Tiere, die in den Abend- und Morgenstunden in Schwärmen [13] auftreten, ihr eigenes Fluggeräusch von dem vorbeifliegender oder in den Schwarm eindringender Weibchen trennen können. Aus den Beobachtungen von A. M. Mayer [5] schließen wir, daß die hohe Empfindlichkeit bei 380 Hz durch die mechanische Resonanz der beiden Geißeln bedingt ist.

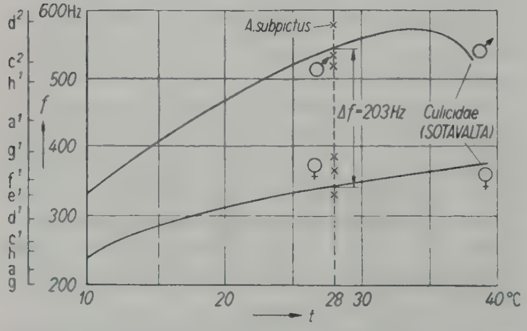

Abb. 4. Subjektiv wahrgenommene Flugtöne von Stechmücken.

Ein Blick auf den zeitlichen Verlauf des Schallpotentials liefert Aufschlüsse über den Umwandlungsprozeß des Schallvorganges im Johnston-Organ. Der elektrische Störpegel bei einer sehr kleinen Amplitude des äußeren Störgeräusches gibt eine unregelmäßige Kurve (Abb. 5a). Dieses und die nachfolgenden Oszillogramme zeigen als untere Kurve jeweils den Verlauf des Schalldruckes oder eine Zeitmarke. Ähnlich ist das Ergebnis bei einem Schallvorgang mit 140 Hz (Abb. 5b). Die Aufnahmen wurden mit einem Zweistrahloszillographen und einer Leica-Kamera gemacht. Oszillograph und Kamera befanden sich in etwa 1 m Abstand von dem Mikrophon. Durch das Öffnen des Schlitzverschlusses der Kamera entstand ein Geräusch, dessen Spektrum zum Teil in den Hörbarkeitsbereich der Mücke fällt. Die Auswirkung dieses Geräusches auf das Schallpotential ist in dem rechten Teil des Oszillogramms zu erkennen.

Bei einer Besprechung des Tieres mit 240 Hz (Abb. 5c) erscheint ein völlig regelmäßiger Verlauf des Schallpotentials, bei dem die zweite Harmonische stark hervortritt. Dies ist charakteristisch für jeden sinusförmigen Vorgang unterhalb der Frequenz größter Empfindlichkeit. Es kommt auch vor, daß bei dicht benachbarten Frequenzen der Phasenwinkel des Grundtones sich schnell gegenüber dem der zweiten Harmonischen dreht. Oberhalb 380 Hz tritt der Grundton immer mehr hervor; bei 400 Hz ist er fast ausschließlich vertreten (Abb. 5d).

Es ist lehrreich, die Reaktion von Stechmücken auf die menschliche Stimme zu studieren. Auf Singen des Vokals „a“ durch eine männliche Stimme reagiert das Tier mit einer Grundfrequenz von 320 Hz und guter Frequenzverdopplung

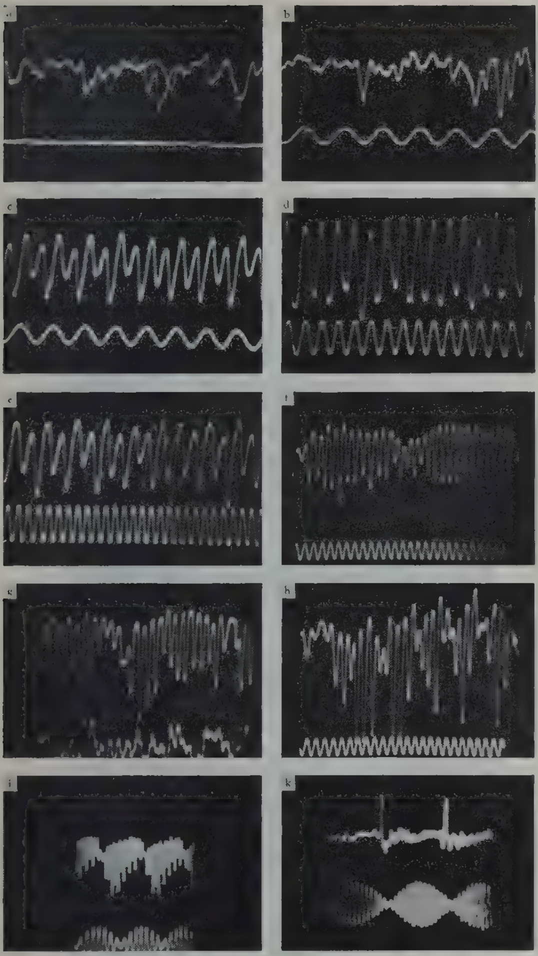

Abb. 5. (a) Störpegel des Schallpotentials.
(b) Schallpotential bei 140 Hz.
(c) Schallpotential bei 240 Hz.
(d) Schallpotential bei 400 Hz.
(e) Schallpotential des Vokals „a“.
(f) Schallpotential des Lautes „sch“.
(g) Schallpotential des Einschaltstosses eines Lautsprechers.
(h) Schallpotential des Dschungelgeräusches.
(i) Schwebung des Schallpotentials 340/391 Hz.
(k) Schwebung des Schallpotentials 370/392 Hz.

(Abb. 5e). S-Laute werden wegen ihrer hohen Formantbereiche zwischen 5···10 kHz nicht mehr wahrgenommen; dagegen wird der Laut „sch“ (Abb. 5f) sehr gut vom Tier registriert. Im Johnston-Organ entsteht eine Frequenz von 770 = 2 × 385 Hz. Man kann sich das Vergnügen machen, die an der Stechmücke abgegriffene Spannung über Verstärker einem Kopfhörer zuzuführen und die Sprache abzuhören, wie sie im Johnston-Organ erscheint. Sie ist nur noch sehr unvollkommen verständlich. Das dem engen Durchlaßbereich entsprechende Frequenzband tritt deutlich hervor. Die Anordnung wirkt als ausgesprochener Bandpaß. Unterhalb der optimalen Durchlaßfrequenz wird also die Frequenz verdoppelt, oberhalb bleibt das Potential sinusförmig.

Die Bandpaßwirkung kommt auch bei der Aufnahme von Einschaltstößen des Lautsprechers zum Ausdruck (Abb. 5g). Aus dem unregelmäßigen Verlauf des Schallvorganges wird die Frequenz 720 = 2 × 360 Hz heraussortiert. Wichtig ist die Reaktion des Moskitos auf das Dschungelgeräusch. Die Messung erfolgte abends 10 Uhr, als die Insektenwelt in voller Bewegung war. Auch aus diesem Geräusch (Abb. 5h) wird die Frequenz 2 × 360 Hz ausgewählt. Die untere Kurve ist wie bei den Abb. 5e und f eine Zeitmarke.

Die Natur achtet streng auf die Trennung der Arten. Da die Flugtonhöhe nach den Beobachtungen von O. Sotavalta [12] bei allen Stechmückenarten praktisch die gleiche ist und auch zeitlich konstant bleibt, müssen andere Unterscheidungsmerkmale für das Fluggeräusch der einzelnen Arten vorliegen. Es liegt nahe, die Unterschiede in dem Modulationsrhythmus und der Hüllkurve des von den Flügeln abgestrahlten Schallvorganges zu suchen. W. Lottermoser [14] beobachtete die große Regelmäßigkeit der von Waldgrillen und Heuschrecken hervorgebrachten Locklaute. Die einzelnen Arten unterscheiden sich durch die Form der Hüllkurve und die Tastfrequenz. Auch zwischen A. subpictus und A. stephensi war der subjektiv gewonnene Eindruck des Fluggeräusches bei etwa gleicher Flugtonhöhe verschieden. Neben der Amplitudenmodulation ist auch eine Frequenzmodulation denkbar.

Um einen Anhaltspunkt für diese Auffassung zu gewinnen, wurden durch die Überlagerung zweier sinusförmiger Spannungen ein sinusförmig amplitudenmodulierter Schallvorgang hergestellt und das zugehörige Schallpotential gemessen. So wurden zwei Spannungen von 340 und 391 Hz zwei Schwebungssummern entnommen und addiert (Abb. 5i). Auch hier tritt im Schallpotential die doppelte Frequenz der resultierenden Schwingung von 2 × 365 Hz klar hervor. Die Schwebungen weisen eine relativ große Verzögerungszeit von 10,95 ms auf. Völlig anders ist das Bild, wenn zwei Spannungen von 370 und 392 Hz überlagert werden (Abb. 5k). An die Stelle der Schwebungen des Schallpotentials treten scharfe Spitzen. Diese Erscheinung läßt darauf schließen, daß jetzt eine besondere Art der Schallumwandlung vor sich geht, die für den Anlockungsmechanismus von Bedeutung ist. Die Einstellung der beiden Frequenzen ist ziemlich kritisch. Die auch hier beobachtete große Schwebungslaufzeit von 18,4 ms ist nicht auf die endliche Fortpflanzungsgeschwindigkeit der Schallpotentiale in den Nerven zurückzuführen; sie hat, wie im Anhang dargelegt ist, rein physikalische Ursachen, die durch die Resonanzeigenschaften der Geißeln mit ihrer Einspannung bedingt sind.

3. Zur Deutung der Ergebnisse

Aus den elektrophysiologischen Beobachtungen ergab sich die Empfindlichkeitskurve und die frequenzverdoppelnde Wirkung des Johnston-Organs. An Hand der von C. M. Child [2] und H. Risler [9] durchgeführten morphologischen Studien lassen sich nun Vorstellungen von der Wirkungsweise des Gehörorgans von Stechmücken entwickeln. Diese vor allem beim männlichen Tier relativ großen Organe befinden sich in den am Kopf vor den Augen gelegenen Pedicellen der Fühler (Abb. 6). In ihnen wurzeln die beim Männchen besonders lang und dicht behaarten Geißeln. Ein Längsschnitt durch den Pedicellus (Abb. 7) zeigt den nicht ganz einfachen Aufbau des Johnston-Organs. In der aus dieser Abbildung abgeleiteten halbschematischen Darstellung (Abb. 8) [15] wurzelt die Geißel G, die im Innern ein Blutgefäß und Nerven enthält, in einer Fußplatte Pl, die an Spangen Sp verankert ist. Die durch die Bewegung der Geißel an der Platte entstehenden Druckschwankungen wirken über die ringförmig angeordneten Spangen auf die Endfasern F der Stifte St_1 im äußeren Ring, welche

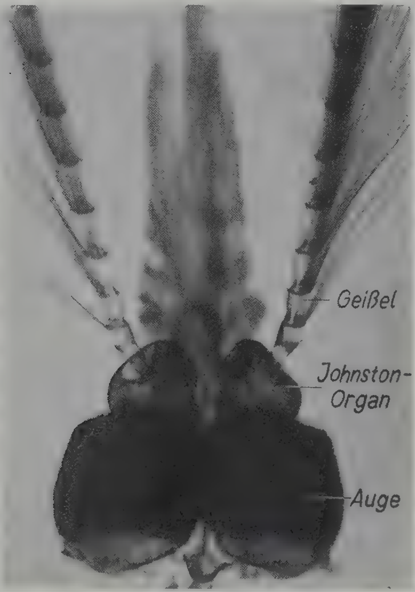

Abb. 6. Dorsalsansicht des Kopfes von A. subpictus.

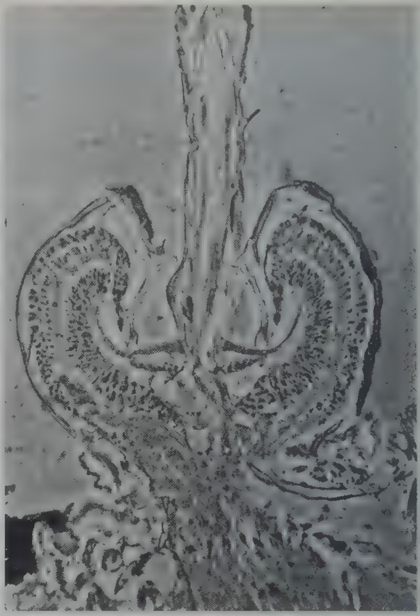

Abb. 7. Längsschnitt durch die Antennenbasis (sagittal). Phasenkontrastaufnahme.

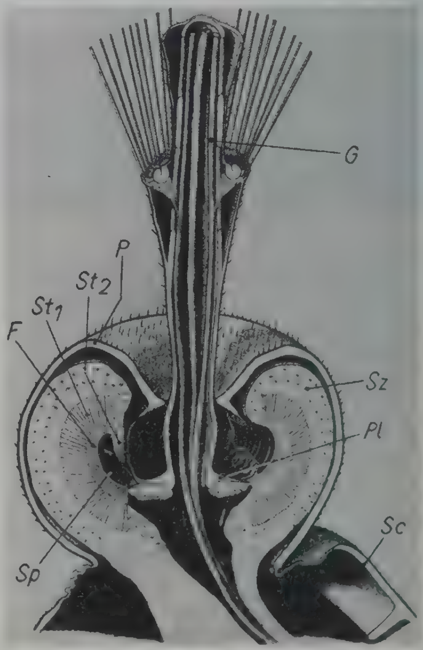

ventral ⟷ dorsal

Abb. 8. Rekonstruktion von Scapus, Pedicellus und Geißel. Rechts ein Teil der inneren Pedicelluswand und die Stifte des inneren Ringes entfernt. Schnittflächen weiß.

G Geißel, Pl Fußplatte, Sp Spangen, F Endfasern, St_1 Stifte des äußeren Ringes, St_2 Stifte des inneren Ringes, Sz Sinneszellen, P Pedicellus, Sc Scapus.

in Gestalt einer Hohlkugel um die Platte herum zusammengefaßt sind. Die ihnen zugeordneten Sinneszellen Sz liegen nahe der Außenwand des Pedicellus P. Der ringförmige Scapus Sc und der Pedicellus werden durch Muskeln bewegt, um der gesamten Antenne eine bestimmte Richtung relativ zum Kopf zu geben. Neben den äußeren Stiften St_1 besteht ein zweiter innerer Ring von Stiften St_2, die mit ihren Endfasern an der Basis der Spangen haften. Ein Querschnitt (Abb. 9) durch den Pedicellus in Höhe der Fußplatte Pl läßt die Spangen Sp mit den Endfasern F, die Stifte St_1 und die Sinneszellen Sz erkennen. Das Organ ist im wesentlichen rotationssymmetrisch um die Antennenachse herum aufgebaut. Eine weitere Schematisierung zeigt Abb. 10. Die Stifte St_2 münden in die Sinneszellen Sz, die an dem von der Platte Pl entfernten Ende angeordnet sind.

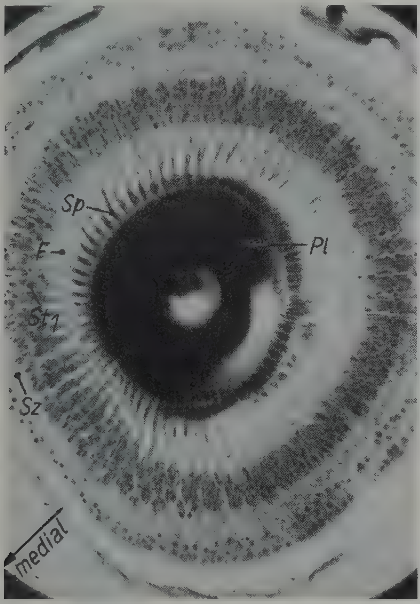

Abb. 9. Querschnitt durch den Pedicellus in Höhe der Fußplatte.
Sp Spangen, F Endfasern, Sz Sinneszellen, Pl Fußplatte, St_1 Stifte des äußeren Ringes.

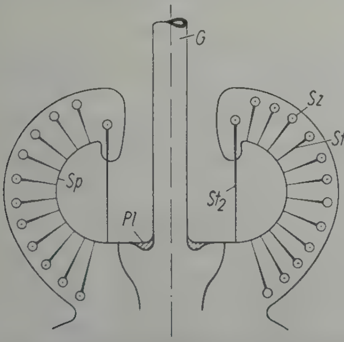

Abb. 10. Vereinfachte Darstellung des Längsschnittes Abb. 7 und 8.

Im Schallfeld verursacht eine Schnellekomponente in Richtung der Geißel eine Bewegung der Platte parallel zu sich selbst. Beim Niedergang drücken die Spangen Sp auf die Stifte St_1 der unteren Sinneszellen Sz, bei der Aufwärtsbewegung auf die Stifte St_1 der oberen Zellen. Ein sinusförmiger Ton hat so ein Schallpotential der doppelten Frequenz zur Folge, wie es unterhalb 380 Hz beobachtet wurde (Abb. 5c). Darüber hinaus erscheint der Grundton, der durch die Bewegung der Stifte St_2 hervorgebracht wird. Wegen der geringeren Zahl der Stifte ist auch seine Amplitude kleiner. In Abb. 5c beträgt die erste Harmonische 60 % der zweiten.

Tritt eine Schnellenkomponente senkrecht zur Antennenrichtung auf, so wird die Platte gekippt. Auch die Stifte St_2 geben nunmehr die doppelte Frequenz des Schallvorganges. Daraus folgt, daß das Tier die Richtung, aus der der Schall kommt, feststellen kann. Der Grundton verschwindet um so mehr, je kleiner die Schnellenkomponente in Richtung der Geißel ist. Die Wellenlänge des Schalles bei 380 Hz ist etwa 1 m, so daß die Phasenverschiebung zwischen den beiden Geißelbewegungen keine Rolle spielt. Der Abstand zwischen den beiden Geißeln an ihrer Einmündung in die Johnston-Organe beträgt 0,2 mm. Diese Phasenverschiebung ist nur bei größeren Abständen der beiden Gehörorgane (Wirbeltiere) von wesentlicher Bedeutung. Die Natur hat mit der Konstruktion des Johnston-Organs die Möglichkeit geschaffen, sehr kleine Empfänger durch die Erfassung des Klirrfaktors richtungsempfindlich zu machen. Dies gelingt um so besser, als durch die Bandpaßwirkung der Geißeln aus dem weiblichen Fluggeräusch nur ein praktisch sinusförmiger Anteil von ungefähr 380 Hz für die Signalübermittlung abgesondert wird.

Bei höheren Frequenzen als 380 Hz tritt die zweite Harmonische zurück (Abb. 5d). Es scheint, als ob das Johnston-Organ nicht mehr in der Lage ist, den raschen Schwankungen des Schallfeldes zu folgen.

ANHANG

Die zeitliche Verzögerung der Bewegung in Resonanzschaltungen bei Schwebungsvorgängen

Die Geißeln der Stechmücken sind resonanzfähige Gebilde. Die Masse wird durch die Geißel mit ihren Härchen und die Platte (Abb. 8) dargestellt; die Einspannung der Fußplatte ist der elastische Teil der schwingenden Anordnung. Die Bewegung x der Geißel gehorcht, wenn man annimmt, daß sie als Ganzes schwingt, der Differentialgleichung

$$m\ddot{x} + r\dot{x} + cx = P_0 \, e^{i\omega t}, \qquad (1a)$$

wobei m die Masse, r die Dämpfungskraft je Schnelleeinheit, c die Rückstellkraft je Wegeinheit, P_0 die Amplitude der erregenden Kraft, ω ihre Kreisfrequenz bei sinusförmigem Antrieb und t die laufende Zeitkoordinate bedeuten. Die Lösung der Gleichung für den eingeschwungenen Zustand ist

$$x = x_0 \, e^{i(\omega t - \varepsilon)} \qquad (1b)$$

mit x_0 als Bewegungsamplitude und ε als Nacheilwinkel der Bewegung gegenüber der Kraft. Durch Einsetzen der Lösung in Gl. (1a) erhält man mit den Abkürzungen $\eta \equiv \omega\sqrt{m/c}$; $D \equiv r/2\sqrt{mc}$ im Anschluß an K. KLOTTER [16]:

$$x_0 \, e^{-i\varepsilon} = \frac{P_0}{c(1-\eta^2+i2D\eta)}. \qquad (1c)$$

Mit $cx_0/P_0 \equiv y$ ensteht

$$y = \frac{1}{\sqrt{(1-\eta^2)^2 + 4D^2\eta^2}}; \quad \varepsilon = \operatorname{arctg} \frac{2D\eta}{1-\eta^2}. \qquad (1d)$$

Die reduzierte kinetische Einflußzahl y stellt als Funktion der normierten Frequenz η die bekannte Resonanzkurve (Abb. 11) dar; der Nacheilwinkel ε steigt von Null über $\pi/2$ bei $\eta = 1$ auf π.

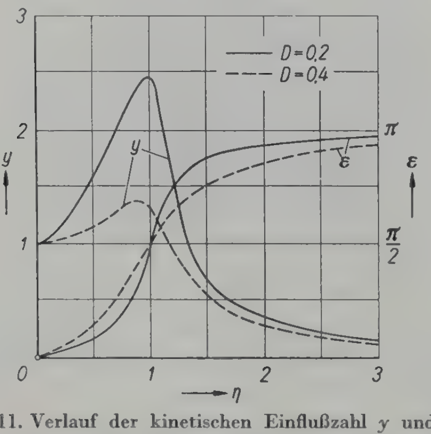

Abb. 11. Verlauf der kinetischen Einflußzahl y und des Nacheilwinkels ε als Funktion der normierten Frequenz η.

Wirken zwei Kräfte mit den Amplituden P_{01} und P_{02} mit den Kreisfrequenzen ω_1 und ω_2 auf das schwingende System, so überlagern sich wegen des durch die Gl. (1a) ausgedrückten linearen Verhaltens die Einflußzahlen y_1 und y_2 mit den entsprechenden Nacheilwinkeln ε_1 und ε_2 zu

$$y \, e^{-i\varepsilon} = y_1 \, e^{-i\varepsilon_1} + y_2 \, e^{-i\varepsilon_2}. \qquad (2a)$$

Um zu einer einfachen Diskussion der Ergebnisse zu gelangen, wird angesetzt, daß $P_{01} = P_{02}$ ist und daß die Kräfte den Phasenwinkel Null zueinander im Zeitpunkt $t = 0$ haben. So wird die antreibende Kraft in reeller Schreibweise:

$$f(t) = P_{01}(\sin\omega_1 t + \sin\omega_2 t). \qquad (2b)$$

Wir wählen die Vorgänge aus, deren Einflußzahlen y_1 und y_2 gleich sind, legen uns also auf bestimmte Werte η_1 und η_2, bzw. ω_1 und ω_2 fest. Damit wird in reeller Schreibweise der zeitliche Ablauf der Bewegung:

$$g(t) = y_1[\sin(\omega_1 t - \varepsilon_1) + \sin(\omega_2 t - \varepsilon_2)],$$

oder

$$g(t) = 2y_1 \cos\frac{(\omega_1-\omega_2)\,t + (\varepsilon_2-\varepsilon_1)}{2} \cdot \sin\frac{(\omega_1+\omega_2)\,t - (\varepsilon_2+\varepsilon_1)}{2}. \qquad (2c)$$

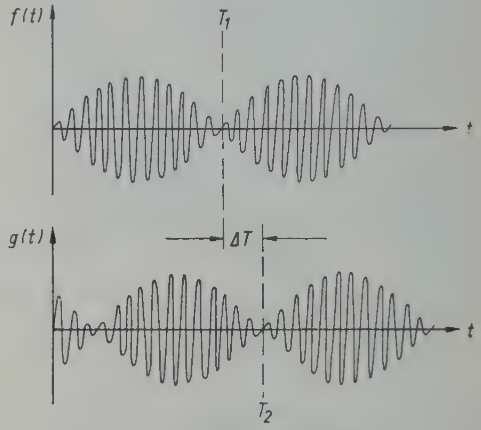

Abb. 12. Die Schwebungslaufzeit.

Die Funktionen $f(t)$ und $g(t)$ stellen amplitudenmodulierte Schwingungen (Abb. 12) dar. Die Nullstellen der Hüllkurven liegen bei

$$\frac{(\omega_1-\omega_2)\,T_1}{2} = (2n-1)\frac{\pi}{2} \quad (n=1,2,3\ldots) \qquad (3a)$$

bzw.

$$\frac{(\omega_1-\omega_2)\,T_2 + (\varepsilon_2-\varepsilon_1)}{2} = (2n-1)\frac{\pi}{2} \quad (n=1,2,3\ldots). \qquad (3b)$$

So ist eine zeitliche Verzögerung

$$T_2 - T_1 = \Delta T = \frac{\varepsilon_2-\varepsilon_1}{\omega_2-\omega_1} = \frac{1}{\omega_0}\cdot\frac{\varepsilon_2-\varepsilon_1}{\eta_2-\eta_1} \qquad (3c)$$

der Bewegung gegenüber der antreibenden Kraft zu verzeichnen, wobei $\omega_0\eta_1 = \omega_1$ bzw. $\omega_0\eta_2 = \omega_2$

gesetzt ist. Da stets $\varepsilon_2-\varepsilon_1 \leqq \pi$ ist, wird die Schwebungslaufzeit

$$\Delta T \leqq \frac{1}{2 f_0 (\eta_2-\eta_1)}. \tag{3d}$$

Sie ist um so größer, je kleiner der Unterschied zwischen den erregenden Frequenzen ist. Für den Fall der Abb. 5i ist $f_0 = 380$ Hz; $\eta_2-\eta_1 = 0{,}135$ und $\Delta T = 10{,}95$ ms. Gemäß Gl. (3d) ist $\Delta T \leqq 9{,}65$ ms zu erwarten. Bei dem Versuch nach Abb. 5k wird unter der Annahme, daß der Impuls dem Maximum der Schwebung entspricht, mit $f_0 = 380$ Hz; $\eta_2-\eta_1 = 0{,}058$ und $\Delta T = 18{,}4$ ms. Die maximal mögliche Verzögerungszeit beträgt 22,6 ms. Die gemessenen, auf den ersten Blick überraschend großen Verzögerungszeiten haben damit eine eindeutige physikalische Ursache, die sich zwanglos aus dem Verhalten des Empfangsapparates als resonanzfähiges System ergibt. Die Tatsache, daß die gemessenen Laufzeiten nahe an den maximal möglichen liegen, deutet auf eine scharf ausgeprägte Resonanz mit einem steilen Anstieg des Nacheilwinkels hin.

Dem Direktor des Indian Institute of Technology, Kharagpur (Indien), Herrn Dr. J. C. Ghosh, danke ich für das Interesse, das er dieser Arbeit entgegenbrachte, ebenso den Herren M. Kundu M. Sc. und P. C. Dhar, die mich bei den Messungen unterstützten. Mein besonderer Dank gilt den Herren Prof. Hans H. Weber (Physiologisches Institut der Universität Tübingen) und Prof. Hermann Weber (Zoologisches Institut der Universität Tübingen), die mir in Unterhaltungen Gelegenheit zu einer Urteilsbildung auf einem Gebiet gaben, das mir bei Beginn der Arbeiten neu war.

(Eingegangen am 20. März 1953.)

Schrifttum

[1] Johnston, C., J. microsc. Science, Old Series III [1855], zitiert nach C. M. Child.

[2] Child, C. M., Z. wiss. Zool. **56** [1894], 475—528.

[3] z. B. Natur und Museum, Senckenberg-Nachrichten **62** [1932], 30—31.

[4] Maxim, Sir H., Brief an die London Times vom 29. Oktober 1901, zitiert nach [6].

[5] Mayer, A. M., Amer. J. Science and Arts, ser. 3, **8** [1874], 85—103.

[6] Howard, L. O., Dyer, H. G. and Knab, F., The Mosquitoes of North and Central America and the West Indies. Carnegie Inst. Washington 1912, vol. I, p. 36.

[7] Roth, L. M., Amer. Midland Naturalist **40** [1948], 265—352.

[8] Kahn, M. C. und Offenhauser jun., W., Amer. J. tropical Medicine **25** [1949], 811—836; J. acoust. Soc. Amer. **21** [1949], 259—263.

[9] Risler, H., Zool. Jahrbücher, Abt. f. Anatomie **73** [1953], 165—186.

[10] Wever, E. G. and Bray, C. W., Proc. nat. Acad. Sci. **16** [1930], 344—350.

[11] Röhrenvoltmeter und Kathodenstrahloszillograph von Philips; Zweistrahloszillograph von Cossor (England).

[12] Sotavalta, O., Acta entomologica Fennica 4—5, Helsinki 1947.

[13] Muirhead-Thomson, R. C., Mosquito behaviour in relation to malaria transmission and control in the Tropics, London 1951, S. 12.

[14] Lottermoser, W., Acustica, Beiheft 2 [1952], AB 66 bis AB 71.

[15] Die Abb. 7—9 sind der Arbeit von Risler, H., [9] mit seiner freundlichen Genehmigung entnommen.

[16] Klotter, W., Messung mechanischer Schwingungen. Springer-Verlag, Berlin 1943, S. 27.

“Aeronautical Acoustics, in particular Jet Noise”

With this title a symposium was held, under the joint auspices of the British Acoustics Group and the Royal Aeronautical Society, at the Institution of Mechanical Engineers on May 21st, 1953. The first paper by Prof. E. J. Richards discussed the work being done in several Universities on sounds of supersonic jets. He was followed by Mr. J. B. Greatrex who described the measurements by Rolls-Royce, Ltd., on the distribution of noise round jet engines and its reduction. Mr. G. M. Lilley discussed the theory of aerodynamic noise, in particular that which results from the interaction of turbulence with shock waves and from shear in boundary layers.

The remaining papers were concerned with the noise associated with actual aircraft in flight; Mr. Warren's on the 'bangs' heard by listeners on the ground as the aircraft breaks through the 'sound barrier', Mr. Hayhurst's on the sounds heard in the neighbourhood of the starting-up and Mr. Fleming on the spectra and loudness of the steady noise produced at the ground by aircraft passing overhead.

A long and interesting general discussion followed ranging from the theory of the generation of supersonic noise to what constitutes a noise nuisance and the legal aspects of the problems of its mitigation.

The papers presented in the symposium will be published by the Royal Aeronautical Society, 4 Hamilton Place, London, W. 1.

E.G.R.

THE RELATION BETWEEN THE SONE AND PHON SCALES OF LOUDNESS

by D. W. Robinson

National Physical Laboratory, Teddington, Middlesex, England

Summary

Several previous investigators have studied the relation between loudness level and loudness sensation but have obtained discordant results. It is thought that a cause of these differences is that results are influenced by the test procedure. A new set of experiments is described in which a variety of sounds having known loudness level-intensity relations was used to make independent estimates of the phon-sone scale law over a wide intensity range. The uniqueness of this relation, which is prerequisite to its existence, is strongly demonstrated by the agreement of results for entirely different sounds and also by the consistency of the data for widely different test ratios. An unexplained difference remains between the scales for sounds ordered in ascending and descending loudness respectively, as has been found previously. The experiments were conducted in a manner directly related to the practical use of the sone scale, and were made with statistical control. The nature of the sone scale near the absolute threshold is discussed. A review of previous work leads to a single set of data representing tolerably well the results of various authors which may serve as a basis for future discussion of the standardisation of the phon-sone relation.

Sommaire

Plusieurs chercheurs ont déjà étudié la relation existant entre le niveau sonore subjectif en phones et l'impression sonore subjective en sones, mais ne sont pas arrivés à des résultats concordants. L'auteur estime que ce désaccord est dû à la différence des méthodes de mesure. Il décrit une nouvelle série d'expériences effectuées sur tout une variété de sons, dont on connaissait la relation entre l'intensité physique et l'intensité subjective, afin d'établir indépendamment la relation entre l'échelle des phones et celle des sones sur une gamme étendue d'intensités. L'unicité de cette relation, condition nécessaire de son existence, est nettement démontrée par le bon accord entre des résultats relatifs à des sons entièrement différents et aussi par la consistance des résultats concernant des rapports très différents. Il reste une différence inexpliquée entre les échelles à intensités croissantes et décroissantes, respectivement, différence déjà constatée antérieurement. On a fait les essais en se plaçant dans des conditions voisines des conditions d'emploi de l'échelle des sones, et sous contrôle statistique. On discute la nature de l'échelle des sones près du seuil absolu. L'examen des travaux antérieurs conduit à une série unique de valeurs qui représente suffisamment bien l'ensemble des résultats des différents auteurs et qui peut servir de base pour une discussion ultérieure en vue de la normalisation de la relation entre les phones et les sones.

Zusammenfassung

Bei mehreren früheren Untersuchungen der Beziehung zwischen Lautstärke und Lautheitsempfindung ergaben sich voneinander abweichende Resultate. Es wird angenommen, daß eine Ursache hierfür in einer Beeinflussung der Ergebnisse durch den Testvorgang liegen könnte. In einer hier beschriebenen neuen Versuchsreihe wurde eine Anzahl verschiedener Schallvorgänge mit bekannter Lautstärke-Intensitäts-Beziehung benutzt, um in einem großen Intensitätsbereich unabhängige Bestimmungen des Gesetzes der Phon-Sone-Skala durchzuführen. Die Allgemeingültigkeit dieser Beziehung, die eine Vorbedingung für deren Existenz ist, wird durch die Übereinstimmung der Ergebnisse für völlig verschiedene Schallvorgänge und auch durch die Konstanz der Werte bei sehr verschiedenen Testverhältnissen überzeugend nachgewiesen. Es bleibt eine unerklärte Abweichung zwischen den Werten, wenn man die Schallvorgänge nach zu- oder abnehmender Lautstärke anordnet, was schon früher festgestellt wurde. Die Versuche wurden mit statistischer Kontrolle und in direkter Beziehung zur praktischen Benutzung der Sone-Skala durchgeführt, deren Verlauf in der Nähe der Hörschwelle diskutiert wird. Ein Überblick über frühere Untersuchungen führt zu einem einzigen Satz von Werten, der ziemlich gut die Ergebnisse verschiedener Autoren wiedergibt und als Grundlage für weitere Diskussionen über die Normierung der Phon-Sone-Beziehung dienen kann.

1. Introduction

In recent years it has become common practice to express the loudness of noise by means of the "phon" scale, that is to say, in terms of the sound pressure level of an equally loud pure tone of frequency 1000 c/s [1]. The tentative international agreement on the phon scale reached in 1937 has brought about a welcome uniformity in the terminology of noise measurement. However, loudness values expressed on this scale do not immediately suggest the actual magnitude of the sensation of loudness and this sometimes leads to difficulty in interpretation on the part of engineers and other users who need to translate the phon values of noise into terms of common experience. For instance, the sequence 10—40—70—100 phons suggests a quantity rising by equal increments, but these values do not in fact correspond to sensations having this simple relationship.

It has often been proposed that to meet this difficulty there should be a supplementary scale, of which the "sone" scale has been proposed as an example [2], by means of which a number representing the average observer's judgment of sensation is assigned to a noise as an aid to the interpretation of the loudness level. If, for instance, the value of one sound on the sone scale were double that of another, the first sound would be judged by the average listener to be about "twice as loud" as the second, and similarly for other ratios.

It was the purpose of the present investigation to provide data which may assist in establishing the scale relation between phons and sones and to provide a basis for any future discussion on the standardisation of the scale for practical purposes.

2. General

A number of reports of similar experiments have already appeared in the literature [3]···[8]. Rather large discrepancies are found between the results obtained by different workers, and it seems that details of procedure of the subjective measurements involved may have a relatively large influence on the judgments of observers. In this new series of subjective loudness experiments an effort has been made to avoid as far as possible the causes which are thought to influence the judgment of subjects, and in addition the experimental plan has been so devised as to reveal its own self-consistency or otherwise in a rather sensitive manner.

At least three methods of determining the relationship between intensity and loudness have been described, namely:

(1) by direct subjective estimation of the intensity increment required to produce an assigned ratio of loudnesses,

(2) by observing the intensity increment required to maintain constant loudness on changing from binaural to monaural listening,

(3) by comparing the intensity of a complex sound built up of a number of equally loud components with that of one of the component tones judged to be of the same loudness as the complex sound.

Whereas the first method is direct, the last two methods, an account of which has been given by Fletcher and Munson [9] are indirect, and their validity rests on assumptions about the mechanism of hearing. There seems to be some justification for considering experiments of types (2) and (3) as being more of the nature of tests of the assumptions than as a basis for the subjective loudness scale itself.

It was concluded by Geiger and Firestone [5] on the basis of direct determinations by method (1) that the concordance of the three methods was established. However, in order to reach this conclusion it was necessary to find fault with the determinations of previous workers [3], [4]. Since the paper by Geiger and Firestone, other determinations have been reported, notably by Churcher, King and Davies [6], Pollack [7] and Garner [8]. Some of these later results show more affinity with those of the workers criticised than with Geiger and Firestone's own results, and their conclusion on the equivalence of the direct and indirect methods does not now appear so certain.

It therefore seemed desirable to attempt a new determination of the intensity-loudness relation by a direct method under conditions which were as far as possible free from the objections which have been or might be levelled against previous experimental techniques.

In practice, the loudness scale has its main application in assessing the effectiveness of noise reduction projects and other cases involving the immediate comparison of two noises according to a numbered scale. This suggests that the method by which the subjective measurements ought to be made is by direct comparison of pairs of stimuli, the loudness ratio of which is judged in relation to an assigned numeral. This direct method also permits proper comparison to be made with the results of earlier investigations similarly carried out.

With the exception of Ham and Parkinson's work and a few supplementary measurements by Laird, each of the previous direct loudness-scale determinations has been made using earphones. There are some limitations attached to this procedure. The field of practical importance of noise measurement does not ordinarily include sounds heard through earphones; consequently it is preferable in laboratory tests to work with free sound fields so that in this respect at least the conditions of the laboratory tests may approximate to those met with in practice. Further, the use of free sound fields admits of more accurate specification and simpler measurement of the test sounds, especially if these are complex in character.

With regard to the nature of the subjective judgments and the possibility of their expression in numerical ratios, there exist divergent opinions. The standpoint adopted in this paper is that the issue may properly be decided by experimental investigations. The self-consistency of the experimental results may be expected to indicate, given sufficiently crucial tests, the extent to which the resulting loudness scale is real and useful. It appears from the present study that experimental evidence strongly indicates that the loudness scale is real, even though it may still be imperfectly known, and that it can provide a useful numerical guide in the consideration of noise problems.

In spite of the scepticism sometimes heard, neither the author, nor apparently most other experimenters, have found that subjects have much difficulty in making repeatable direct loudness ratio judgments associated with simple numbers such as 2, $\frac{1}{2}$, 10, and the purposes of this investigation are adequately and appropriately met by direct tests so long as it can be shown that the results are consistent to a sufficiently high degree of statistical significance. This condition is found to be fulfilled by the results of the present investigation. It may be argued that even if the results are consistent they are not necessarily true. Of the various authors, **Garner** [8] alone states that some of his observers could easily be persuaded to change their criteria and yet remain consistent. Careful observation and interrogation of the subjects who took part in the present experiments lend no support to this. The explanation of discrepancies between the various results of different experimenters is likely to be found in differences of procedure and the objective conditions of test rather than in mere "suggestibility" or "faulty numerical sense" of the subjects.

There is, in principle, a method of deducing the numerical loudness scale without actually making judgments associated with numbers. The method, which has been mentioned by **Garner** [6], has some theoretical interest and the possibility of pursuing it had been considered in the present connection. The basis of the method is the estimation of "equal-loudness ratios" and "equal loudness intervals", that is, the estimation of equal geometrical and arithmetical intervals on the scale of sensation. The difficulty about this procedure lies in presenting the comparison-stimuli in a satisfactory manner, since there are three of them. It may also be doubted whether the subtle distinction between ordering three stimuli by equal ratios and by bisection would be sufficiently intelligible to ordinary observers, so that the logical advantage of the method might well be outweighed by the experimental hazards. It would be interesting to know whether results would be obtained similar to those from direct ratio judgments but it should not be assumed that this is certain. It was decided that, for the stated purposes of the present investigation, this method is not appropriate, because the user of the sone scale does not have occasion to consider whether *three* noises stand in geometrical or arithmetical loudness relations but is concerned with more immediate comparisons.

3. Choice of psychophysical method

Two testing procedures are available for experiments of the present kind, namely, the "constant stimulus" and "average error" methods[1]. Each of these basic methods may have a number of variants of a detailed kind. Opinions differ as to which method yields the more *reliable* data in particular experiments. In a paper devoted to this topic **Kellogg** [10] concluded that the constant-stimulus procedure was more reliable for experiments in loudness. **Stevens** [11], on the other hand, advocates the opposite but with the reservation that practical or theoretical considerations may modify the choice. **Churcher** and **King** [12] have also discussed the relative merits of the two procedures.

In the present case, several factors weigh in favour of using the constant-stimulus method. The question involved from the acoustical engineer's point of view is whether a reduced noise is substantially or inappreciably less than the original, and he has usually to exercise his judgment in circumstances where he has no control of the stimulus. It seems most appropriate to make the laboratory judgments under similar conditions.

---

[1] These terms mean roughly the following. In C.S. pairs of stimuli are presented and the subject's sole function is to judge whether the relation between them stands on one side or other of an assigned criterion; for instance, "Is A louder than B?", or "Is A more than twice as loud as B?" In A.E. the subject adjusts one stimulus until it stands in the appropriate relation to the other. Thus, in the first example, B would be adjusted to sound as loud as A; in the second example, twice as loud.

Some of the other considerations appropriate to loudness ratio tests may also be mentioned. The manipulation of the switch or switch and volume control which are required in average-error procedure necessarily diverts attention from the judgment. In these circumstances some observers may take a short-cut to an apparently stable final value which they do not repeat on subsequent occasions [5]. Another objection to the average-error procedure is that it provides the experimenter with little evidence regarding the quality of the judgments, whereas in the constant stimulus method, a spurious judgment, such as may happen through a slip of the tongue, is immediately apparent to the experimenter. Furthermore, the comparison stimuli may be presented at random intervals of intensity, thus forcing the observer to give independent consideration to each judgment, and encouraging him to be more discriminating in the search for barely detectable differences. There is, however, one drawback, namely, that the method undoubtedly occupies more time. A large number of the judgments made and recorded express the trivial fact that the stimuli were far removed from the desired value. This is the price to be paid for the outstanding advantage of randomisation.

In the present investigation "don't know" judgments were ruled out, but the comparison was repeated if necessary. "About right" judgments were discouraged but were finally admitted if the subject remained non-committal. This rarely happened.

4. Experimental plan

The experiments to be described covered the intensity range of practical importance. Some work at rather low intensities was included for completeness; the upper limit of about 110 phon was to some extent determined by instrumental limitations.

Three quite distinct types of sound were employed. These were a pure tone of 1000 c/s, a thermionically-generated white noise, the spectrum of which was approximately constant per cycle band width up to a cut-off frequency of 6000 c/s, and finally two reproductions of engine noises. Referring to Table I, the series I, II and V is approximately parallel with III, IV and VI, and the purpose of using different types of sounds was to check the overall consistency of the ratio determinations by appeal to a logical proposition. Suppose A_1 and A_2 are two signals of 1000 c/s tone such that A_2 is judged to be twice as loud as A_1. If, also, B_1 and B_2 are two signals of noise respectively judged to be equal in loudness to A_1 and A_2, then the existence of a numerical scale of loudness would imply that B_2 should be twice as loud as B_1. It is interesting, and important for the practical utility of such a scale, to obtain direct experimental verification. Determinations of the equivalent loudness of the white noise were used to express the data of III, IV and VI in terms of equivalent 1000 c/s loudness, that is to say, in phons, and the converted data were then compared with the results of I, II and V. A similar conversion was used for the results with reproduced engine noises (VII). The truth of the proposition was amply demonstrated.

Further satisfactory evidence of the reality of the numerical loudness scale was obtained by comparing the data for 2-fold and 10-fold ratios.

The experimental programme was spread over a period of rather more than one year, the tests being completed in a non-systematic order in order to avoid any systematic bias due to habituation of the team.

The duration of a testing session was about 15 minutes during which two separate tests were usually conducted.

5. Details of experimental procedure

The observer was seated at a distance of one metre from a direct-radiator loudspeaker in a sound-absorbent room, in which the ambient noise level was below the auditory threshold.

Table I

Plan of experiments

Series	Type of judgment	Sound
I	Doubling loudness	1000 c/s tone
II	Halving loudness	1000 c/s tone
III	Doubling loudness	white noise
IV	Halving loudness	white noise
V	10-fold magnification and reduction	1000 c/s tone
VI	10-fold magnification and reduction	white noise
VII	Doubling loudness	reproductions of engine noises
VIII	Investigation of the effect of varying the interval of silence between the stimuli in loudness ratio judgments.	
IX	Investigation of the effect on the results of employing monaural earphone listening.	
X	Investigation of the limiting behaviour of the ratio scale near the absolute threshold.	

In addition, 10 determinations were made of the equivalent loudness of the white noise at various intensity levels covering the range used in series III, IV and VI, and similar determinations for the engine noises at appropriate intensity levels.

The sound field of the loudspeaker was constant to within ±0.5 dB over distances of 20 cm transverse to the axis, and obeyed the inverse distance law along the axis. The greatest harmonic distortion tolerated was just under 1 %, which occurred when the intensity level of the 1000 c/s tone was 110 dB above 0.0002 dyne/cm^2 at the listening position; at lower intensity levels the distortion was much less than this.

The sounds for comparison were gated by an electronic switch having a time constant of 0.15 s and low distortion during transients. A mechanical sequence generator controlled the switch, and this had normal mark and space periods of one second each. A single test group consisted of four marks and four spaces, 8 s in all (Fig. 1). For experiments VIII only, the spaces were increased to 3 s, so that one test group occupied 16 s.

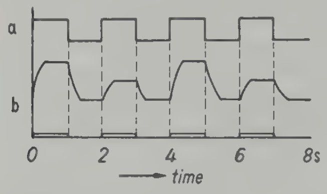

Fig. 1. Unit test sequence.
(a = sequence generator, b = sound intensity, 0···1, 4···5, ··· seconds = fixed stimulus, 2···3, 6···7, ··· seconds = variable stimulus.)

The time during which the maximum sound intensity persisted was chosen as short as possible to avoid unnecessary prolongation of the tests. The duration was adequate to ensure that full loudness sensation was reached [13].

The choice of the space period is of some importance. As will be seen, the results are usually repeated quite closely when this is increased from 1 to 3 s. Indeed it is quite possible that the results would be repeated if a very prolonged silence separated the stimuli although the dispersion would no doubt be relatively great. In practice a period of months may be relevant, as for instance in the subjective assessment of the efficacy of noise reduction projects. At the other end of the scale, however, too short an interval is objectionable in that adaptation to the first stimulus may influence the apparent loudness of the second. It is believed that the combination of 1 second mark and space is the most suitable experimental arrangement which at the same time gives results representative of useful practice.

The electrical circuit included separate attenuators controlling the "reference" and "test" channels which were switched for final amplification by contacts operated by the sequence generator. The attenuator controlling the "test" stimulus had a range of 60 dB in 1 dB steps. The range over which the comparison stimulus was varied depended on the type of test, and was typically 35 or 40 dB for 2-fold ratio judgments. After a few initial judgments the stimuli were mainly confined to a narrower interval of 15 or 20 dB with occasional "easy" groups to prevent the observer as far as possible from memorising an absolute intensity. A test consisted of 25 to 40 groups, and a verbal judgment was recorded by the experimenter after each. The intensity of the comparison stimulus was varied in a nonsystematic way but attempts to employ tables of random numbers were not very successful owing to the inefficiency which resulted from the fact that the "equality" datum varied considerably from one observer to another. In practice a qualified randomisation was used, in which stimuli were offered in a random sequence around a rough placing of the "equality" point obtained fairly early in the test.

In ratio judgments, comparisons were not offered for judgment which lay on the wrong side of objective equality since it was found that this procedure was liable to be interpreted as a fault condition in which the order of presentation had been accidentally reversed. In all ratio judgments the reference stimulus was presented first[2] and was maintained constant throughout a test.

A team of 18 male and 7 female subjects was employed whose ages ranged from 18 to 52 and averaged 28. Some care was taken in the initial briefing of the team to avoid any mention of decibels, phons or sones. The instructions were cast in the simplest possible form, the observer being asked merely to state whether the loudness of the second sound heard was greater or less than twice (half, etc.) the loudness of the first.

6. Experimental results

The average results for each of the ratio tests are given first in Table II in terms of the decibel interval between reference and compared sounds.

Of the two measures of average shown those in the column headed $\Phi(\gamma)$ are the preferred values. They refer to the form of probit analysis described by **Guilford** [14] by which the best-fitting normal ogive curves are deduced with a preferential weighting for central values (see appendix A).

---

[2] **Garner** reports measurements in which the order was deliberately inverted. This procedure seems to be open to criticism, since the stimulus to be estimated has been withdrawn before the standard of comparison is disclosed.

Table II. Results of loudness ratio determinations

Series	Type of test	Sound used	Reference intensity dB rel. 0.0002 dyne/cm²	Average dB interval		Standard error of		Reference level [phon]	Average phon interval	Average figure of merit [dB]
				$\Phi(\gamma)$ (median)	mean	median	mean			
I	times 2	1000 c/s tone	29.6	17.6	17.7	1.6	1.2	29.6	17.6	2.6
			29.6	17.4	18.0	1.5	1.2	29.6	17.4	3.2
			39.6	17.2	17.0	1.2	0.8	39.6	17.2	3.6
			49.6	17.0	16.9	1.4	1.0	49.6	17.0	2.6
			54.6	17.0	16.9	1.2	0.8	54.6	17.0	3.0
			69.6	14.6	14.5	1.0	0.7	69.6	14.6	2.9
			82.6	10.3	9.6	0.8	0.5	82.6	10.3	3.0
			94.5(1)	10.3	10.3	1.1	0.7	94.5	10.3	2.7
II	times ½	1000 c/s tone	39.6	10.3	10.2	0.7	0.5	39.6	10.3	3.1
			52.6	11.6	11.7	1.0	0.8	52.6	11.6	2.6
			79.6	11.6	11.6	0.8	0.5	79.6	11.6	3.2
			82.6	10.6	10.6	0.9	0.6	82.6	10.6	3.0
			94.6	10.8	10.7	1.0	0.7	94.6	10.8	2.6
			109.6	10.3	10.2	1.1	0.7	109.6	10.3	3.5
III	times 2	white noise	18	12.7	12.9	2.0	1.1	32.5	17.5	3.6
			30	13.6	13.3	1.2	0.8	49.0	17.8	3.0
			40	14.5	14.7	1.6	1.1	62.4	16.0	2.4
			45	12.3	12.4	1.1	0.8	68.9	12.1	1.9
			60	11.3	11.5	1.1	0.7	83.1	9.0	2.1
			80	8.1	8.0	0.5	0.5	97.7	7.3	3.1
IV	times ½	white noise	28	7.3	7.3	0.6	0.4	46.4	10.4	2.5
			42	9.6	9.7	0.8	0.5	65.0	12.5	2.4
			50	10.0	10.1	0.9	0.6	74.1	11.6	2.3
			75	12.5	12.6	1.0	0.9	94.6	9.3	2.8
			95	12.3	11.7	1.1	0.6	111.9	11.9	2.6
V	times 10	1000 c/s tone	52.6	43.4	43.1	1.4	1.1	52.6	43.4	4.4
V	times 1/10	1000 c/s tone	80.6	38.2	38.3	2.4	1.7	80.6	38.2	6.5
VI	times 10	white noise	35	41.3	41.3	1.9	1.4	56.0	39.6	4.3
VI	times 1/10	white noise	60	32.5	33.0	1.7	1.2	83.1	37.6	4.2
VI	times 1/10	white noise	90	30.9	31.1	2.3	1.6	107.5	25.1	4.8
VII	times 2	reproductions of engine noises	93	8.0	7.8	0.5	0.4	90.5	8.0	3.7
VII	times 2		70	12.0	11.9	0.6	0.4	71.0	12.0	3.8
VIII	times 2	white noise	40(2)	13.1	13.6	1.5	0.9	62.4	14.8	2.8
VIII	times 1/2	1000 c/s tone	64.6(2)	12.8	12.4	1.3	0.9	64.6	12.8	2.8
VIII	times 1/2	white noise	93(2)	12.4	11.5	1.6	1.1	110.3	11.6	2.6
VIII	times 1/10	white noise	60(2)	30.9	32.5	1.7	1.3	83.1	35.4	4.2
VIII	times 1/10	white noise	90(2)	35.8	34.5	2.1	1.5	107.5	30.6	4.1
IX	times 2	1000 c/s tone	40(3)	18.0	18.7	1.6	1.2	40 approx.	18.0	2.7
X	times ½	1000 c/s tone	10 phons(4)	5.0	4.8	0.5	0.4	10	5.0	1.6

(1) For this experiment the observers' head position was reduced to 40 cm from loudspeaker.
(2) For these tests the silent interval was increased from 1 to 3 s.
(3) Monaural telephone test. The reference intensity was 40 ± 3 dB in 25 left ears.
(4) 10 phon means, in this case, 10 dB above individual minimum audible field.

The other measure of average shown is the arithmetic mean, obtained from estimations of individual decibel intervals from the test records, examples of which are shown in Table III. The values adopted were estimated from the test records to the nearest ½ dB.

7. Determination of equivalent loudness of the white noise and engine noises

In order to compare the results obtained in ratio judgments with the pure tone and the noises it was necessary to obtain accurate equivalent loudness data for the latter. The testing procedure was very similar to that used for the ratio judgments, the main differences being that a slightly larger team (30) was employed, and that "equality" judgments were positively excluded. The results were found to depend on the order of presentation of the noise and tone signals, the difference being 0.98 dB in the sense that preferential judgments of "louder" were made in case of the second sound heard. The "order" difference is highly significant by statistical test. A mean was taken in practice and the results for the white noise are shown in Fig. 2.

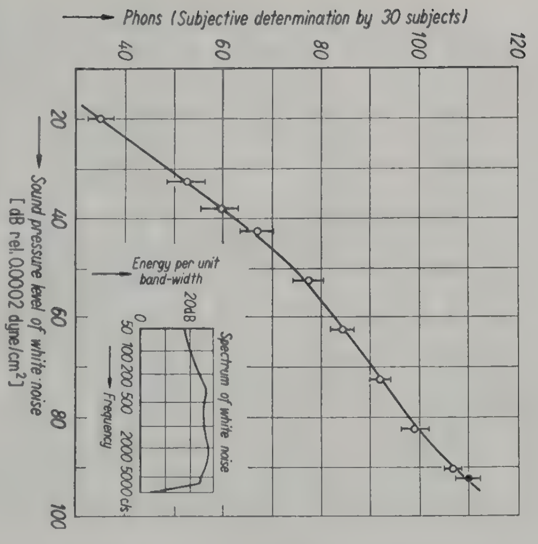

Fig. 2. Equivalent loudness of white noise.
Mean for 30 observers, with 98 % confidence limits;
● Data obtained by the method described in appendix B.

An interesting variant of the "constant-stimulus" method was used to determine the equivalent-loudness of white noise at the highest intensity. This is described in appendix B.

Table III. Specimen test records for loudness doubling

Observer	dB interval from objective equality																																								Value recorded	Figure of merit*
	0	1	2	3	4	5	6	7	8	9	10	11	12	13	14	15	16	17	18	19	20	21	22	23	24	25	26	27	28	29	30	31	32	33	34	35	36	37	38	39		
A	L		L		L	L	L	L	L	L	L	L	L	L	G	G	G	G	G	G	G	G		G			G				G					G				G	13.5	1
B	L	L		L	L	L	L	L	L	G	L	G	G	G	G	G	G	G		G		G	G	G				G						G							9.5	3
C		L	L		L	L	L	L	L	L		L	L	L	L	R	L	G	G	G	G	G	G	G		G	G	G		G		G		G				G			16.0	3
D	L		L		L	L	L	L	L	L	L	L	L	L	L	L	G	G	L	G	G	G	G	G	G	G	G	G	G		G	G	G	G			G				16.5	4
E		L		L	L	L	L	L	L	L	L	L	L	L	L	L	R	L	L	G	L	G	G	G	G	G	G	G		G	G	G	G			G				G	17.5	6
F	L	L	L	L	L	L	L	L	L	L	G	G	L	L	G	G	G	G	G	G	G		G	G		G	G	G	G		G		G			G		G			11.5	5

Key: L = test sound not loud enough, G = test sound too loud, R = about right.

* The number of dB steps between unbroken sequences of L and G judgments. The minimum value (1 dB) was recorded in 37 % of all tests.

8. Analysis of results of ratio-judgments

8.1. Table II shows the results of all the ratio-judgment tests, with the terminating levels of each interval expressed both in decibels and phons. When the intervals are expressed in phons in accordance with the experimental equivalent loudness determinations, the results for the different types of sound are in close agreement. This may be seen especially clearly in Fig. 3a and 3b[3]. It is important to note, however, that if the intervals are expressed in decibels alone, this concordance is largely lost.

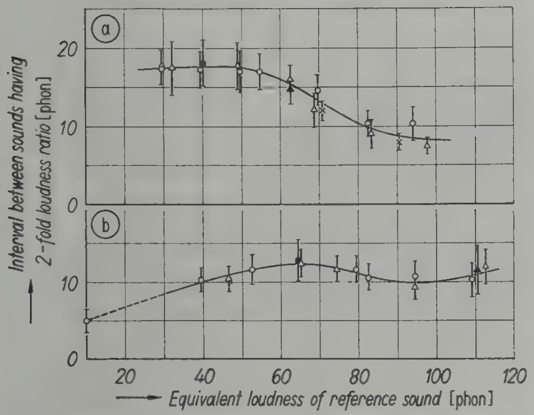

Fig. 3. Results of 2-fold loudness ratio estimations expressed in phons (average of 25 observers).
(a) Doubling judgments I 98 % confidence limits;
(b) Halving judgments I 98 % confidence limits.
○ 1000 c/s tone (free field),
△ white noise (free field),
● 1000 c/s tone (earphone),
■ 1000 c/s tone (free field) 3 second spaces,
▲ white noise (free field) 3 second spaces,
× reproductions of engine noises (free field).

The consistency between the results using 1000 c/s tone and the noises justifies single smooth curves to represent the data, as shown in Fig. 3a and 3b respectively. However, it is not possible to amalgamate the fractional and multiple data without offending both. They differ in the same sense as found by previous investigators [5], [8], namely, that the interval for doubling at low absolute intensities exceeds that for halving and the contrary at high intensities. The difference, which appears from Fig. 3 to be considerable in relation to the dispersion of the results, is certainly much less so in relation to the diversity of data by various authors. A tentative explanation of the effect is that it represents a predilection for *moderate* levels of the adjustable stimulus superimposed on and mildly biassing the judgment of pure ratio.

Not only do the various types of sound give results agreeing as to average but they also exhibit a high degree of consistency on the part of individual observers. This is illustrated in Table IVa, which shows the correlation between the various observers' average results for each of the four sets of tests I-IV.

Table IVa
Correlation between individual results for white noise and pure tone

Experimental series correlated	Correlation coefficient
I against III	0.64**
II against IV	0.79**
I, II against III, IV	0.77**

** indicates that the significance level was 0.001 or less, that is, the chance of obtaining such values by pure chance is less than one in a thousand.

Although, as mentioned above, the *mean* results for doubling and halving are significantly different, individual subjects nevertheless show substantial correlation in respect of this classification. This is illustrated in Table IVb.

Table IVb
Correlation between individual results for doubling and halving judgments

Experimental series correlated	Correlation coefficient
I against II	0.64**
III against IV	0.65**
I, III against II, IV	0.71**

** See note to Table IVa.

Loudness scales for loudness reduction and magnification are shown in Fig. 4. These are derived straightforwardly from the smooth curves of Fig. 3. The curve standardised by the A.S.A. [2] is shown for comparison, the data having been arbitrarily aligned at 75 phon. It will be seen that there is substantial similarity between the shapes of the curves, especially if the A. S. A. curve is compared with the geometric mean of the other two. To bring the data into coincidence the *logarithms* of loudness must be transformed by a scale factor.

8.2. Concordance of the results of 2-fold and 10-fold ratio judgments

The data from experiments V and VI are illustrated in Fig. 4. The general agreement between the direct observation of 10-fold ratios and data read from Fig. 4 (which is based on 2-fold ratios) is very close. These comparisons are shown in Table V. The only significant discrepancy occurs in the case of 10-fold reduction from the loudest reference level (white noise), and this is believed to be due to 1-second periods between the stimuli being insufficient when the first sound is excessively loud. When the same experiment was repeated with 3-second intervals the discrepancy was brought below the level of statistical significance. The point is further discussed in section *8.3.*

---

[3] The 98 % confidence bands shown on Fig. 3a and 3b extend ± 2.49 × standard error in phons about the mean values, 2.49 being the value of STUDENT's *t* for 24 degrees of freedom. They indicate that the true value lies within the bands shown with probability 0.98.

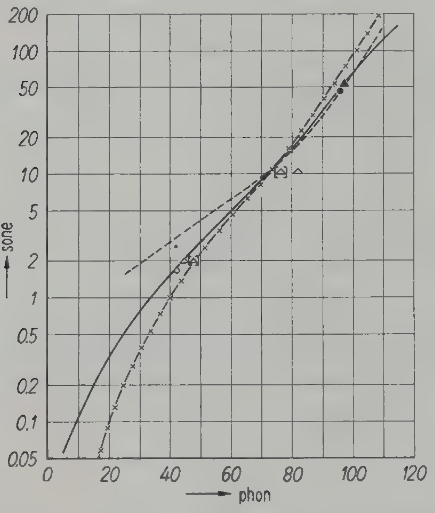

Fig. 4. Loudness function relating phon and sone scales.
——— this paper, loudness halving,
– – – – this paper, loudness doubling,
×——× American Standards Association data.
(Note: The curves are arbitrarily aligned at 75 phon. The American Standard defines 1 sone as the loudness of a 1000 c/s tone, having loudness level 40 dB above threshold i. e. 40 phon for normal observers.)

Results of 10-fold ratio tests
● 1000 c/s tone, 10-fold magnification (52.6),
▲ white noise, 10-fold magnification (56.0),
○ 1000 c/s tone, 10-fold reduction (80.6)
△ white noise, 10-fold reduction (107.5 and 83.1).
The figures in brackets are loudnesses of reference sounds in phon. The 10-fold reduction results shown thus [△] were obtained with the time sequence 1 second mark—3 seconds space.

It should be noted that the agreement is between 10-fold *magnification* and predictions from *doubling;* alternatively between 10-fold *reduction* and *halving*. The discrepancy between the halving and doubling intervals appears to persist in a general distinction between increasing and decreasing sensations, perhaps for the reason suggested in section *8.1.*

Table V
Comparison of phon intervals for 10-fold loudness ratios

Type of sound and equivalent loudness of reference sound in phons	Type of test	Interval for 10-fold loudness ratio in phons		Error of prediction [phon]
		Predicted from doubling (Fig. 4)	Observed	
1000 c/s tone 52.6	times 10	43.0	43.4	−0.4
white noise 56		41.3	39.6	+1.7
		Predicted from halving (Fig. 4)	Observed	
1000 c/s tone 80.6	times 1/10	39.1	38.2	+0.9
white noise 83.1		38.5	37.6	+0.9
white noise 107.5		33.9	25.1	+8.8
white noise* 83.1	times 1/10	38.5	35.4	+3.1
white noise* 107.5		33.9	30.6	+3.3

* In these cases only, the sequence of stimuli was 1-second mark, 3-seconds space.

The concordance illustrated by Table V is actually more deep-seated than the average figures show. By constructing curves of the type shown in Fig. 3 for each observer, individual predictions of the 10-fold range were made from 2-fold observational data. The correlation of the predicted and observed 10-fold intervals is shown in Table VI. It is strongly concluded that observers are individually and collectively consistent in making ratio judgments over the wide sensation range connoted by the numerals 2 and 10.

Table VI
Correlation of predicted and observed 10-fold ratio intervals

Type of sound and reference intensity, in dB rel. 0.0002 dyne/cm²	Type of test	Correlation coefficient between predicted and observed dB interval for 10-fold loudness ratio	Probability level
1000 c/s tone 52.6	times 10	0.60	0.003
white noise 35		0.53	0.011
1000 c/s tone 80.6	times 1/10	0.59	0.002
white noise 60		0.82	0.001
white noise 90		0.63	0.001
white noise* 60		0.66	0.001
white noise* 90		0.54	0.010
All 10-fold tests		0.59	0.001

* See note to Table V.

8.3. The effect of increasing the silent interval

It will be recalled from section 5 that some investigation was made of the extent to which the judgments of loudness ratio depended on the time interval between the stimuli (experiment VIII). In all, five tests were made with a time sequence different from that used in most of the tests. The mark periods of 1 second were not changed, but the space was increased to 3 seconds. These tests were suitably combined with others in which the normal 1:1 sequence was employed, in such a way as to provide controls on the effect under investigation. For ease of comparison, the relevant data are shown in Table VII. Four of the five results, involving the ratios 2, ½ and 1/10 and different types of sound, show no significant difference for the altered time sequence. The 2-fold results are seen to fit in quite well with the other data, as shown in Fig. 3.

The two results involving the ratio 1/10 are shown in Fig. 4. Only one of these is in significant disagreement with the appropriate loudness curve based on ½-fold data, namely, the case of 10-fold reduction from a disagreeably loud reference level. It seems possible that under this exceptional condition the shorter period of silence is not adequate for the ear to recover its sensitivity to the much quieter sound following. This is confirmed by the much reduced disagreement which resulted when the same test was repeated with longer silent spaces. Probably because the second sound has not so marked a contrast with the very loud reference sound no such difference was observed between the results of *halving* judgments at comparable intensities when the time sequence was altered.

It was concluded that with the one exception just discussed, the 1-second space period was adequate.

Table VII
Comparison of results for normal and altered time sequence

Type of sound and equivalent loudness of reference sound in phons		Type of test	Interval in phons	
			1 s mark 3 s space	1 s mark 1 s space
1000 c/s tone	64.6	times ½	12.8	12.6*
white noise	62.4	times 2	13.1	14.5
white noise	110.3	times ½	12.4	12.3+
white noise	83.1	times 1/10	30.9	32.5
white noise	107.5	times 1/10	35.8	30.9

* interpolated from results of Series II.
+ reference sound 111.9 phon.

8.4. Classification of the results by sex and experience

In most of the ratio tests, the average results for males and females were about the same, but the number of female subjects was too few to allow a precise conclusion to be drawn.

As far as the acoustical experience of the observers is concerned the conclusion reached is that this has no effect on the results. 17 out of the 25 persons employed had no special knowledge of the subject or none at all, and had had no previous experience of this kind of test.

8.5. The reliability of individual ratio judgments and the manner of variation of the 2-fold interval with absolute intensity level

In addition to the concordance between 2- and 10-fold ratio judgments which has already been discussed, there is substantial evidence that observers maintain a constant criterion over a considerable period of time.

An identical replication occurs in the case of the first two tests of series I, and in view of the null results of certain tests in series VIII and IX, it is admissible to regard these also as replications. The method of handling these data is outlined in appendix C and the conclusions may be briefly stated as follows:

(i) the error standard deviation is of the order 2.5-3.0 dB for 2-fold ratio tests, and greater though not proportionately greater for 10-fold tests,

(ii) the results of individual observers show a strong constant tendency with regard to their departures from average,

(iii) the trend of the curves shown in Fig. 3a and 3b is broadly speaking the same for all observers.

9. The effect of earphone listening (experiment IX)

Comparison data for 1000 c/s loudness doubling judgments at 40 dB using the free field and monaural earphone methods may be seen in Table II (cf. IX and the third of I). In view of the null result only one such test was made. The result is also shown in Fig. 3a. The small difference observed (0.85 phon) offers no basis for an explanation of the discrepant results in the literature.

The earphone test was made using a pair of moving-coil telephones, only one of which was energised. The force of application was 400 g-weight. Probe microphone measurements showed that the sound pressure varied by ± 3 dB from one ear to another for constant excitation.

Most observers commented unfavourably on the monaural earphone test, particularly because adventitious noises of physiological origin or from the clothing seemed so much more noticeable than when listening to the loudspeaker.

10. The nature of the loudness scale near the absolute threshold

The limiting behaviour of the loudness scale close to the absolute threshold is of theoretical interest. Most of the previous data indicate a progressive diminution of the intensity interval for a ratio of half-loudness as intensity level decreases, but the data appear to be inconclusive. If it were not for the essentially quantal nature of the sensation of loudness, the intensity intervals for a given ratio would ultimately have to contract to infinitesimal values to accommodate infinite subdivision of the scale.

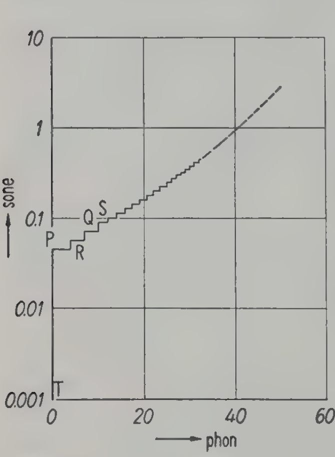

Fig. 5. Diagrammatic form of a possible loudness function for an observer with normal threshold. (N. B. The width of the horizontal steps, representing the differential intensity threshold and the particular form of the curve shown, are not intended to have any but diagrammatic significance.)

Fig. 5 shows diagrammatically a possible loudness function for an observer with normal auditory threshold. Suppose S has been found to sound twice as loud as P, and that Q is then used as the reference level for judgments of halving. Evidently both R and P will be "greater than half", whilst T is inaudible. In such a test, then, one would obtain a test record consisting exclusively of "greater" and "inaudible" judgments, no audible stimulus appearing to be "less than half".

In the actual tests the 25 subjects were each asked to make loudness ratio judgments on stimuli-pairs, the first of which was adjusted to 10 dB above the *individual* minimum audible field intensity at 1000 c/s (experiment X). In practice difficulty was experienced in preventing some of the subjects from making bisection judgments and the results are inconclusive. The mean phon interval for halving actually found was about 5, but this figure excludes 2 test records which did in fact consist exclusively of "greater" and "inaudible" judgments. In view of the fact that 5 phon is little more than the accepted value of the differential threshold [15], little reliance can be placed on the result.

11. Assessment of previous data

An attempt has been made to reassess the available data, which include three new determinations since the review given by Churcher [16] in 1935. Only such results are considered as are properly comparable, which entails the omission of a large part of the work of Laird and of Ham. The data for comparison are shown in Fig. 6a-h together with an abridged annotation of the test conditions.

In the case of Laird, only the data for 1024 c/s are shown. Data for other frequencies are omitted. It may be noted that Laird and his co-authors remarked on the consistency of their results for various frequencies, but this agreement would appear to be more apparent than real, since the results were compared in decibels rather than in terms of equivalent loudness.

Ham and Parkinson's procedure required the subject to estimate a percentage loudness relation between fixed stimuli. From the results given in their paper a loudness scale can be directly derived. The data for Fig. 6b were determined from such a scale, obtained by averaging their 350, 1000 and 2500 c/s data.

Fig. 6c and d shows the 2- and 4-fold data from Geiger and Firestone's paper, the latter being included by appropriate adjustment. It is noteworthy that the 2- and 4-fold data are in reasonable agreement. It is also true that the 10- and 100-fold data are concordant with the 2- and 4-fold data as may be confirmed by constructing loudness scales from Fig. 6c and d and comparing the 10- and 100-fold results given in their paper. Geiger and Firestone seem to have over-emphasised the discrepancy between their results for different numerical ratios. There is some doubt, however, whether all the intervals reported by Geiger and Firestone are not too small. The author's experience is that a 100-fold judgment could not be made from a starting-point as high as 55 dB, whilst a 1/100-fold judgment from 30 dB is virtually a determination of one difference limen or so above absolute threshold. The fact that Geiger and Firestone criticised Laird for presenting a rather wide range of stimuli suggests that they may themselves have tended too far in the opposite direction.

The halving data from Churcher, King, and Davies' paper are shown in Fig. 6e. Their ¼-fold data are included by a suitable adjustment.

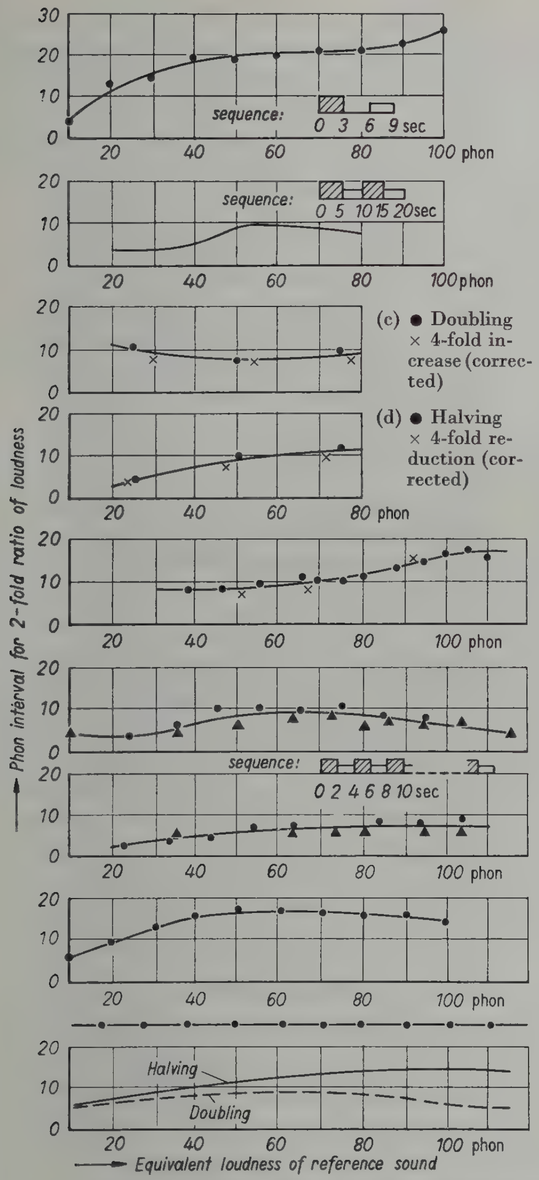

(a) Laird, Taylor and Wille
Constant-stimulus method, 10 observers. Monaural earphone listening. Halving, 1024 c/s).

(b) Ham and Parkinson
Method: Subjective assessment of fractional reduction as percentage. Free-field listening, ca. 50 observations per point selected from 175 observers.
Data for 50 % reduction (derived from average loudness function for 350, 1000 and 2500 c/s).

Geiger and Firestone
Average-error method.
Binaural earphone listening.
ca. 40 observations per point (number of subjects not known); 1000 c/s.

(e) Churcher, King and Davies
Average-error method. 34 observers. Binaural earphone listening. 800 c/s.
● Halving
× 4-fold reduction (corrected)

(f) Doubling
● 1000 c/s
▲ white noise

(g) Halving
● 1000 c/s
▲ white noise

Pollack
Average-error method. 7 observers. Monaural earphone listening.

(h) Garner
Average-error method. 18 observers. Monaural earphone listening. Halving, 1000 c/s.
Sequence: mark 1s, space 1s, mark 1s, space 3s (repeated).

(i) Smoothed unweighted average of previous determinations.
These data may be compared with Fig. 3.

Fig. 6. Previous determinations of phon interval for 2-fold loudness ratio.

The data for 1000 c/s doubling and halving given by Pollack are replotted directly. The data for noise have been converted to phons and phon intervals by means of Fig. 2 of Pollack's paper, and are included in Fig. 6f and g. Although the data for noise and tone are somewhat discrepant a mean curve has been drawn to represent both, for halving and doubling respectively.

The halving results of Garner for a tone of 1000 c/s are replotted in Fig. 6h.

By averaging the ordinates of the curves in Fig. 6 the fairly smooth curves shown in Fig. 6i result. There are six determinations of the halving interval but only two of the doubling interval, contributing to these averages. The results of the present determinations conform quite well to the average halving curve but rather less well to the doubling curve (cf. Fig. 3). Unfortunately the only comparison data for loudness doubling are those from the papers by Geiger and by Pollack who happen to be those whose results for halving are much smaller than others. This may be the reason for the relatively poor agreement between the curves of Fig. 3b and 6i.

The curves of Fig. 6i taken in conjunction with Fig. 3 suggest that a reasonable approximation to the function for loudness reduction is given by the formula $\log S = 0.029(P - 40)$ for the range 20-110 phon, the loudness being S in the sone scale and P in the phon scale. At lower intensities the function must be regarded as undetermined.

It is difficult to find systematic procedural differences between the various results which correlate with the discrepancies, except possibly on the basis of the duration of the interval of silence between presentation of stimuli. For instance, LAIRD, GARNER and the author, using 1 or 3 second intervals, obtain intervals higher than most, whereas HAM and POLLACK obtained low values. In HAM's procedure there was no interval of silence; the same is inferred from POLLACK's paper though the description given is not entirely clear on this point. In the view of the author, tests conducted without a silent interval are of doubtful relevance to the main purposes of the sone scale.

12. Conclusions

The conclusions drawn from this investigation of the relation between the sone and phon scales are as follows:

(1) Highly consistent loudness scales are obtainable by direct subjective ratio estimations. Estimates of the loudness scale obtained by loudness ratio judgments involving the numeral "2" agree closely with those obtained using "10".

(2) The scale for loudness reduction and also for magnification proved to be closely the same for entirely different types of sound, namely, a pure tone of 1000 c/s, a "white noise" with a spectrum level approximately constant up to 6000 c/s, and reproductions of engine noises.

(3) There is a significant difference between the scales relating to increase and decrease of sensation respectively, especially at low levels of loudness. The interval on the phon scale for a given loudness ratio is approximately constant for *decreasing* sensation, but for loudness *magnification* it decreases as the absolute loudness is raised.

(4) The shape of the function defining the loudness scale for individual observers is much the same for all observers.

(5) The results of the present work combined with data from other determinations indicate that there is no appreciable difference between the results for free-field and earphone listening.

(6) Judgments are not affected by a substantial change in the period of silence elapsing between the test sounds if this is of the order of seconds. There is some indication from comparisons with other work that the apparent loudness change is greater if no silent period is used. However, the use of judgments in which the sounds are presented without a gap does not seem to be relevant to the main objectives of the sone scale.

(7) The scale based on loudness reduction from the present investigation is in fair agreement with previous work. The results may be approximated by the formula:

$$\log S = 0.029(P - 40)$$

for the range 20-110 phons,

P being the loudness level in phons and S the loudness sensation in sones. No simple formula expresses the results for loudness magnification.

Acknowledgements

The author wishes to acknowledge the cooperation of the staff of the Physics Division, National Physical Laboratory, who took part in the subjective tests, and many valuable discussions with Mr. R. S. DADSON. The work described has been carried out as part of the research programme of the National Physical Laboratory, and the paper is published by permission of the Director of the Laboratory.

(Received 29th January, 1953.)

APPENDIX A

Estimates of the average in loudness ratio tests

The method which was preferred was a form of probit analysis [14]. The data to be fitted were the total judgments cast in favour of the "test" sound exceeding the datum of comparison. In the present results, "about right" judgments were relatively infrequent and were counted as half a vote, thus avoiding the complication of deducing separate but barely distinguishable ogives for "exceeding" and "falling short" respectively. In every case the fit of the observed data to the best-fitting normal ogive ranged from good to exceptionally good by the chi-square test. Two specimens are shown in Fig. 7. The process employed (URBAN's constant process) estimates a median. The corresponding standard error, $1.253 s_1/\sqrt{n}$, is given in Table II. s_1, which is an estimate of the standard deviation of the parent population, is inversely related to the abruptness of transition of the ogive curves.

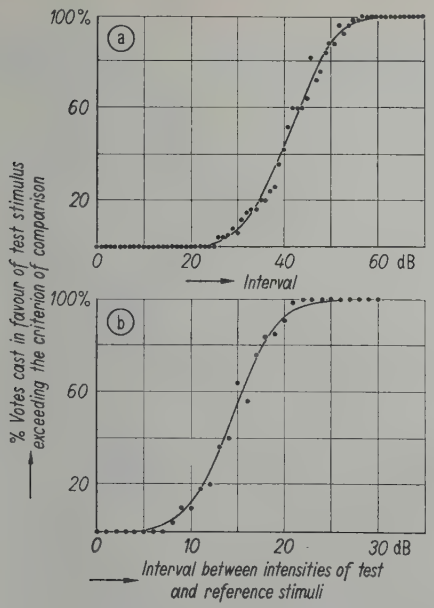

Fig. 7. Specimen test results with ogive curves fitted by URBAN's process.

(a) White noise, 10-fold increase judgments, reference intensity 35 dB rel. 0.0002 dyne/cm^2.
(Estimate of median intensity interval (50 % votes) = 41.3 dB.)

(b) 1000 c/s tone, double-loudness judgments, reference intensity 69.6 dB rel. 0.0002 dyne/cm^2.
(Estimate of median intensity interval (50 % votes) = 14.6 dB.)

The arithmetic mean result was obtained as described in the text and was distinct from, though generally quite close to, the median obtained from the ogive curves. The standard error of the mean, which has also been shown in Table II is $s_2/\sqrt{n}$, s_2 being the observed standard deviation of the individual estimates obtained from the test records. s_2 is generally more optimistic than the cognate statistic s_1.

APPENDIX B

A variant of the "constant-stimulus" method

A special method was applied to the determination of the equivalent loudness of white noise at the highest intensity. Since this procedure has other applications it is considered worth describing in detail. In the usual constant-stimulus method, it is necessary to have in hand quite a wide range, at least sufficient to carry the "test" signal well beyond the balance point for extreme observers. For loud levels of the reference signal this requirement becomes very difficult to meet. The case of 92.4 dB (white noise) affords a good illustration. Extrapolation from determinations at lower intensities predicates a mean result of some 110 phon (Fig. 2) with a spread of perhaps 20 phon. The extreme observer may be expected to judge equality at about 120 phon. Consequently the circuit would have to be capable of reproducing 1000 c/s signals of up to 130 dB. This was beyond the undistorted capacity of the available loudspeakers at the 1 metre listening position.

A method is available for substantially reducing the maximum level required; indeed, in principle, levels falling slightly short of the predicted average may suffice. In the present case that would be, say, 110 dB. Instead of presenting numerous pairs of stimuli to one observer, a single comparison repeated any number of times is offered. This is arranged to lie fairly close to the predicted average result. A single judgment is recorded for each subject. The process is repeated on subsequent occasions at one or two other intensities of the 1000 c/s signal in a fairly narrow range. The fractions of observers judging "test stimulus louder" are then used to deduce a normal ogive curve by the same process described in appendix A. The curve is interpolated (or even extrapolated) to the 50 % fraction. This method has been found to be in excellent concordance with the conventional procedure (Fig. 2). The observed fractions and the best-fitting ogive are shown in Fig. 8 for the case cited. Some of the observers at no time judge the test stimulus louder, consequently the ogive curve must be assumed to be symmetrical. There is ample justification for this by reference to the corresponding curves at lower intensities, which of course are determinate over their whole length.

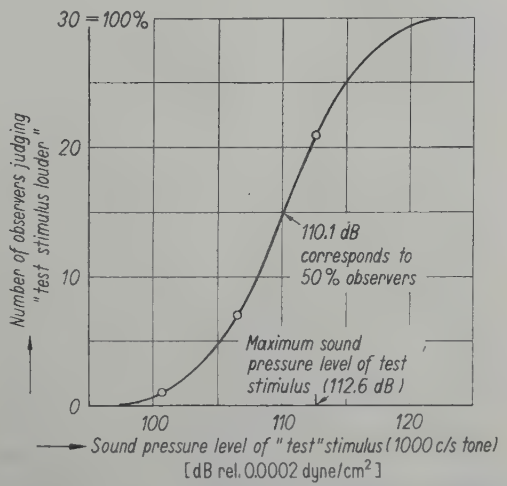

Fig. 8. Ogive curve determining the equivalent loudness of white noise. (Sound pressure level of white noise 92.4 dB rel. 0.0002 dyne/cm^2.)

APPENDIX C

Statistical analysis of 2-fold test results

The analyses of variance for series I-IV are shown in Table VIII. The components of variance between individuals and between reference intensities are significant in each case in relation to the error variance. Evidence of "observer × intensity" interaction is necessarily indirect. The residual variances shown in Table VIII contain this interaction, if any, together with random error.

Table VIII
Analysis of variance and coefficients of concordance

Group of tests	"Between individuals" variance		"Between intensities" variance		Residual variance		Coefficient of concordance	Probability on the random hypothesis
	(dB)^2	DF*	(dB)^2	DF	(dB)^2	DF		
I	9.5	24	9.6	6	7.9	144	0.593	<0.0001
II	5.5	24	4.2	6	6.6	144	0.530	<0.0001
III	7.5	24	4.0	5	9.7	120	0.481	<0.0001
IV	3.5	24	3.9	4	4.3	96	0.538	<0.0001

* DF signifies the number of degrees of freedom.

The further analysis of the residual variance requires an independent estimate to be made of the error variance. This is possible on the basis of sample replication data shown in Table IX.

Table IX
Replication data from doubling tests

Test replicated	Shift of average [phon]	Estimates of error variance (dB)^2	Known difference
(i) 1000 c/s tone, × 2, 29.6 dB	0.20	13.5	lapse of 3 months
(ii) white noise, × 2, 40 dB	1.20	2.6	mark/space ratio
(iii) 1000 c/s tone, × 2, 39.6-40 dB	0.85	20.4	earphone vs free field plus lapse of 12 months
(iv) white noise, × ½, 93-95 dB	0.30	10.9	mark/space ratio plus lapse of 5 months

The estimates of error variance in (i), (iii) and (iv) of Table IX are homogeneous by **Barlett**'s test. The estimate in (ii) is abnormally low, but can probably be left out of account in view of the much shorter lapse of time between the tests compared (a matter of minutes) as being too optimistic. The error variance is estimated to be of the order 14 dB^2 for 2-fold tests in general. This is actually rather larger than the residual variances shown in Table VIII, and must therefore account for the whole of it. The conclusion is that the estimates of error variance (Table IX) and the residual variances (Table VIII) are estimates of the same variance, and that consequently there is no significant component of variance arising from observer × intensity interaction.

The same conclusion is reached by calculating the coefficients of concordance [17] for the respective series of experiments. This statistic, which is obtained by placing the observed decibel intervals in rank order and summing over the various intensities, expresses the extent to which the observers giving high or low intensity intervals continue to do so at each absolute intensity. In the presence of a large observer × intensity interaction, the rankings would become confused and the coefficient of concordance would be low. The very high coefficients actually found for each experimental series I-IV strongly support the view that this interaction is not present to any extent, and that individuals on the whole maintain a constant tendency with regard to their departure from average. The significance of the coefficients of concordance is estimated by the f-test against the variance to be expected with random ranking. The details are shown in Table VIII.

References

[1] Brit. Stand. BS. 661: 1936.
[2] Amer. Stand. Z24. 2-1942.
[3] **Laird**, D. A., **Taylor**, E. and **Wille**, H. H., J. acoust. Soc. Amer. **3** [1932], 393.
[4] **Ham**, L. B. and **Parkinson**, J. S., J. acoust. Soc. Amer. **3** [1932], 511.
[5] **Geiger**, P. H. and **Firestone**, F. A., J. acoust. Soc. Amer. **5** [1933], 25.
[6] **Churcher**, B. G., **King**, A. J. and **Davies**, H., J. Instn Elect. Engrs. **75** (454), [1934], 401.
[7] **Pollack**, I., J. acoust. Soc. Amer. **23** [1951], 654.
[8] **Garner**, W. R., J. acoust. Soc. Amer. **24** [1952], 153.
[9] **Fletcher**, H. and **Munson**, W. A., J. acoust. Soc. Amer. **5** [1933], 82.
[10] **Kellogg**, W. W., Archives of psychology No. 106 New York 1929.
[11] **Stevens**, S. S., Handbook of experimental psychology, J. Wiley & Sons, New York 1951, p. 44.
[12] **Churcher**, B. G. and **King**, A. J., J. Instn Elect. Engrs. **81** (487) [1937], 57.
[13] **Munson**, W. A., J. acoust. Soc. Amer. **19** [1947], 584.
[14] **Guilford**, J. P., Psychometric methods. McGraw-Hill Book Co., New York 1936, Ch. VI.
[15] **Licklider**, J. C. R., Handbook of experimental psychology. J. Wiley & Sons, New York 1951, p. 999. The magnitude of the differential threshold is about 5 phon near the absolute threshold and falls to about 1 phon at 40 dB. See also **Stevens**, S. S. and **Davis**, H., Hearing. J. Wiley & Sons, New York 1948, p. 138.
[16] **Churcher**, B. G., J. acoust. Soc. Amer. **6** [1935], 216.
[17] **Kendall**, M. G., Advanced theory of statistics, Vol. I. Charles Griffin & Co., Ltd., London 1943, p. 410.

THE DIRECTIVITY OF SPHERICAL MICROPHONES

by R. L. PRITCHARD

Schenectady, N. Y., U.S.A.

Summary

By employing the reciprocity principle, alternative solutions for the response of spherical microphones considered recently by W. KUHL are given in terms of the response for sound emission. An existing solution for the sound field radiated from a vibrating spherical cap is used to calculate the directional response of a cylindrical microphone mounted in a sphere. Similarly, the frequency response of a completely spherical (non-directional) microphone is calculated with the help of the electroacoustic reciprocity theorem. Results of numerical computations for each type of calculation are given and are compared with KUHL's results, which were obtained by direct integration of the sound pressure over the active surface of the sphere.

Sommaire

On indique, en appliquant le théorème de réciprocité, deux solutions au problème de la réponse à une émission sonore des microphones sphériques considéré récemment par W. KUHL. On calcule la réponse directive d'un microphone cylindrique monté dans une sphère, en utilisant des résultats antérieurs obtenus dans le calcul du champ sonore émis par une capsule sphérique qui vibre. De même, on calcule au moyen du théorème de réciprocité électro-acoustique la réponse en fréquence d'un microphone entièrement sphérique (non directif). On donne les résultats numériques obtenus pour chaque mode de calcul et on les compare avec les résultats de KUHL qui proviennent d'une intégration directe de la pression sonore sur la surface active de la sphère.

Zusammenfassung

Unter Verwendung des Reziprozitätsprinzips werden weitere Lösungen für die Richtcharakteristik kugelförmiger Mikrophone, wie sie kürzlich von W. KUHL behandelt wurden, aus der Richtcharakteristik bei Schallabstrahlung bestimmt. Eine Lösung für das Schallfeld bei Abstrahlung von einer schwingenden Kugelkappe wird benutzt, um die Richtcharakteristik eines in eine Kugel eingebauten zylindrischen Mikrophons zu berechnen. In ähnlicher Weise wird mit Hilfe des elektroakustischen Reziprozitätstheorems die Frequenzkurve eines kugelförmigen Mikrophons ohne jegliche Richtwirkung bestimmt. Numerische Ergebnisse für jede Berechnungsmethode sind angegeben und werden mit den von KUHL durch direkte Integration über die wirksame Kugeloberfläche gewonnenen Resultaten verglichen.

In a recent paper [1], W. KUHL has calculated the directional response of a cylindrical microphone of diameter $2d$ mounted in a sphere of radius a as shown in Fig. 1. The method employed was that of numerically integrating over the spherical cap $0 \leqq \Theta \leqq \Theta_0$ (which corresponds approximately to the circular area of the microphone diaphragm) the sound pressure existing on a rigid sphere [2] due to a plane wave incident upon the sphere from the direction Θ. In a similar manner, the frequency response of a completely spherical microphone also was calculated.

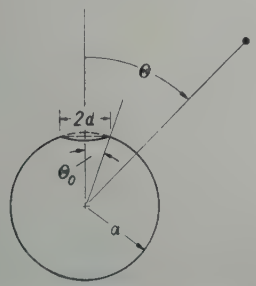

Fig. 1. Cylindrical microphone of diameter $2d$ in a sphere of radius a; approximation by spherical cap of angle Θ_0.

It is the purpose of this paper to point out that exact solutions to the problems considered by KUHL may be obtained by employing the reciprocity principle. In the first case, the directional response of the spherical cap for reception of an incident plane wave is identical with the directional response of a radiating spherical cap. For the second problem, the frequency response of the spherical microphone in sound reception may be calculated from the easily-determined frequency response for sound transmission with the help of the electroacoustic reciprocity theorem.

A radiating spherical cap is defined as a rigid sphere having a radial velocity distribution that is a function only of the polar angle Θ and is defined as

$$v(\Theta) \equiv \begin{cases} v_0 & 0 \leqq \Theta < \Theta_0, \\ 0 & \Theta_0 < \Theta \leqq \pi. \end{cases}$$

An exact solution for the sound field radiated from such a source with an arbitrary cap angle Θ_0 has been given by MORSE [3] and by STENZEL [4]. The directional response $f(\Theta,\Theta_0)$ may be defined as the ratio of the sound pressure at a large distance r in the direction Θ radiated by the spherical cap of angle Θ_0 to the pressure that would be produced at the distance r by a non-directional radiator of equivalent strength. (Equivalent strength is defined as the product of the normal velocity v_0 and the radiating surface area of the cap.) In the notation of STENZEL, $f(\Theta,\Theta_0)$ may be written as

$$f(\Theta,\Theta_0) = \frac{1}{(1-\cos\Theta_0)} \cdot \sum_{n=0}^{\infty} \mathrm{j}^{n+1} \left[\frac{\mathrm{P}_{n-1}(\cos\Theta_0) - \mathrm{P}_{n+1}(\cos\Theta_0)}{\mathrm{U}_n(ka) + \mathrm{j}\mathrm{V}_n(ka)} \right] \mathrm{P}_n(\cos\Theta), \tag{1}$$

where $k = 2\pi/\lambda$ is the phase constant (λ = wavelength of radiated sound), $\mathrm{P}_n(\cos\Theta)$ is the Legendre function of the first kind, $\mathrm{P}_{-1}(\cos\Theta_0) \equiv 1$, and $\mathrm{U}_n(ka)$ and $\mathrm{V}_n(ka)$ are functions involving combinations of the Bessel functions $\mathrm{J}_{m+1/2}(x)$ of half-integer order:

$$\begin{aligned} \mathrm{U}_n(x) &\equiv (\pi x/2)^{1/2} [x \cdot \mathrm{J}_{n+3/2}(x) - n\,\mathrm{J}_{n+1/2}(x)], \\ \mathrm{V}_n(x) &\equiv (-1)^{n+1} (\pi x/2)^{1/2} [x \cdot \mathrm{J}_{-n-3/2}(x) + \\ &\qquad + n\,\mathrm{J}_{-n-1/2}(x)]. \end{aligned} \tag{2}$$

By the reciprocity principle, it can be shown that $f(\Theta,\Theta_0)$ also represents the ratio of the average pressure existing over the surface of the spherical cap of angle Θ_0 due to a plane wave incident upon the sphere from the direction Θ to the free-field sound pressure due to the incident plane wave. This latter ratio is the directional response considered by KUHL. A proof of the equivalence of the two directional responses is given in the Appendix.

When Θ_0 is set equal to zero[1], corresponding to a point radiator at the (north) pole of the sphere, the right-hand member of eq. (1) becomes identical with the expression (eq. (35)) used by SCHWARZ [2] for the relative pressure existing at a point on the sphere due to an incident plane wave. The reciprocal relation between the sound field due to a point radiator on a sphere and the sound pressure at a point on the sphere due to an incident plane (or spherical) wave was pointed out first by RAYLEIGH [5], and has been noted by many writers [6].

STENZEL has given many graphical illustrations of the variation of the function $f(\Theta,\Theta_0)$ with Θ for $ka = 10$ for different values of Θ_0. However, the particular case of $\Theta_0 = 20°$, which corresponds to the value considered by KUHL, is not included. On the other hand, numerical values of the coefficients (the bracketed terms) in the series of eq. (1) have been given by STENZEL [7] for the case of $ka = 10$, $\Theta_0 = 20°$. Using these coefficients, the writer has calculated the directional response for this particular case. The results are indicated by points in Fig. 2, where the solid curve is a tracing of the curve calculated by KUHL and shown in his Fig. 6 as curve b. The agreement is quite good, except for values of Θ between 160° and 180°. In this region, the sound pressure at a point on the sphere changes quite rapidly with Θ (cf. curve a of KUHL's Fig. 6), and consequently reduced accuracy might be expected with the numerical integration used by KUHL. It might be noted that the values indicated by the points in Fig. 2 for Θ between 160° and 180° are in fairly good agreement with the experimentally-obtained values of KUHL (cf. the crosses, or curve c, in KUHL's Fig. 6).

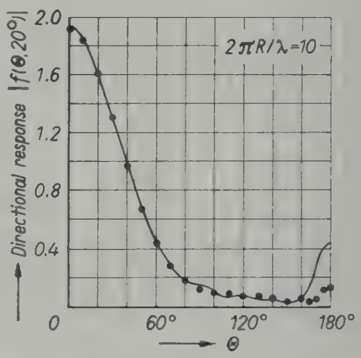

Fig. 2. Magnitude of the directional response $f(\Theta,\Theta_0)$ of a spherical cap of angle $\Theta_0 = 20°$ as a function of the angle Θ of arrival of an incident plane wave, for $ka = 10$. Solid curve: tracing of KUHL's calculated curve; points: values calculated from eq. (1) above.

In the conclusion of his paper, KUHL has calculated the frequency response of a completely spherical microphone by graphical integration of the sound pressure over the surface of the sphere. This problem also may be solved exactly by employing the electroacoustic reciprocity theorem. The free-field voltage response (sensitivity) of a microphone, or the ratio of the open-circuit voltage e_{oc} at the microphone terminals to the free-field pressure p_0 at the location of the microphone, may be calculated in terms of the transmitting current response, or the ratio of the sound pressure p_s produced at a large distance r

---

[1] When Θ_0 is set equal to 0, the factor $(1-\cos\Theta_0)^{-1}$ $[\mathrm{P}_{n-1}(\cos\Theta_0) - \mathrm{P}_{n+1}(\cos\Theta_0)]$ reduces to $(2n+1)$.

from the microphone acting as a sound source when a current i_s is applied to the terminals, by the relation [8]

$$|e_{oc}/p_0| = |p_s/i_s|(2r\lambda/\varrho c). \qquad (3)$$

Here, ϱc is the characteristic impedance of the medium, and λ is the wavelength of the radiated and received sound.

To determine the ratio p_s/i_s, the radial velocity v_0 of the sphere (assumed to be constant over the entire spherical surface) may be introduced; thus

$$p_s/i_s = (p_s/v_0)(v_0/i_s). \qquad (4)$$

The first term, due to sound-radiation considerations only, may be determined readily from the solution for the sound pressure due to a zero-order vibrating sphere of radius a as [9]

$$(p_s/v_0) = (\varrho c a/r)(ka)[1+(ka)^2]^{-1/2}. \qquad (5)$$

On the other hand, the ratio (v_0/i_s) of eq. (4) depends upon the nature of the electromechanical system. For an electrostatic transducer, the velocity is directly proportional to the a–c charge, $i_s/j\omega$, where ω is the circular frequency ($\omega = kc$), and is inversely proportional to the mechanical impedance [10]. With a stiffness-controlled mechanical system, i.e., for frequencies below the fundamental-resonance frequency of the diaphragm, as assumed by Kuhl, the mechanical impedance is inversely proportional to frequency. Hence, in this frequency range, v_0 becomes directly proportional to applied current, independent of frequency. Under these conditions, the microphone sensitivity is directly proportional to the function (p_s/v_0) and to wavelength. Thus, combining eqs. (3), (4), and (5),

$$|e_{oc}/p_0| = (4\pi a^2)|v_0/i_s|\cdot[1+(ka)^2]^{-1/2}. \qquad (6)$$

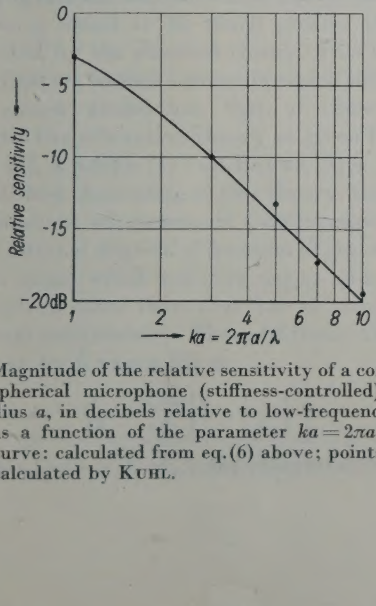

Fig. 3. Magnitude of the relative sensitivity of a completely spherical microphone (stiffness-controlled), of radius a, in decibels relative to low-frequency value, as a function of the parameter $ka = 2\pi a/\lambda$. Solid curve: calculated from eq. (6) above; points: values calculated by Kuhl.

A curve of the frequency-dependent term of eq. (6), i.e., the term within the brackets, expressed in decibels relative to the low-frequency value of unity, is shown in Fig. 3 as a function of the parameter $ka = 2\pi a/\lambda$. The points in Fig. 3 represent values calculated by Kuhl, which were obtained from his Fig. 8. In general the agreement is fairly good.

In conclusion, the writer would like to emphasize that the reciprocity theorem is a useful tool for solving problems of sound reception and transmission. Quite often, as in the cases described above, it is easier to solve the sound-radiation problem than to solve the corresponding problem in sound reception.

Appendix

A proof of the equivalence of the directional response of the spherical cap for sound reception with that for sound transmission may be constructed by the use of the Green's function, along the lines employed by Foldy and Primakoff [11] for a general proof of the electroacoustic reciprocity theorem. For further details of this method, the reader is referred to their paper [12].

Points in space will be described by a radius vector $\vec{R}$ from the origin of an arbitrary coordinate system, while a point on the surface of the sphere will be denoted by $\vec{r}$. The Green's function for the spherical surface S is denoted by $G(\vec{R},\vec{R}')$. Physically, $G(\vec{R},\vec{R}')$ represents the pressure at the point $\vec{R}$ due to a point source of sound of unit stength at point $\vec{R}'$ in the presence of the surface S when the latter is perfectly rigid. From the symmetry of the Green's function, $G(\vec{R},\vec{R}') = G(\vec{R}',\vec{R})$, there follows the reciprocity theorem for the sound field.

When the spherical cap is to be used as a sound radiator, the pressure $p(\vec{R}_0)$ at a point $\vec{R}_0$ may be written as [11], [12]

$$p(\vec{R}_0) = (j\omega\varrho/4\pi)\iint_S G(\vec{r},\vec{R}_0)\, v_n(\vec{r})\, dS. \qquad (A1)$$

The integral is taken over the surface S of the sphere, and $v_n(\vec{r})$ is the normal velocity on the surface S (positive normal outward from the surface). An $e^{j\omega t}$ time dependence is assumed. Over the spherical cap ($0 \leq \Theta \leq \Theta_0$ of Fig. 1) $v_n(\vec{r}) \equiv v_0$, while $v_n(\vec{r}) = 0$ elsewhere on the sphere. On the other hand, the pressure at the point $\vec{R}_0$ due to a point source of strength $v_0 S_{cap}$ located at the centre $\vec{R}_c$ of the sphere may be written as

$$p_0(\vec{R}_0) = (j\omega\varrho v_0 S_{cap}/4\pi)\, e^{-jk|\vec{R}_0-\vec{R}_c|}/|\vec{R}_0-\vec{R}_c|, \qquad (A2)$$

where S_{cap} denotes the surface area of the cap. The directional response f_T for sound transmission may be defined as the ratio $p(\vec{R}_0)/p_0(\vec{R}_0)$, which is a function of the direction defined by the vector $\vec{R}_0 - \vec{R}_c$, for a constant $R \equiv |\vec{R}_0 - \vec{R}_c|$; thus

$$f_T = [\iint_S G(\vec{r}, \vec{R}_0)\, v_n(\vec{r})\, \mathrm{d}S]/[v_0 S_{cap}\, \mathrm{e}^{-\mathrm{j}kR}/R]. \quad \text{(A 3)}$$

For sound reception by the spherical cap, a point source of strength Q is located at the point $\vec{R}_0$. In this case, the pressure $p_g(\vec{r})$ existing at a point $\vec{r}$ on the sphere is given by

$$p_g(\vec{r}) = (\mathrm{j}\,\omega\varrho Q/4\pi)\, G(\vec{r}, \vec{R}_0).$$

If the point $\vec{R}_0$ is at sufficient distance from the sphere, the wavefront due to the point source will be substantially plane at the sphere. The average pressure over the spherical cap may be written as an integral over the entire sphere by introducing the function $v_n(\vec{r})/v_0$ used above to define the location of the cap in the arbitrary coordinate system. Thus,

$$\begin{aligned} p_{avg} &= (1/v_0 S_{cap}) \iint_S p_g(\vec{r})\, v_n(\vec{r})\, \mathrm{d}S \qquad \text{(A 4)} \\ &= (1/v_0 S_{cap})\, (\mathrm{j}\,\omega\varrho Q/4\pi) \iint_S G(\vec{r}, \vec{R}_0)\, v_n(\vec{r})\, \mathrm{d}S. \end{aligned}$$

Free-field pressure p_0 at the centre $\vec{R}_c$ of the sphere is given by the relation

$$p_0(\vec{R}_c) = (\mathrm{j}\omega\varrho Q/4\pi)\, \mathrm{e}^{-\mathrm{j}kR}/R. \qquad \text{(A 5)}$$

The ratio $p_{avg}/p_0(R_c)$ for a fixed magnitude R is the directional response f_M of the spherical cap for sound reception (microphone) as defined by KUHL; thus

$$f_M = [(1/v_0 S_{cap}) \iint_S G(\vec{r}, \vec{R}_0)\, v_n(\vec{r})\, \mathrm{d}S]/[\mathrm{e}^{-\mathrm{j}kR}/R]. \qquad \text{(A 6)}$$

Comparison of the right-hand members of eqs. (A 3) and (A 6) shows that the directional response for sound reception is equal to that for sound transmission, i.e., $f_M = f_T$.

It might be noted that formally, both the radiated pressure and the average pressure on the cap in sound reception are calculated by means of the same integral, cf. eqs. (A 1) and (A 4), which is difficult to evaluate in practice. The simplicity offered by the use of the reciprocity principle to calculate the microphone directional response in terms of the expression for radiated pressure resides in the fact that the latter may be evaluated by the alternative and simpler method of solving a boundary-value problem.

(Received 1st February, 1953.)

References

[1] KUHL, W., Acustica **2** [1952], 226.

[2] Calculations for the sound pressure on the rigid sphere were based on the paper of SCHWARZ, L., Akust. Z. **8** [1943], 91.

[3] MORSE, P.M., Vibration and sound, 1st Ed. McGraw-Hill, New York 1936, pp. 250, 253.

[4] STENZEL, H., Leitfaden zur Berechnung von Schallvorgängen. Springer Verlag, Berlin 1939, pp. 86—89.

[5] Lord RAYLEIGH, Theory of sound. Macmillan & Co., London 1896, Vol. II, Section 334.

[6] For example a) MORSE [3], p. 270.
b) STENZEL [4], p. 109.
c) SCHWARZ [2], p. 105.

[7] See [4], Table p. 90.

[8] See, for example, Institute of Radio Engineers Standards on Electroacoustics, Proc. Instn Radio Engrs **39** [1951], 516 or FOLDY, L. L. and PRIMAKOFF, H., J. acoust. Soc. Amer. **17** [1945], 118.

[9] See, for example, STENZEL [4], Eq. (142), p. 81.

[10] See, for example, FISCHER, F.A., Grundzüge der Elektroakustik. Fachverlag Schiele u. Schön, Berlin 1950, Eq. (287), p. 104.
MASON, W.P., Electromechanical transducers and wave filters, 2nd Ed. D. van Nostrand Co, New York 1948, Eqs (6.21-4), (6.21-6), p. 389.

[11] See [8], pp. 113—114.

[12] See also FOLDY, L., J. acoust. Soc. Amer. **21** [1949], 597.

VARIATION OF ULTRASONIC ABSORPTION WITH FREQUENCY IN ORGANIC LIQUIDS

by S. PARTHASARATHY, S. S. CHARI and D. SRINIVASAN

National Physical Laboratory of India, New Delhi 12

Summary

The absorption (α) of ultrasonic waves has been measured by a radiation pressure method at 5, 10 and 15 Mc/s. The variation of α/f^2 with frequency (f) is discussed in relation to relaxation theory. In esters, generally, a pronounced decrease of α/f^2 with frequency occurs, thus justifying to some extent the relaxation theory.

Sommaire

On a mesuré par la méthode de la pression de radiation l'absorption des ultrasons aux fréquences 5, 10 et 15 MHz.

On étudie la variation de α/f^2 avec la fréquence au point de vue de la théorie de la relaxation. Il y a généralement dans les esters une diminution marquée de α/f^2 avec la fréquence, ce qui justifie dans une certaine mesure la théorie de la relaxation.

Zusammenfassung

Die Absorption von Ultraschallwellen wurde bei 5, 10 und 15 MHz mit der Strahlungsdruckmethode gemessen. Die Abhängigkeit der Größe α/f^2 von der Frequenz wird im Zusammenhang mit der Relaxationstheorie diskutiert. Bei Estern findet man im allgemeinen einen merklichen Abfall von α/f^2 mit der Frequenz und kann damit bis zu einem gewissen Grad die Relaxationstheorie rechtfertigen.

1. Introduction

The classical formula for the absorption of sound in liquids is not found adequate to explain the anomalous nature of absorption in benzene, carbon disulphide and some other non-associated polyatomic liquids. In most of these liquids, the absorption coefficient of sound waves varies as the square of the frequency in accordance with the classical prediction assuming the absorption to be due to viscosity [1] and conduction of heat [2], but the amount of absorption in all these liquids is found to be much greater than that predicted by the classical theory. This led many investigators to find a formula which will explain this excess absorption. Out of these various theories the relaxation theory as given by **Herzfeld** [3], **Kneser** [4] and **Bauer** [5] is now well established. According to this theory, there exists a relaxation of structural perturbation and of some internal degrees of freedom of the molecules of the liquid which will give rise to an additional absorption other than that due to viscosity and thermal conductivity. This additional absorption is given by **Kneser** [4] as

$$\frac{\alpha}{f^2} = \frac{2\mu_m}{c f_m}\left[1 + \left(\frac{f}{f_m}\right)^2\right]^{-1} \tag{1}$$

where $\mu_m = \alpha_m c/f_m$, f_m is the relaxation frequency and c the velocity of sound. At low frequencies $\frac{\alpha}{f^2} \approx \frac{2\mu_m}{c f_m} = A$ (say). Then **Kneser**'s equation can be simplified into

$$\frac{1}{\alpha} = \frac{1}{A}\left(\frac{1}{f^2} + \frac{1}{f_m^2}\right). \tag{2}$$

This equation can be used to find the relaxation frequency from a plot of $1/\alpha$ and $1/f^2$. The above equations lead to the conclusion that when $f > f_m$, α/f^2 falls with the frequency finally approaching the classical value when $f \gg f_m$.

In most of the non-associated polyatomic liquids, this relaxation frequency is far above the experimentally obtainable range which makes it impossible to put this theory to test. **Rapuano** [6] made measurements of absorption in a number of liquids between 75 and 280 Mc/s, but in none of them did he find a decrease of α/f^2 with frequency. Even in carbon disulphide he did not observe any fall in the value of α/f^2 up to 280 Mc/s in spite of the fact that the relaxation frequency in carbon disulphide is 52.5 Mc/s which is well within the range of his experiments. A number of experiments were made in water [7], [8] and in no case a drop of α/f^2 with frequency is noticed as indicated by theory.

The experiments performed in acetic acid [7], [8] up to 100 Mc/s and copper acetate and ethyl acetate [9] up to 50 Mc/s give some weight to the relaxation theory. In these liquids, the value of α/f^2 falls with the frequency as demanded by the theory but the value of α/f^2 never reaches the classical one. It is probable that the value of α/f^2 may attain the classical value at a still higher frequency than the one reached by the experiment.

In view of the limited data available to test the relaxation theory, we felt the need to determine the variation of α/f^2 with frequency in a number of organic liquids not investigated so far and this explains the purpose of the present paper.

2. Experiment

The radiation pressure method is used to determine the absorption coefficient. Every liquid is doubly distilled and used immediately after distillation. The experiment is performed at 5, 10 and 15 Mc/s. The value of α/f^2 is calculated for each frequency for all the liquids measured and is tabulated in Table I. Fig. 1 gives the curves relating α/f^2 with f for the liquids mentioned in Table I.

Table I
Variation of α/f^2 with frequency

No.	Liquid	Temperature [°C]	$\alpha/f^2 \times 10^{15}$ at 5 Mc/s	10 Mc/s	15 Mc/s	Classical value of $\alpha/f^2 \times 10^{15}$
1.	Cyclohexanone	27.0	1.59	0.89	0.49	0.223
2.	n-Butyl acetate	27.0	2.27	0.92	0.57	0.100
3.	n-Butyl alcohol	27.5	1.10	0.72	0.80	0.840
4.	Iso propyl alcohol	26.5	0.92	0.90	0.92	0.460
5.	Pyridine	27.0	5.10	3.94	3.60	0.900
6.	Toluene	27.0	1.29	1.24	1.23	0.078
7.	Cyclohexanol	28.0	5.00	5.10	—	4.890
8.	Capryl alcohol	27.0	2.07	1.95	1.90	—
9.	Diethyl malonate	28.0	3.68	0.61	0.52	0.210
10.	m-Xylene	27.0	0.89	0.80	0.72	0.079
11.	Ethyl acetate	25.0	1.90	1.07	0.78	0.080

3. Discussion

The results given in Table I show that the value of α/f^2 for non-associated polyatomic liquids like toluene and m-xylene, remains approximately constant as also in alcohols and the viscous liquids like cyclohexanol. In esters, there is a pronounced decrease in the value of α/f^2 when the frequency is increased from 5 to 15 Mc/s, the value falling at 15 Mc/s to nearly one-third of its value at 5 Mc/s. Our results in ethyl acetate agree very well that of **Beyer** and **Smith** [9]. The value of α/f^2 is tending towards the classical value as the frequency increases in esters.

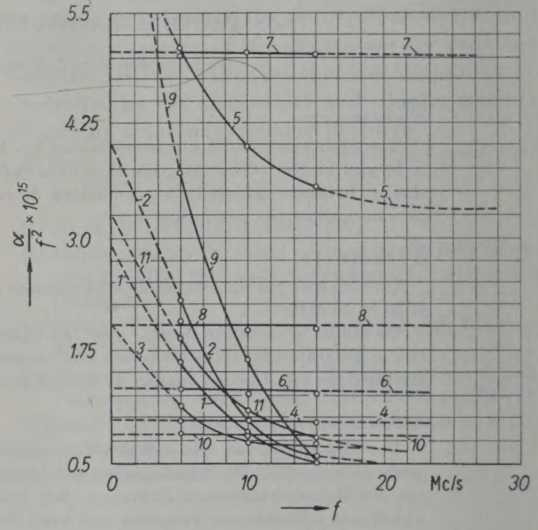

Fig. 1. Variation of α/f^2 with frequency for liquids indicated in Table I.

It is probable that the value of α/f^2 in esters may reach the classical value at still higher frequencies. Our results in esters support to some extent the relaxation theory. It is not possible to trace a fall in the value of α/f^2 in non-associated polyatomic liquids like toluene and m-xylene as their relaxation frequencies lie far above the range in which we have measured.

(Received 20th October, 1952.)

References

[1] **Stokes**, G. G., Camb. phil. Trans. **8** [1845], 287.
[2] **Kirchhoff**, G. G., Pogg. Ann. **134** [1868], 177.
[3] **Herzfeld**, K. F., J. acoust. Soc. Amer. **13** [1941], 33.
[4] **Kneser**, H. O., Ann. Phys. **32** [1938], 277.
[5] **Bauer**, E., Proc. phys. Soc. London **A 62** [1949], 141.
[6] **Rapuano**, R. A., Phys. Rev. **72** [1947], 78.
[7] **Pinkerton**, J. M. M., Nature **162** [1948], 106.
[8] **Lamb**, J., **Andreae**, J. H. and **Bird**, R., Nature **162** [1948], 993.
[9] **Beyer**, R. T. and **Smith**, M. C., J. acoust. Soc. Amer. **18** [1947], 424.